Key bioactive reaction products of the NO/H_2S interaction are S/N-hybrid species, polysulfides, and nitroxyl

Miriam M. Cortese-Krott[a], Gunter G. C. Kuhnle[b,1], Alex Dyson[c,1], Bernadette O. Fernandez[d,1], Marian Grman[e], Jenna F. DuMond[f], Mark P. Barrow[g], George McLeod[h], Hidehiko Nakagawa[i], Karol Ondrias[e], Péter Nagy[j], S. Bruce King[f], Joseph E. Saavedra[k], Larry K. Keefer[l], Mervyn Singer[c], Malte Kelm[a], Anthony R. Butler[m], and Martin Feelisch[d,2]

[a]Cardiovascular Research Laboratory, Department of Cardiology, Pneumology and Angiology, Medical Faculty, Heinrich Heine University of Düsseldorf, 40225 Dusseldorf, Germany; [b]Department of Nutrition, University of Reading, Whiteknights, Reading RG6 6AP, United Kingdom; [c]Bloomsbury Institute of Intensive Care Medicine, University College London, London WC1E 6BT, United Kingdom; [d]Clinical and Experimental Sciences, Faculty of Medicine, University of Southampton, Southampton General Hospital and Institute for Life Sciences, Southampton SO16 6YD, United Kingdom; [e]Center for Molecular Medicine, Slovak Academy of Sciences, 83101 Bratislava, Slovak Republic; [f]Department of Chemistry, Wake Forest University, Winston-Salem, NC 27109; [g]Department of Chemistry, Warwick University, Coventry CV4 7AL, United Kingdom; [h]Bruker UK Ltd., Coventry CV4 9GH, United Kingdom; [i]Department of Organic and Medicinal Chemistry, Graduate School of Pharmaceutical Sciences, Nagoya City University, Nagoya-shi, Aichi 467-8603, Japan; [j]Department of Molecular Immunology and Toxicology, National Institute of Oncology, 1122 Budapest, Hungary; [k]Leidos Biomedical Research, Inc., National Cancer Institute–Frederick, Frederick, MD 21702; [l]National Cancer Institute–Frederick, Frederick, MD 21702; and [m]Medical School, University of St. Andrews, St. Andrews, Fife KY16 9AJ, Scotland

Edited by Louis J. Ignarro, University of California, Los Angeles School of Medicine, Beverly Hills, CA, and approved July 2, 2015 (received for review May 12, 2015)

Experimental evidence suggests that nitric oxide (NO) and hydrogen sulfide (H_2S) signaling pathways are intimately intertwined, with mutual attenuation or potentiation of biological responses in the cardiovascular system and elsewhere. The chemical basis of this interaction is elusive. Moreover, polysulfides recently emerged as potential mediators of H_2S/sulfide signaling, but their biosynthesis and relationship to NO remain enigmatic. We sought to characterize the nature, chemical biology, and bioactivity of key reaction products formed in the NO/sulfide system. At physiological pH, we find that NO and sulfide form a network of cascading chemical reactions that generate radical intermediates as well as anionic and uncharged solutes, with accumulation of three major products: nitrosopersulfide ($SSNO^-$), polysulfides, and dinitrososulfite [*N*-nitrosohydroxylamine-*N*-sulfonate (SULFI/NO)], each with a distinct chemical biology and in vitro and in vivo bioactivity. $SSNO^-$ is resistant to thiols and cyanolysis, efficiently donates both sulfane sulfur and NO, and potently lowers blood pressure. Polysulfides are both intermediates and products of $SSNO^-$ synthesis/decomposition, and they also decrease blood pressure and enhance arterial compliance. SULFI/NO is a weak combined NO/nitroxyl donor that releases mainly N_2O on decomposition; although it affects blood pressure only mildly, it markedly increases cardiac contractility, and formation of its precursor sulfite likely contributes to NO scavenging. Our results unveil an unexpectedly rich network of coupled chemical reactions between NO and H_2S/sulfide, suggesting that the bioactivity of either transmitter is governed by concomitant formation of polysulfides and anionic S/N-hybrid species. This conceptual framework would seem to offer ample opportunities for the modulation of fundamental biological processes governed by redox switching and sulfur trafficking.

sulfide | nitric oxide | nitroxyl | redox | gasotransmitter

Nitrogen and sulfur are essential for all known forms of life on Earth. Our planet's earliest atmosphere is likely to have contained only traces of O_2 but rather large amounts of hydrogen sulfide (H_2S) (1). Indeed, sulfide may have supported life long before the emergence of O_2 and NO (2, 3).* This notion is consistent with a number of observations: H_2S is essential for efficient abiotic amino acid generation as evidenced by the recent reanalysis of samples of Stanley Miller's original spark discharge experiments (4), sulfide is an efficient reductant in protometabolic reactions forming RNA, protein, and lipid precursors (5), and sulfide is both a bacterial and mitochondrial substrate (6), enabling even multicellular lifeforms to exist and reproduce under conditions of permanent anoxia (7). Thus, although eukaryotic cells may have originated from the symbiosis of sulfur-reducing and -oxidizing lifeforms within a self-contained sulfur redox metabolome (8), sulfide may have been essential even earlier by providing the basic building blocks of life.

The chemical reactions of sulfur-centered nucleophiles with a range of nitrogen-containing species have been studied for different reasons and as independent processes for more than a century, and early reports indicated complex reaction mechanisms (9–13). The recent surge of interest in this chemistry in

Significance

Reactions of sulfur-centered nucleophiles with nitrogenous species have been studied independently for more than a century for synthetic/industrial purposes; to understand geochemical, atmospheric, and biological processes; and to explain the origins of life. Various products and reaction mechanisms were proposed. We here identify a singular process comprising a network of cascading chemical reactions that form three main bioactive products at physiological pH: nitrosopersulfide, polysulfides, and dinitrososulfite. These anionic products scavenge, transport, and release NO/HNO or sulfide/sulfane sulfur, each displaying distinct chemistries and bioactivities. Our observations provide a chemical foundation for the cross-talk between the NO and H_2S signaling pathways in biology and suggest that the biological actions of these entities can be neither considered nor studied in isolation.

Author contributions: M.F. conceived, initiated, and coordinated the study; M.M.C.-K., G.G.C.K., A.D., B.O.F., J.F.D., M.P.B., G.M., K.O., P.N., S.B.K., M.S., A.R.B., and M.F. designed research; M.M.C.-K., G.G.C.K., A.D., B.O.F., M.G., J.F.D., M.P.B., G.M., and M.F. performed research; M.M.C.-K., G.G.C.K., M.P.B., G.M., H.N., S.B.K., J.E.S., L.K.K., and M.F. contributed new reagents/analytic tools; M.M.C.-K., G.G.C.K., A.D., B.O.F., M.G., J.F.D., M.P.B., G.M., K.O., P.N., S.B.K., J.E.S., M.S., M.K., A.R.B., and M.F. analyzed data; M.M.C.-K. and M.F. wrote the paper; and G.G.C.K., A.D., B.O.F., M.G., J.F.D., M.P.B., G.M., H.N., K.O., P.N., S.B.K., L.K.K., M.S., M.K., and A.R.B. contributed to manuscript writing.

The authors declare no conflict of interest.

This article is a PNAS Direct Submission.

Freely available online through the PNAS open access option.

[1]G.G.C.K., A.D., and B.O.F. contributed equally to this work.

[2]To whom correspondence should be addressed. Email: M.Feelisch@soton.ac.uk.

This article contains supporting information online at www.pnas.org/lookup/suppl/doi:10.1073/pnas.1509277112/-/DCSupplemental.

*H_2S is a weak acid (pK_a1 = 7.0, pK_a2 = 14.1); at physiological pH, approximately three-quarters of the dissolved H_2S exist in the form of hydrosulfide (HS^-) with negligible amounts of S_2^-. The combination of all three forms (H_2S, HS^-, and S_2^-) will hereinafter be referred to as sulfide.

the biological community (13–15) was triggered by a growing appreciation that NO and sulfide exert similar and often interdependent biological actions within the cardiovascular system and elsewhere (NO/H_2S "cross-talk") (16, 17), resulting in mutual attenuation or potentiation of their responses. This cross-talk is possibly mediated by chemical interactions (18–20), but much of the older chemical work seems to have been forgotten. Recently, low concentrations of sulfide were shown to quench NO-mediated vascular responses through formation of an uncharacterized "nitrosothiol" (RSNO) (18–20), assumed to be thionitrous acid (HSNO) (13–15).

A recent report of the detection by MS of the highly unstable HSNO at physiological pH (21) has attracted considerable attention from the biological community, because it could be an intermediate in the reaction of sulfide with RSNOs (22) and a precursor for NO, nitrosonium (NO^+) equivalents, and nitroxyl (HNO). However, a key aspect of HSNO's properties that seems to have been overlooked in these discussions is its mobile hydrogen, allowing facile 1,3 hydrogen shift and formation of four isomers with the same chemical equation (13)—a feature described in the seminal studies by Goehring in the 1950s (23) and by Müller and Nonella later on (24, 25) that distinguishes HSNO from all other RSNOs (26). The same feature also contributes to the short half-life of the molecule at ambient temperatures, making it more probable that other yet unknown entities are involved as biological mediators of the NO/H_2S cross-talk. Chemical studies by Seel and Wagner (9, 10) showed that NO readily reacts with HS^- in basic aqueous solution or organic solvents under anoxic conditions to form the yellow nitrosopersulfide ($SSNO^-$). Accumulation of this product was also observed after reaction of RSNOs with sulfide at pH 7.4 (26, 27); moreover, $SSNO^-$-containing mixtures were found to release NO, activate soluble guanylyl cyclase (sGC) (26), and relax vascular tissue (28), although a contribution of other reaction products to these effects cannot be excluded. Meanwhile, other sulfane sulfur molecules, including persulfides (RSSH) and polysulfides (RSS_n^- and HS_n^-), have come to the fore as potential mediators of sulfide's biological effects (29–31), but little is known about their pathways of formation, prevalence in biological systems, and relationship with NO.

In view of this confusion, we sought to carry out an integrative chemical/pharmacological investigation to study the chemical biology of the reaction of NO with sulfide more thoroughly and systematically identify potentially bioactive reaction products. We here report that the NO/H_2S interaction leads to formation of at least three product classes with distinct in vivo bioactivity profiles: nitrosopersulfide ($SSNO^-$), polysulfides (HS_n^-), and dinitrososulfite [$ONN(OH)SO_3^-$ or *N*-nitrosohydroxylamine-*N*-sulfonate (SULFI/NO)]; all anions at physiological pH. Their formation is accompanied by both scavenging and release of NO and H_2S and formation of nitrous oxide (N_2O), nitroxyl (HNO), nitrite (NO_2^-), nitrate (NO_3^-), and various sulfoxy species. These results not only offer an intriguing explanation for the quenching and potentiating effects of sulfide on NO bioavailability but also, provide a novel framework for modulation of fundamental biological processes governed by redox switching and sulfur trafficking. This chemistry is likely to prevail wherever NO and sulfide are cogenerated.

Results

Sulfide Modulates NO Bioavailability in a Concentration-Dependent Manner. Effects of sulfide on NO bioavailability and hemodynamics were investigated in anesthetized rats. Pilot studies confirmed that sodium hydrosulfide (NaHS; 1.8–18 μmol/kg) lowers blood pressure and heart rate in a dose-dependent manner; effects were short-lived and accompanied by alterations in NO metabolite status in RBCs and plasma (*SI Appendix*, Fig. S1 and Table S1). As with inhaled NO (32), higher sulfide doses increased total nitroso (RXNO) levels in RBCs (*SI Appendix*, Fig. S1). Inhibition of NO synthase by *S*-ethylisothiourea prolonged the action of sulfide and markedly increased its toxicity (*SI Appendix*, Fig. S1 *A* and *B*), showing that endogenous NO production modulates sulfide bioactivity and attesting to the reciprocal nature of interaction of these signaling molecules. In subsequent experiments, NaHS was administered by continuous infusion (2.8 μmol/kg per minute in PBS, pH 7.4) to counter the rapid rate of sulfide elimination (33), and blood was collected repeatedly for measurement of circulating NO biomarkers (Fig. 1 and *SI Appendix*, Fig. S2 and Table S2). Consistent with the notion that vascular sulfide levels rise only after inactivation (binding/elimination) pathways become saturated, no significant hemodynamic changes were observed in the

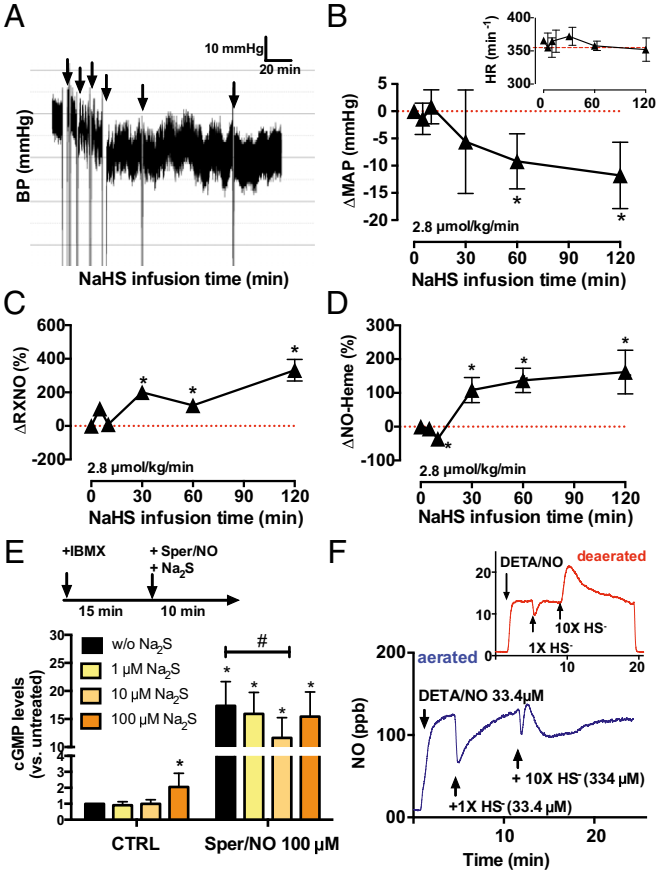

Fig. 1. Sulfide affects NO bioavailability in vivo and in vitro. (*A* and *B*) Continuous i.v. infusion of sodium hydrosulfide (2.8 μmol/kg per min NaHS in PBS, pH 7.4) progressively decreases blood pressure (BP) in rats. (*A*) Original recording depicting progressive decrease in BP during ongoing sulfide infusion; incisions (arrows) are caused by interruption of pressure recording during blood collection. (*B*) Changes in mean arterial blood pressure (MAP; $n = 5$; ANOVA $P = 0.0256$) and (*Inset*) heart rate (HR). *Dunnett's $P < 0.05$ vs. baseline. (*C*) Gradual increases in circulating nitroso species (RXNO) levels in RBCs ($n = 3$; ANOVA $P = 0.0032$). *Dunnett's $P < 0.05$ vs. baseline. (*D*) Concomitant transient decrease followed by an increase in NO-heme levels during continuous sulfide infusion (2.8 μmol/kg per min NaHS in PBS, pH 7.4; $n = 3$; ANOVA $P = 0.0126$). *Tuckey $P < 0.05$ vs. baseline. (*E*) Sulfide (10 μM Na_2S) decreases Sper/NO (100 μM)-mediated sGC activation in RFL-6 cells pretreated with the phosophdiesterase inhibitor 3-isobutyl-1-metylxanthine (IBMX). The scheme represents the experimental setup ($n = 6$; ANOVA $P < 0.001$). CTRL, control. *Tuckey $P < 0.01$ vs. untreated. # t test $P < 0.05$ (*F*) Equimolar concentrations of sulfide (33.4 μM) scavenge NO released form NO donors (33.4 μM DETA/NO) as assessed by time-resolved chemiluminescence detection under both aerated and (*Inset*) deaerated conditions, whereas excess sulfide (334 μM) transiently elevates NO release (representative of $n = 3$ independent experiments); DETA/NO, diethylenetriamine NONOate.

first 30 min of infusion (Fig. 1 *A* and *B* and *SI Appendix*, Table S2), albeit NO-heme levels dropped significantly (Fig. 1*D*). After 1 h of sulfide infusion, blood pressure was significantly lower, whereas heart rate remained constant (Fig. 1 *A* and *B* and *SI Appendix*, Table S2). The lack of a compensatory rise in heart rate and the decrease in respiratory rate that accompanied the fall in mean arterial pressure are consistent with the recognized metabolic effects of sulfide, capable of inducing a state of suspended animation (34). Concomitant with these changes in blood pressure, erythrocyte RXNO and NO-heme levels gradually increased (Fig. 1 *C* and *D*).

The effect of sulfide on NO-induced sGC stimulation was tested in an NO reporter cell line in the presence of a phosphodiesterase (PDE) inhibitor. Low sulfide concentrations (10 μM) inhibited sGC stimulation by the NO donor, spermine NONOate (Sper/NO; 100 μM), whereas cGMP levels at equimolar concentrations of sulfide and Sper/NO did not differ from those of Sper/NO alone (Fig. 1*E*). Although constitutive cGMP–PDE activity in these cells is very low (26) and cells were pretreated with a PDE inhibitor, 100 μM sulfide increased cGMP on its own (Fig. 1*E*), prohibiting the use of higher sulfide concentrations to investigate NO responses in these cells. Additional chemical experiments with NO donors/sulfide in cell-free buffer systems confirmed that sulfide, dependent on concentration, either quenches or transiently enhances NO as detected by chemiluminescence (Fig. 1*F*).

Collectively, these data show a dual effect of sulfide on NO bioavailability, with lower doses inhibiting and higher doses restoring (or in some cases, potentiating) NO bioactivity in cell-free systems, cells in vitro, and rats in vivo.

Sulfide Reacts with NO to Form Polysulfides and Two NO-Containing S/N-Hybrid Species. Our next efforts were directed toward elucidating whether there is a chemical foundation for this NO/H_2S cross-talk by identifying specific reaction products. UV-visible spectroscopy offered a first glimpse into the chemistry of the NO/sulfide interaction. A dominant product of the reaction of sulfide with NO (Fig. 2*A*), the NO donor DEA/NO (Fig. 2 *B–D* and *SI Appendix*, Fig. S4), or RSNOs (SNAP in Fig. 2*E*) (other RSNOs are in ref. 26) in aqueous buffer at pH 7.4 in both the absence and the presence of O_2 is a yellow compound (λ_{max} = 412 nm), in particular when sulfide is in excess (Fig. 2 *C* and *D*). We (13, 26) and others (9, 10, 27, 35) attributed this species to $SSNO^-$. We here extend those earlier observations with RSNOs to NO itself (as shown by the reaction of sulfide with aqueous NO solution and NO donors). Absorbance increases in the regions of 250–300 nm and below 250 nm are also apparent (Fig. 2, arrows).

The reaction products absorbing in the region around 300 nm (λ = 290–350 nm) seem to be HS_n^-, because this feature disappeared on addition of the classical sulfane sulfur-reducing reagents DTT or cyanide (*SI Appendix*, Fig. S5 *A* and *B*) or millimolar concentrations of cysteine and glutathione (26). Contrary to HS_n^-, the $SSNO^-$ peak was resistant toward thiols and cyanide (*SI Appendix*, Fig. S5 *A* and *B*), and its decomposition rate was hardly affected by the presence of these chemicals (*SI Appendix*, Fig. S5*C*). Like HS_n^- but contrary to classical RSNOs, $SSNO^-$ is relatively stable at neutral and basic pH levels (*SI Appendix*, Fig. S5*C*) but rapidly decomposes with formation of colloidal sulfur and H_2S on acidification as shown previously (26). Interestingly, HS_n^-s are not only products of $SSNO^-$ decomposition (*SI Appendix*, Fig. S5*D*) but also, likely intermediates with clear catalytic effects on $SSNO^-$ formation (Fig. 2*F*). Under conditions of no/low added HS_n^-, an induction period is observed that disappears at higher HS_n^- concentrations (Fig. 2*F*), pointing to possible autocatalytic effects of HS_n^- formed during the reaction between sulfide and NO/RSNO. The product yield in the reaction of SNAP with excess sulfide approached 30% for $SSNO^-$ as estimated by measuring the concentrations of either H_2S or sulfane sulfur atoms liberated by reduction, cyanolysis, or chloroform extraction

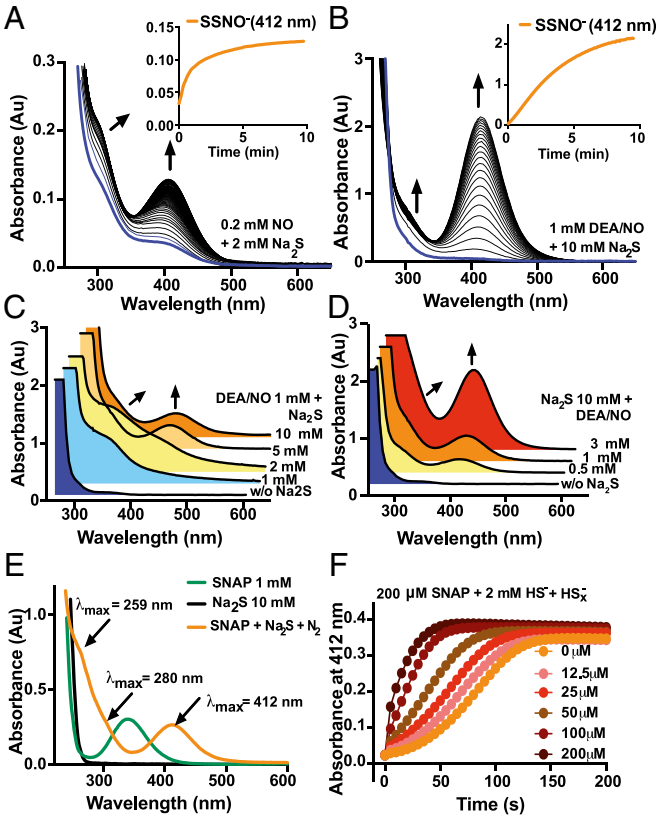

Fig. 2. The reaction of NO with sulfide leads to formation of three major products, which we assign to be $SSNO^-$ (λ_{max} = 412 nm), HS_n^- (λ_{max} = 290–300 nm), and SULFI/NO (λ_{max} = 259 nm). (*A*) Reaction of aqueous solutions of NO (200 μM) with sulfide (2 mM) under deaerated conditions in buffer at pH 7.4 leads to formation of a peak with λ_{max} = 412 nm ($SSNO^-$) and increases in absorbance at λ_{max} < 300 nm (HS_n^-). Products with λ_{max} < 250 nm are not discernable from sulfide because of the high concentration of HS^- (λ_{max} = 230 nm) in these experiments; spectra were taken at the reaction start (blue) and every 5 s after the addition of NO. (*Inset*) kinetics of $SSNO^-$ formation. (*B*) Reaction of the NO donor DEA/NO (1 mM) with sulfide (10 mM) under aerated conditions forms $SSNO^-$ and HS_n^-. The blue line indicates the spectrum before the addition of sulfide. (*Inset*) Kinetics of formation of $SSNO^-$. (*C* and *D*) The yield of $SSNO^-$ formation depends on both (*C*) sulfide concentration and (*D*) the rate of NO release; all spectra were taken 10 min after the start of the reaction. (*E*) $SSNO^-$ (λ_{max} = 412 nm), HS_n^- (λ_{max} = 290–300 nm), and SULFI/NO (λ_{max} = 259 nm) are formed in the reaction of sulfide with the *S*-nitrosothiol SNAP (1 mM SNAP + 10 mM Na_2S; 10 min); SULFI/NO is detectable after removal of sulfide by gassing with N_2 for 10 min. (*F*) Addition of HS_n^- (12.5–200 μM) increases the rate of formation of $SSNO^-$ from the reaction of SNAP (200 μM) and sulfide (2 mM); the induction period observed at no/low added HS_n^- points to an autocatalytic effect of HS_n^- (n = 3). All spectra in *A–E* are representative of 3–10 independent experiments. Au, arbitrary unit; DEA/NO, dietylamine/NONOate; SNAP, S-nitroso-N-acetyl-penicillamine.

during formation and/or decomposition of $SSNO^-$ (*SI Appendix*, Fig. S5) and was calculated to be ∼34% in nonaqueous media (ε = 2,800 M^{-1} cm^{-1}, λ_{max} = 448 nm) (35). Furthermore, $SSNO^-$ decomposition in the presence of DTT released two times as much sulfide as sulfane sulfur (*SI Appendix*, Fig. S5 *D* and *E*). Therefore, $SSNO^-$ contains two sulfur atoms, one of which is a sulfane sulfur.

In the reaction of NO with sulfide, in basic aqueous and nonaqueous conditions under exclusion of air, Seel and Wagner (9) also observed the formation of SULFI/NO ($[ONN(OH)SO_3]^-$), a complex formed by the reaction of sulfite with NO. This product is also known as dinitrososulfite (36) (λ_{max} = 259 nm, ε = 8,198 M^{-1} cm^{-1}), which we find to be another product of the reaction of NO and sulfide at physiological pH. Indeed, a peak with λ_{max} = 259 nm appears in RSNOs/sulfide incubates after

removal of excess unreacted sulfide by bubbling with N_2 (Fig. 2*E*). The formation of SULFI/NO from DEA/NO/sulfide mixtures cannot be followed spectrophotometrically, because DEA/NO (like SULFI/NO) is a diazeniumdiolate (36) that absorbs in the same wavelength range. Other putative reaction products are sulfoxy species, including sulfite, sulfate, thiosulfate ($S_2O_3^{2-}$), and polythionates ($[O_3S\text{-}S_x\text{-}SO_3]^{2-}$), all absorbing at wavelengths <250 nm and spectrophotometrically difficult to distinguish from each other.

Taken together, these results show that the reaction of sulfide with NO or RSNO under physiologically relevant conditions leads to formation of three major reaction products: $SSNO^-$, HS_n^-, and SULFI/NO. These products have been described in different contexts before, but we find that all three are formed in sequential reactions of the same chemical system under physiologically relevant conditions. With high NO fluxes and excess sulfide, $SSNO^-$ is a major reaction product.

Mass Spectrometric Identification of the Products of the Sulfide/NO Reaction. To definitively identify the reaction products of NO (1 mM DEA/NO) or RSNOs (1 mM SNAP) with sulfide (2 mM Na_2S), incubation runs in phosphate or Tris buffer at pH 7.4 were subjected to electrospray ionization (ESI)–high-resolution MS (HRMS) analysis (Fig. 3 and *SI Appendix*, Table S7). Because many of the key reaction products were suspected to be negatively charged species at pH 7.4, negative ionization mode was used throughout. The S/N-hybrid species $SSNO^-$ (compound 1; *m/z* theoretical = 93.94268, *m/z* found = 93.9427, error = 0.39 milli mass units, mmu) and SULFI/NO (compound 2; $HO_5N_2S^-$; *m/z* theoretical = 140.96061, *m/z* found = 140.9612, error = 0.35 mmu) and multiple polysulfide species, including HS_3^-, HS_4^-, and HS_5^-, were identified as reaction products of sulfide with either NO donor (Fig. 3). For $SSNO^-$ and SULFI/NO, assigned structures were confirmed by analysis of their fragmentation pattern (Fig. 3 *A*, *Center* and *B*, *Center*); the former was found to eliminate NO by hemolytic cleavage, forming the persulfide radical ($S_2{\cdot}^-$) (Fig. 3*A*), whereas N_2O elimination and sulfate formation (detected as HSO_4^-) characterized the latter (Fig. 3*B*). The structural assignments were unequivocally confirmed using ^{15}N labeling, resulting in an *m/z* shift of 1 for $SSNO^-$ and 2 for SULFI/NO (Fig. 3 *A*, *Right* and *B*, *Right*). Changes in relative abundance of reaction products over time were monitored during direct infusion of the reaction mixture into the ionization chamber. These studies revealed that both $SSNO^-$ and SULFI/NO are formed surprisingly quickly (≤2 s, which was evidenced by additional experiments using NO/sulfide coinfusion by a T piece close to the ionization source) from both NO and RSNOs followed by gradual accumulation of medium-chain/long-chain HS_n^-.

More in-depth analysis of reaction mixtures by ESI-HRMS and HPLC revealed the presence of additional anionic products, including nitrite, hyponitrite, nitrate, sulfite, sulfate, thiosulfate, and polythionates (Fig. 3*C* and *SI Appendix*, Fig. S6), with evidence for traces of a persulfide NONOate ($[ONN(OH)S_2]^-$). The previously reported intermediate in the formation of $SSNO^-$, thionitrite (SNO^-)/thionitrous acid (HSNO) (9, 10, 21, 22, 26), proved impossible to be detected from RSNO/sulfide mixtures using this technique, even with cryospray ionization at −20 °C (*SI Appendix*, Figs. S8 and S9); although stable at very low temperature (12 K) in a frozen argon matrix (24), detection of HSNO at room temperature as presented in an earlier publication (21) is difficult to understand.

Collectively, these data suggest that the chemical foundation of the NO/sulfide cross-talk is not limited to formation of a single molecular entity but is underpinned by a mixture of compounds, including HS_n^- and two S/N-hybrid molecules ($SSNO^-$ and SULFI/NO) along with other nitrogen oxides and sulfoxy species. With sulfide in abundance, HS_n^- and $SSNO^-$ are the major products accumulating.

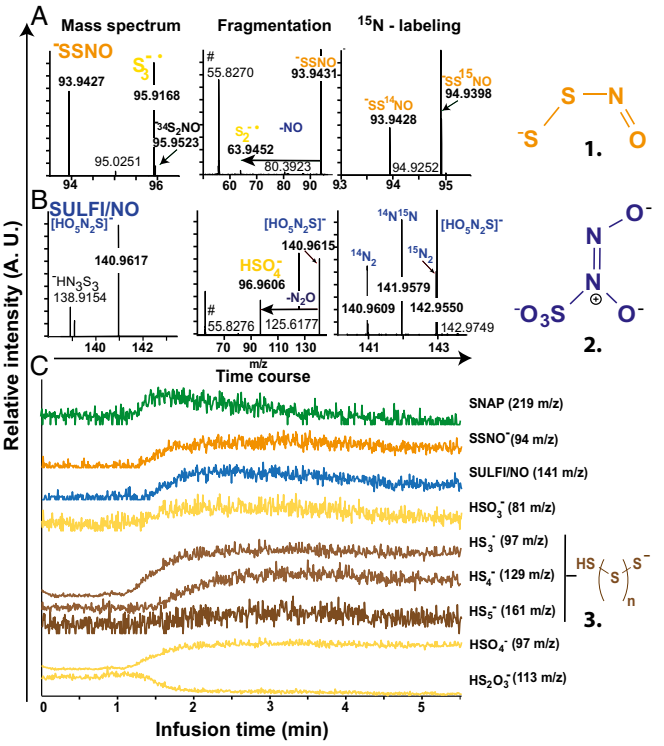

Fig. 3. Identification by ESI-HRMS of SULFI/NO and $SSNO^-$ as S/N-hybrid species formed by the reaction of sulfide with DEA/NO or SNAP. (*A*) Formation of $SSNO^-$ from DEA/NO (1 mM)/sulfide (2 mM) and SNAP (1 mM)/sulfide (2 mM) incubates. (*Left*) Mass and (*Center*) fragmentation spectra of $SSNO^-$ (compound 1) from DEA-NO-sulfide incubates; (*Right*) shift in *m/z* of $SSNO^-$ using an equimolar mixture of $^{14}N/^{15}N$-labeled SNAP with sulfide. (*B*) Formation of SULFI/NO (compound 2) from DEA/NO (1 mM)/sulfide (2 mM) and SNAP (1 mM)/sulfide (2 mM) incubates. (*Left*) Mass and (*Center*) fragmentation spectra of SULFI/NO; (*Right*) *m/z* shifts of one and two by reacting an equimolar mixture of $^{15}N/^{14}N$-SNAP (1 mM) with sulfide (2 mM). (*C*) Extracted ion chromatograms showing SNAP consumption accompanied by formation of SULFI/NO and $SSNO^-$ together with polysulfides (compound 3; $n = 2$–7), including monoprotonated tri-, tetra-, and pentasulfide (HS_3^-, HS_4^-, and HS_5^-, respectively), sulfite (HSO_3^-), sulfate (HSO_4^-), and thiosulfate ($HS_2O_3^-$). *SI Appendix*, Table S7 has details on predicted molecular masses. A.U., arbitrary unit; DEA/NO, dietylamine NONOate; SNAP, S-nitroso-N-acetylpenicillamine; m/z, mass-to-charge ratio.

NO- and HNO-Mediated Bioactivity in Vitro. Both $SSNO^-$ and SULFI/NO may have the potential to generate NO and/or its redox congener, HNO (26, 36). We, therefore, compared the NO and HNO releasing properties of $SSNO^-$-enriched mixtures ("$SSNO^-$ mix") with the properties of solutions of authentic SULFI/NO. $SSNO^-$ is a potent NO donor as assessed by chemiluminescence (Fig. 4*A*) and a weak HNO donor as assessed by triarylphosphine trapping (Fig. 4*D*) (37); however, no signal was obtained using the specific nitroxyl probe P-Rhod (38) (Fig. 4*B*). Other methods, such as methemoglobin trapping and ferricyanide oxidation of HNO into NO, suffer from artifacts caused by reaction with sulfide (*SI Appendix*, Fig. S10). In agreement with earlier findings (39), we found SULFI/NO to be a weak combined NO/HNO donor compared with DEA/NO and Angeli's salt (Fig. 4 *B* and *C* and *SI Appendix*, Figs. S10 and S11). Interestingly, N_2O (the main decomposition product of SULFI/NO) is generated at high yield under aerobic and anaerobic conditions on reaction of sulfide with DEA/NO (Fig. 4*C*) and RSNOs (*SI Appendix*, Fig. S11). Thus, as with acidified nitrite and sulfide (12), NO, HNO, and N_2O are common end products of the reaction of sulfide with NO or RSNOs.

As shown recently, the $SSNO^-$ mix concentration-dependently increases cGMP in RFL-6 cells (26) and relaxes aortic rings (28)

in an NO- and sGC-dependent manner. In Fig. 4*E*, we show that low concentrations of SULFI/NO do not increase intracellular cGMP levels, except in the presence of very high concentrations of superoxide dismutase (SOD) facilitating noncatalytic, copper-mediated conversion of HNO to NO (40). The effects of SULFI/NO were quenched by trapping either HNO by cysteine or NO by cPTIO (Fig. 4*F*). HS_n^- and colloidal sulfur did not significantly increase cGMP. Considering that $SSNO^-$ and SULFI/NO are the major S/N-hybrid molecules formed from sulfide and NO and that SULFI/NO is rather inefficient at releasing NO/HNO, these observations suggest that $SSNO^-$ is the main carrier of bioactivity in the NO/sulfide interaction. The formation of sulfite from sulfide may be important in redox switching by virtue of sulfite's ability to trap NO (*SI Appendix*, Fig. S3) and form SULFI/NO, allowing conversion of NO into HNO.

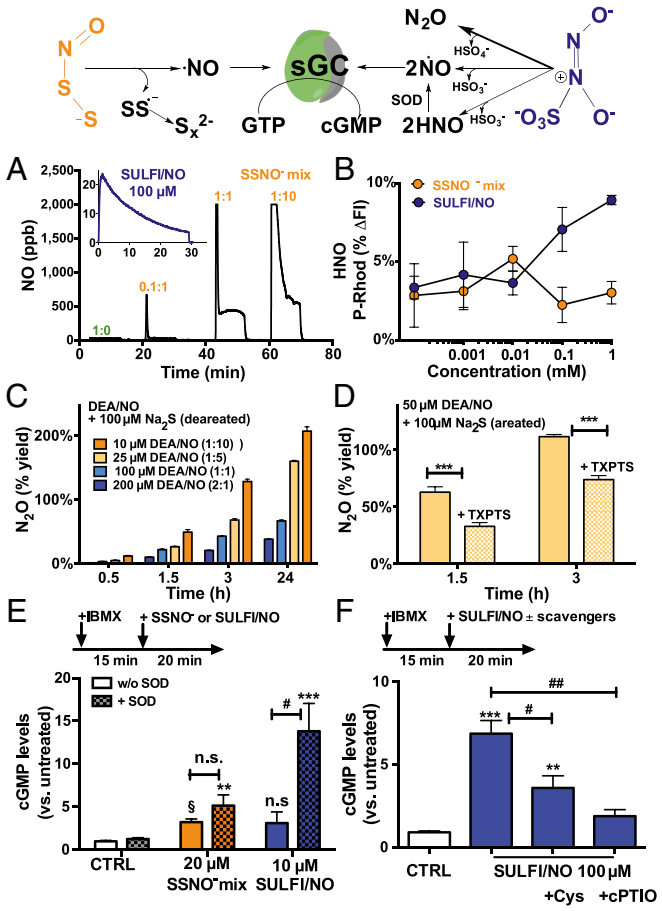

Fig. 4. NO and HNO bioactivity of $SSNO^-$ and SULFI/NO in vitro. The scheme shows that the release of NO and HNO from $SSNO^-$ and SULFI/NO leads to activation of sGC in cells. (*A*) Kinetics of NO release from $SSNO^-$ after incubation of SNAP (0.1 or 1 mM) and Na_2S (1 or 10 mM) for 1 min as determined by chemiluminescence (final dilution of 1:100). (*Inset*) NO release from authentic SULFI/NO (100 µM) in the absence of sulfide. (*B*) Release of nitroxyl (HNO) as assessed by P-Rhod fluorescence from increasing concentrations of SULFI/NO (blue) and $SSNO^-$ (orange; 1 mM SNAP, 10 mM Na_2S; gassed). ΔFI, fluorescence intensity-background. (*C*) The reaction of DEA/NO (10–200 µM) with sulfide (100 µM) generates N_2O over prolonged periods of time. (*D*) HNO scavenging by triphenylphosphine reveals that part of the N_2O formed during the DEA/NO/sulfide reaction originates from HNO dimerization/dehydration. ***Dunnett's $P < 0.001$. (*E*) $SSNO^-$ (20 µM) activates sGC in RFL-6 cells in both the presence and the absence of SOD, whereas equivalent concentrations of SULFI/NO (10 µM) activate sGC only in the presence of SOD after conversion of HNO into NO (n = 6–12; one-way ANOVA, $P < 0.001$). **Dunnett's $P < 0.01$; ***Dunnett's $P < 0.001$; $^{§}t$ test vs. untreated $P < 0.001$ (paired t test $P = 0.0056$); $^{\#}P < 0.01$ vs. 10 µM SULFI/NO without SOD. n.s., nonsignificant. (*F*) Higher concentrations of SULFI/NO (100 µM) activate sGC even in the absence of added SOD, an effect that is abolished by the NO scavenger cPTIO (500 µM) and the HNO scavenger Cys (1 mM; n = 5–10; one-way ANOVA, $P < 0.001$; $F = 27.14$). *Sidak's $P < 0.05$ vs. CTRL; ***Sidak's $P < 0.001$ vs. CTRL; $^{\#}P < 0.01$ vs. 100 µM SULFI/NO; $^{\#\#}P < 0.001$ vs. 100 µM SULFI/NO. cPTIO, 2-(4-Carboxyphenyl)-4,4,5,5-tetramethylimidazoline-1-oxyl-3-oxide; CTRL, control; Cys, cysteine; DEA/NO, diethylamine NONOate; IBMX, 3-isobutyl-1-metylxanthine; SOD, superoxide dismutase; TXPTS, triarylphosphine.

In Vivo Bioactivity: Vascular and Cardiac Effects. The in vivo bioactivity of the $SSNO^-$ mix was compared with authentic SULFI/NO by assessing effects on hemodynamics and cardiac function in rats (Fig. 5 and *SI Appendix*, Tables S3–S6). Acute administration of $SSNO^-$ dose-dependently decreases blood pressure, whereas only the highest dose of SULFI/NO tested lowered blood pressure significantly (Fig. 5*A*). However, in contrast to $SSNO^-$, SULFI/NO increases cardiac output, stroke volume, and aortic peak flow velocity without significant changes in heart rate, indicative of increased myocardial contractility (Fig. 5*B* and *SI Appendix*, Table S5). Continuous i.v. infusion of $SSNO^-$ induces a transient but significant drop in blood pressure followed by an increase in cardiac output (Fig. 5 *C* and *D*), whereas heart rate remains constant (*SI Appendix*, Table S6). By comparison, continuous infusion of SULFI/NO had less of an effect on blood pressure than $SSNO^-$ but produced a dramatic increase in cardiac contractility (Fig. 5 *C* and *D*); these results suggest that the positive inotropic effects of the $SSNO^-$ mix may, in fact, be mediated by the presence of SULFI/NO in the reaction mixture. The i.v. bolus administration of a mixture of HS_n^- was found to be of similar potency at lowering blood pressure as sulfide, but HS_n^- seems to be endowed with a longer duration of action (*SI Appendix*, Figs. S12 and 13*A*); preliminary results suggest that they may also increase vascular compliance (*SI Appendix*, Fig. S13). Collectively, our results indicate that the three major reaction products of the NO/sulfide interaction all display potent bioactivity, with a distinct cardiovascular profile for each class of species.

Discussion

The results of this study show that sulfide reacts with NO under physiologically relevant conditions to form three main bioactive products: $SSNO^-$, HS_n^- (where n = 2–7), and SULFI/NO. Specifically, we show that (*i*) in vivo sulfide administration modulates endogenous NO bioavailability; (*ii*) $SSNO^-$ is formed by intermediate polysulfide formation, accumulates at higher sulfide concentrations, is resistant to attack by other thiols, acts as an efficient NO and sulfane sulfur donor, and lowers blood pressure; (*iii*) HS_n^- are also products of the NO/sulfide interaction, are intermediates as well as decomposition products of $SSNO^-$, and lower blood pressure; (*iv*) SULFI/NO is a weak combined NO/HNO donor that has only mild blood pressure lowering but very pronounced positive inotropic effects; and (*v*) various other reaction products, including nitrogen oxides and sulfoxy species, are formed and likely also contribute to the bioactivity of both NO and sulfide. Importantly, our results suggest that the fates of NO and sulfide are intimately intertwined wherever they are cogenerated in biology; as a corollary, the biological actions of NO and H_2S can be neither considered nor studied in isolation, because they form a network of coupled chemical reactions that gives rise to formation of multiple new chemical entities with distinct bioactivity profiles. This unexpectedly rich chemistry would seem to provide nature with ample opportunities for modulation of various fundamental biological and pathophysiological processes related to, for example, electron transfer, sulfur trafficking, and redox regulation.

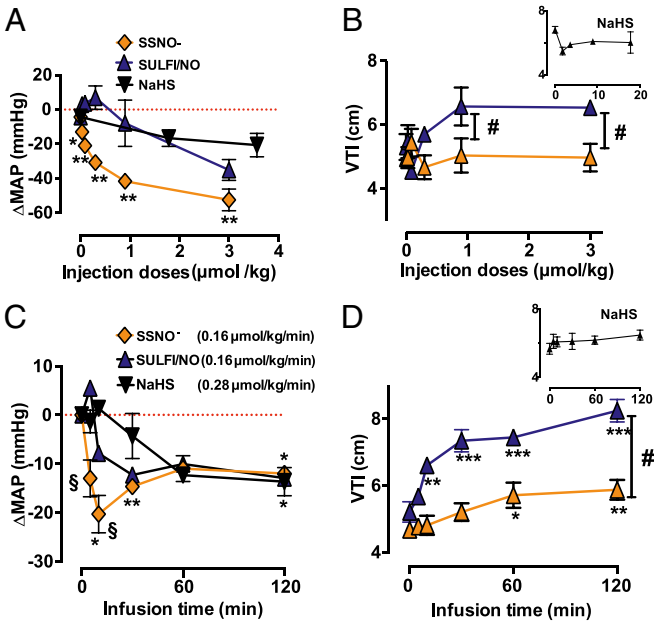

Fig. 5. $SSNO^-$ and SULFI/NO show distinct bioactivity in rats in vivo. (*A*) i.v. Injection of the $SSNO^-$ mix (dose range of 0.03–3 μmol/kg) leads to significant dose-dependent decreases of mean arterial pressure (MAP), whereas only the highest dose of SULFI/NO (3 μmol/kg) decreases MAP ($n = 3$ per group; RM two-way ANOVA, $P < 0.01$ for treatment and doses). *Sidak's $P < 0.01$; **Sidak's $P < 0.01$. At comparable doses, NaHS (1.8 and 3.5 μmol/kg) does not significantly affect blood pressure. (*B*) The $SSNO^-$ mix (dose range of 0.03–3 μmol/kg) does not affect cardiac function, whereas higher doses of SULFI/NO (3 μmol/kg) increase cardiac contractility, which was assessed by changes in velocity time index (VTI), cardiac output (CO), and peak flow velocity (PFV; $n = 3$ per group; RM two-way ANOVA, $P < 0.01$) (*SI Appendix*, Tables S3–S5). (*Inset*) NaHS (dose range of 1.8–18 μmol/kg) does not affect VTI. $^{\#}t$ Test $P < 0.05$. (*C*) Continuous infusion of the $SSNO^-$ mix (0.16 μmol/kg per min) significantly decreases MAP compared with baseline, and its effect is more rapid in onset compared with that of NaHS (2.9 μmol/kg per min). Infusion of SULFI/NO equimolar to $SSNO^-$ (0.16 μmol/kg per min) has only a mild, nonsignificant effect on blood pressure compared with vehicle control (*SI Appendix*, Table S6) ($n = 3$ per group; RM two-way ANOVA treatments, $P = 0.00471$). *Sidak's $P < 0.05$ vs. baseline; **Sidak's $P < 0.01$ vs. baseline; $^{\S}P < 0.01$ vs. NaHS. (*D*) Continuous infusion of $SSNO^-$ mix (0.16 μmol/kg per minute) increases cardiac contractility (VTI, CO, and PFV) after 60 and 120 min of infusion ($n = 3$), whereas NaHS (2.9 μmol/kg per minute; shown in *Inset*) does not have any effect. SULFI/NO markedly increases cardiac contractility already 10 min after the start of infusion ($n = 3$; RM two-way ANOVA, $P < 0.0001$). *Sidak's $P < 0.05$ vs. vehicle; **Sidak's $P < 0.01$ vs. vehicle; ***Sidak's $P < 0.001$ vs. vehicle; $^{\#}$two-way ANOVA SULFI/NO vs. SSNO, $P = 0.0046$. RM, repeated measurements.

Chemistry of the Reaction Between Sulfide and NO. A reaction between NO and sulfide was first described almost a century ago (refs. 11, 41, and 42 and references therein). The main products of this reaction were found to be nitrogen oxides (NO, N_2, and N_2O; measured in the gas phase) and sulfur-bearing anionic solutes, including $SSNO^-$ and HS_n^- (9, 10). These are essentially the same products that were later described in the reaction of RSNOs with sulfide (26, 27) without an understanding of detailed reaction mechanisms. SULFI/NO formation was described by others (9, 42–44), although only in one case (9) in the context of sulfide. We here describe a singular process that occurs under biologically relevant conditions and characterizes the interaction between NO or RSNOs and sulfide. This process comprises cascading chemical reactions, giving rise to formation of three main anionic products ($SSNO^-$, HS_n^-, and SULFI/NO) accompanied by the release of H_2S, NO, HNO and N_2O, NO_2^-, and NO_3^- as well as sulfoxy species, such as SO_4^{2-}, $S_2O_3^{2-}$, SO_4^{2-}, and polythionates. Identification of the S/N-hybrid species was achieved using a variety of techniques, including ESI-HRMS combined with stable isotope labeling.

On the basis of the products identified here and elsewhere (9–11, 41–44), it is possible to propose a unified reaction scheme (summarized in Fig. 6 and explained in more detail in *SI Appendix*). Although it is not difficult to rationalize how HS^- (or the even stronger nucleophile HSS^-) reacts with RSNOs to form $HSSNO/SSNO^-$ (13, 26), formation of the latter from NO and sulfide is less straightforward. The simplest assumption is that, under aerobic conditions, sulfide is nitrosated by NO autoxidation products (NO_2 and N_2O_3), initially leading to transient formation of HSNO with subsequent attack by another HSS^- to form $SSNO^-$ (reactions 1–3 in Fig. 6). However, our results with DEA/NO and aqueous NO solution clearly show that the reaction also occurs (to about the same extent, although with slower kinetics) under strict exclusion of oxygen, showing that there must be another route to formation of $SSNO^-$. A second possibility involves formation of thiyl and perthiyl radicals ($S^{\bullet-}$ and $SS^{\bullet-}$) (reactions 4 and 6 in Fig. 6), which can trap NO directly to form SNO^- and $SSNO^-$ (reactions 5 and 7 in Fig. 6). Formation of $S^{\bullet-}$ can take place by one-electron oxidation of sulfide after (*i*) reaction with O_2 (rather inefficient) or (*ii*) transition metal catalysis (reaction 4 in Fig. 6); alternatively, $S^{\bullet-}$ and $SS^{\bullet-}$ might be also formed by HSNO or $SSNO^-$ hemolysis after these species are formed through other routes (reactions 16 and 17 in Fig. 6) or by homolytic cleavage of long-chain HS_n^- (e.g., reaction 20 in Fig. 6), although the driving force for HS_n^- decomposition to anion radicals is unclear. Nevertheless, as shown here and according to reactions 3 and 7 in Fig. 6, HS_n^- (or its radical intermediates) are substrates of $SSNO^-$ synthesis. Previous work has shown that relatively pure solutions of $SSNO^-$ in acetone can be obtained by passing NO through solutions of inorganic/organic polysulfide as evidenced by ^{15}N NMR (10) and X-ray crystallographic studies (35).

In addition to HS_n^- and $SSNO^-$, we identified SULFI/NO (36, 42, 45) as another important product of the reaction of sulfide

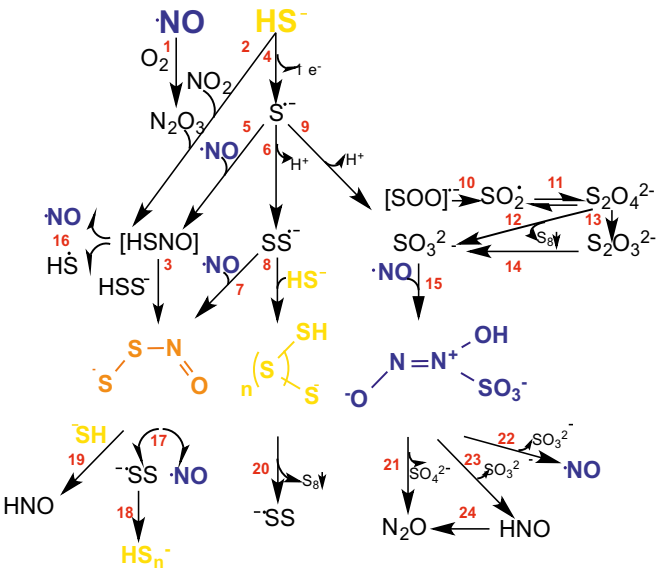

Fig. 6. Chemical reaction cascade depicting pathways of formation and decomposition of $SSNO^-$, HS_n^-, and SULFI/NO. Reactions are not mass balanced; numbers in red refer to the reactions described in the text. A more detailed discussion of the reaction mechanisms can be found in *SI Appendix*. The pK_a values of HS• and HSS• are unknown but likely exceed 7; therefore, at pH 7.4, these species are radical anions.

with either NO or RSNOs. We also found traces of $[ONN(OH)S_2]^-$ as predicted by Seel and Wagner (9). A likely precursor of SULFI/NO formation from NO and sulfide is sulfite (SO_3^{2-}) (reaction 15 in Fig. 6), which was suggested by others not only for the reaction of sulfide with NO under anoxia (9, 11) but also, as a result of the reaction of NO with thiosulfate ($S_2O_3^{2-}$) and $S_2O_4^{2-}$ (11). In aqueous solution, sulfite may be formed by reaction of sulfide with O_2 by formation of $SO_2^{\bullet-}$ and $S_2O_4^{2-}$ (46) (reactions 9–12 in Fig. 6), formation of $S_2O_3^{2-}$ originating from radical reactions (by $SO_2^{\bullet-}$) (reactions 9–13 in Fig. 6), or hydrolysis of HONS (a product of HSNO isomerization) as proposed by Goehring and Messner (23). Because no SO_3^{2-} was detected by ESI-HRMS in freshly prepared sulfide stock solutions and sulfide autoxidation is a rather slow process, production of $S_2O_3^{2-}$ through radical reactions and/or HONS/HSNO seems to be the most plausible route.

The main pathways of decomposition of the key reaction products are as follows (Fig. 6): $SSNO^-$ can undergo homolytic cleavage to $SS^{\bullet-}$ and $NO^{\bullet}$ (reaction 17 in Fig. 6) or secondary reaction with sulfide (reaction 19 in Fig. 6), which according to Seel and Wagner (10), is not efficient, because they observed an equilibrium between the trisulfide radical and NO in sealed systems, making $SSNO^-$ rather stable in excess sulfide (10). HS_n^- may undergo polymerization reaction to *cyclo*-octasulfur (S_8) and/or homolytic cleavage to form sulfur radicals (see above) (reaction 20 in Fig. 6); in the presence of strong nucleophiles (such as DTT), polysulfides undergo decomposition to sulfide, a property that we here used to distinguish them from $SSNO^-$. Decomposition of SULFI/NO leads to formation of SO_3^{2-}, SO_4^{2-}, and N_2O (reactions 21–24 in Fig. 6). Although it has been proposed that this process occurs directly (reaction 21 in Fig. 6) (36), the formation of both HNO and NO from hyponitrite ($ON{:}NOH^-$) has been proposed by others (reactions 22 and 23 in Fig. 6) (42–44). Indeed, evidence for trace levels of $ON{:}NOH^-$ in incubation mixtures of both SULFI/NO and DEA/NO (but not SNAP) with sulfide was observed by us using ESI-HRMS (*SI Appendix*, Fig. S6). Authentic sodium hyponitrite was found to release NO at pH 7.4, which was markedly enhanced in the presence of the one-electron oxidant ferricyanide, consistent with the generation of both NO and HNO (*SI Appendix*, Fig. S7) (47). $ON = NOH^-$ is known to decompose to N_2O and water after protonation to hyponitrous acid ($HNO = NOH$).

Parallel reactions lead to formation of HNO, superoxide ($O_2^{\bullet-}$), and peroxynitrite ($ONOO^-$). These reactions include reduction of NO to HNO by HS_n^-, very potent radical reducing/trapping agents (48), and oxidation of O_2 or NO to $O_2^{\bullet-}$ or $ONOO^-$, respectively, by reaction with sulfur-centered radicals. Moreover, $ONOO^-$ may also be formed after reaction of HNO with O_2; these possibilities are consistent with the rapid consumption of O_2 in the reaction (26). Finally, HNO can be reduced by sulfide to hydroxylamine (NH_2OH), and nitrosation of NH_2OH results in formation of N_2O (12).

Chemical Biology of $SSNO^-$, Polysulfides, and SULFI/NO. The fact that the above reactions occur in aqueous buffers at pH 7.4 does not necessarily mean that they are relevant to biology. What follows is a discussion about whether the chemical properties of $SSNO^-$, HS_n^-, and SULFI/NO are compatible with the biological situation, such that these molecules can conceivably play a role in cell signaling and/or interorgan transport of NO and sulfur equivalents.

$SSNO^-$ is a bioactive product with unusual properties: it is stable in the presence of millimolar concentrations of other thiols [sulfide, (homo)cysteine, and glutathione], carries and releases NO, and generates HS_n^- on decomposition. These properties suggest it would be sufficiently stable if formed in the cellular milieu to participate in and contribute to NO/sulfur trafficking (13, 26). These properties clearly distinguish $SSNO^-$ [and its protonated form perthionitrous acid (HSSNO)] from SNO^-/HSNO (13, 26). $SSNO^-$ is considerably more stable than HSNO, because the latter undergoes rapid isomerization, hemolysis, and polymerization (13). Moreover, HSNO can undergo rapid nucleophilic attack by HS^- to give HSSH and NO^- (reacting with O_2 to form $ONOO^-$), whereas the electron density of the proximate sulfur in HSSNO is increased, making it less susceptible to nucleophilic attack by HS^- and reaction with metals (e.g., Cu^+). Of note, $SSNO^-$ exerts faster and more prominent vasorelaxation compared with its precursor and the prototypical nitrosothiol, GSNO (28), indicative of the ease with which it can cross cell membranes and release NO.

HS_n^- (and their organic counterparts) are not resistant to reducing conditions and high concentrations of thiols, and contain a highly reactive sulfane sulfur (49, 50). Polysulfides were proposed to be the bioactive molecules responsible for "H_2S signaling" and much of the physiological action of sulfide in cells (31, 48, 49). In addition, they are believed to act as storage or buffer molecules of H_2S, with surprisingly high concentrations measured in murine organs/tissues (31). Although their chemistry is reasonably well-understood (48, 50), biosynthetic pathways, speciation, and modes of action in the biological environment are still poorly defined. The results of this study suggest that HS_n^- are also intermediates in $SSNO^-$ formation, possibly through homolytic cleavage to radical species and subsequent reaction with NO. Thus, in addition to their enzymatic formation (33) and as a consequence of sulfide oxidation (50), reaction of sulfide with NO or nitrosothiols may provide another pathway to their production in cells and tissues.

SULFI/NO arises as a result of the trapping of two molecules of NO by sulfite (36, 39, 45), a reaction originally described by Davy in 1802. The substance is also known as dinitrososulfite (51), "Pelouze's salt," or "Stickoxid-sulfite" in the German literature (ref. 42 and references therein). Its structural characteristics were revealed about 100 years later using IR spectroscopy (51) and confirmed by alternative chemical synthesis (42). It belongs to a class of compounds now better known as diazeniumdiolates or NONOates (36). Consistent with earlier reports, we found that SULFI/NO has similar stability characteristics as other diazeniumdiolates (36, 39, 45, 52), cogenerates small amounts of NO and HNO at pH 7.4, and releases N_2O in high yields. An unexpected yet inevitable consequence of its formation in the NO/sulfide system is that SULFI/NO is formed (in addition to $SSNO^-$ and HS_n^-) whenever NO and sulfide are cogenerated; sulfite generation, thus, results in the scavenging of NO, with consecutive redox conversion of part of this NO to HNO. This unexpected chemistry propels this molecule, a rather ineffective NO donor and vasodilator (39), from the chemists' curiosity cabinet to the forefront of biological signaling. Proof for its formation in living organisms will require development of sufficiently sensitive analytical techniques to monitor its formation and fate, but the likelihood of its existence in real life is intriguing.

Taken together, the chemical biology of the three major products of the NO/sulfide reaction system ranges from sulfane sulfur signaling ($SSNO^-$ and polysulfides) through NO release ($SSNO^-$ and SULFI/NO) and NO scavenging (sulfite) to nitroxyl signaling (SULFI/NO), with generation of several other sulfoxy and nitrogen oxide metabolites with known and distinct bioactivity profiles.

Bioactivity of $SSNO^-$, Polysulfides, and SULFI/NO. The different chemical properties attributed to $SSNO^-$, HS_n^-, and SULFI/NO translate into distinct bioactivities in vitro and in vivo. As shown here and elsewhere (26, 28), the $SSNO^-$ mixture (produced from either DEA/NO or SNAP with excess sulfide) contains high concentrations of $SSNO^-$ and HS_n^-, releases NO, is a potent sGC stimulator in the NO reporter cell line RFL-6 (26), induces NO-mediated vasorelaxation in isolated aortic tissue (28), and significantly decreases blood pressure in a dose-dependent fashion with minor effects on cardiac function. No changes in any of these

parameters were observed by equivalent concentrations/doses of sulfide alone. Control experiments with HS_n^- suggest that NO-independent effects on blood pressure may be, in part, dependent on the presence of HS_n^- in the mixture but independent of SULFI/NO. Only rather high (>100 μM) concentrations of SULFI/NO (but not HS_n^- or S_8) activated sGC in RFL-6 cells; these effects were fully inhibited by addition of cysteine (HNO scavenger) or cPTIO (NO scavenger) and potentiated by high but not low concentrations of SOD converting HNO into NO (40, 47). These results are consistent with its predicted chemical biology as a relatively weak combined NO/HNO donor. However, SULFI/NO dramatically increased cardiac output, stroke volume (measured as the velocity–time integral), and peak blood flow velocity while affecting blood pressure and heart rate only minimally (except at high doses), indicative of its propensity to enhance cardiac contractility, an effect likely mediated by the generation of HNO.

In aggregate, these results show that $SSNO^-$ is a potent NO donor mainly affecting peripheral vascular resistance, whereas SULFI/NO is a rather weak NO/HNO donor that affects the tone of resistant vessels to a lesser degree but potently increases cardiac contractility. Although $SSNO^-$ is a major reaction product in NO/sulfide-containing mixtures, one important limitation worth highlighting is that, at present, the biological properties of $SSNO^-$ cannot be studied separately from SULFI/NO, sulfide/HS_n^-, and other reaction products formed. Moreover, the rich possibilities for interaction between defined constituents of the reaction mixture may profoundly affect the chemistry and bioactivity of individual species in the biological setting. For example, by incubating SULFI/NO with sulfide, we observed formation of HS_n^-. Nevertheless, our results clearly show that NO and sulfide react with each other; wherever cogenerated, their reaction leads to formation of molecules with bioactivities distinct from the parent compounds, resulting in quenching, redox switching, or release/transport of NO bioactivity.

What Is the Significance of These Reactions for the Sulfide/NO Cross-Talk in Vivo? Our in vivo data suggest that the well-known scavenging and potentiating effects of sulfide on NO bioavailability in vitro (19, 26) and vascular function in vivo (18) correlate with changes in NO bioavailability. In the first 30 min of sulfide infusion, we observed a drop in NO-heme levels within erythrocytes, whereas no significant changes in hemodynamic parameters were apparent; after 1 h of infusion, allowing sulfide accumulation (53), increases in systemic NO bioavailability (i.e., levels of NO-heme and nitroso species) were accompanied by corresponding decreases in blood pressure. These results are consistent with NO scavenging effects after the addition of low concentrations of sulfide as detected by chemiluminescence as well as in RFL-6 cells and other cell types as shown here and elsewhere (19, 26). A decrease in circulating nitrite and RXNO levels was observed in mice lacking the sulfide-producing enzyme cystathionine-γ-lyase (54); however, this result was ascribed to effects of sulfide on endothelial NO synthase activity. However, effects of sulfide on NOS activity in this context are unlikely, considering that the effects of NOS inhibition on circulating and tissue NO metabolites are less rapid than the functional effects of sulfide observed.

The molecular basis that accounts for scavenging and potentiation of NO bioactivity by sulfide is presently unclear. These effects have been ascribed to formation of a nitrosothiol (19), mutual regulation of enzymatic pathways (e.g., endothelial nitric oxide synthase) (54), modulation of PDE (55), and/or targeting of different vascular beds (56). An interesting alternative possibility that would seem to warrant additional investigation is that sulfide might modulate redox-dependent control mechanisms, regulating vascular tone independently of sGC, such as, for example, through modulation of the redox state of PKGIα by oxidative modification of Cys42 (57). This notion would be consistent with the observation that the vasoactive effects of sulfide are partially attenuated in aortic rings from $PKG1^{-/-}$ mice (58). It is also possible that the effects of sulfide are caused by a chemical interaction by (*i*) formation of *S*-nitroso species (such as $SSNO^-$) acting as a temporary "NO sink" that is able to release NO farther downstream; (*ii*) formation of reactive sulfoxy intermediates, such as $SO_2^{\bullet}$ or SO_3^{2-}, forming NO complexes with a low NO-releasing potential, such as SULFI/NO; or (*iii*) formation of thiyl radicals (such as $HS^{\bullet}$ and $HSS^{\bullet}$) by reaction with O_2. The latter is consistent with our earlier observation that O_2 is consumed in the reaction (26) and would lead to formation of $O_2^{\bullet-}$ and NO scavenging as a result of peroxynitrite ($ONOO^-$) generation. Both formation of sulfoxy species and O_2 consumption are interesting observations not only from a chemical perspective but also, because mitochondrial sulfide oxidation has been linked to physiological oxygen sensing (59) and $SO_3^{2-}/S_2O_3^{2-}$ are reduced to HS^- in mitochondria (59). Final proof of the relevance of these chemical pathways in biological systems will require the detection of these S/N-hybrid molecules, as shown for RSSH (31), in cells and tissues. Similarly important in this context will be a careful kinetic assessment of the reaction yields depending on the rates of formation of NO and sulfide in subcellular compartments. Because such evaluation does not seem to be possible using current analytical techniques, the development of a novel quantitative/nondestructive methodology for in situ detection and monitoring of those molecules in biological matrices merits additional investigation.

Summary and Conclusions

Understanding the basic chemical principles that govern the interactions between sulfide and NO is essential to interpreting and untangling the conflicting observations about mutual potentiating and inhibitory effects presented in the literature. Here, we show that the reaction between sulfide and NO leads to formation of different bioactive intermediates (including $SSNO^-$, HS_n^-, and SULFI/NO) capable of scavenging, transporting, and releasing NO and generating its redox congeners HNO, N_2O, and sulfane sulfur. Each of these products is characterized by a specific biological chemistry and the potential to release other bioactive mediators. With the exception of SULFI/NO, the bioactivity of HS_n^- and $SSNO^-$ cannot be studied in isolation and/or the absence of sulfide at present. Nevertheless, by careful comparison of the effects of different mixtures of these components, we conclude that $SSNO^-$ is a potent NO donor, resistant to the reducing milieu of the cell, and able to release both NO and HS_n^-. SULFI/NO is a weak combined NO/HNO donor and generator of N_2O with potent effects on the heart. Formation of its precursor sulfite and generation of sulfur and/or oxygen-centered free radicals may be responsible for the scavenging effects of sulfide on NO bioavailability. Polysulfides may be formed secondary to the reaction of sulfide with NO, either through HSNO or after decomposition of $SSNO^-$, and may also contribute to NO scavenging and sulfane sulfur signaling. Although admittedly even more speculative, some of this chemistry may also help explain the "Janus-like" face of NO (i.e., the often opposing biological effects of low and high concentrations observed in physiology and pathophysiology). In any case, our findings open the door to a new field of research with $SSNO^-$, HS_n^-, and SULFI/NO taking center stage as biologically important mediators of both the NO and H_2S transduction pathways. Although the cardiovascular system has been the target of our current efforts, this chemical interaction is likely to be relevant to cell/organelle signaling in many other systems, including neuronal and immune cells, plants, and prokaryotes as exemplified by the recent work on antibiotic resistance by bacterial NO/H_2S production (17). Beyond its likely significance for biology and redox signaling, our results may also be of significance for environmental chemistry pertinent to marine and atmospheric processes.

Materials and Methods

A complete and more detailed description of the materials and methods used is provided in *SI Appendix*.

Preparation of Stock Solutions of NO Donors, SULFI/NO, Sulfide, and SSNO$^-$. The potassium salt of SULFI/NO was synthesized as described by Drago and coworkers (60). Stock solutions of DEA/NO, DETA/NO, Sper/NO, SULFI/NO, and Angeli's salt were freshly prepared in 0.01 M NaOH, diluted in PBS, and used immediately. Aqueous stock solutions of ^{15}N-SNAP or SNAP were freshly prepared either from crystalline material or through reaction of the reduced thiols with acidified nitrite (61) and used immediately. Saturated aqueous solutions of NO were prepared and kept sealed under argon as described (62). Sulfide stock solutions for in vitro use (e.g., in cell culture experiments) were prepared fresh before each experiment by dissolving anhydrous Na_2S in a strong buffer (1 M Tris or phosphate buffer, pH 7.4) and diluting further in 100 mM Tris or 50–100 mM phosphate buffer (pH 7.4) immediately before use. For in vivo experiments, NaHS stock solutions were prepared in 300 mM phosphate buffer (pH 7.4), diluted in PBS (pH 7.4), and used immediately (10 mg/mL = 176.7 mM NaHS; anhydrous; Alfa Aesar). Although all precautions were undertaken to avoid the presence of products of sulfide oxidation in the stock solutions, including polysulfide, their presence in stock solutions cannot be excluded. Stock solutions of SSNO$^-$ were prepared by reacting 1 mM SNAP with 10 mM Na_2S in 1 mL PBS or 100 mM Tris (pH 7.4). After 10 min of incubation at RT in the dark, excess sulfide was removed by 10 min of bubbling with N_2. The (theoretical) maximal yield of SSNO$^-$ under these conditions is 1 mM, corresponding to the concentration of added nitrosothiol (*SI Appendix*, Fig. S5 shows the experimental determination of reaction yield). For in vivo experiments, the SSNO$^-$ solution was prepared in phosphate buffer (pH 7.4) and further diluted in PBS to obtain the doses indicated for bolus i.v. injection or used directly for continuous i.v. infusion.

Effects of Sulfide, SSNO$^-$, SULFI/NO, and Polysulfides on Cardiovascular Hemodynamics and Circulating NO Metabolites. All animal experiments were approved either by the Institutional Animal Care and Use Committee (IACUC) at Boston University School of Medicine (Boston, MA), the University College London (London, UK), or the State Veterinary and Food Administration of the Slovak Republic. All procedures were conducted in male Wistar rats (250–300 g; Charles River) anesthetized with 2% (vol/vol) isofluorane. Briefly, the effects of bolus i.v. injection of increasing doses of NaHS (1.8–18 μmol/kg), SSNO$^-$ mix (0.03–3 μmol/kg), or SULFI/NO (0.03–3 μmol/kg) in PBS or vehicle alone on cardiovascular hemodynamics and circulating NO stores were assessed at 10-min intervals. Continuous i.v. infusions of NaHS (2.8 μmol/kg per min in PBS), SSNO$^-$ (0.16 μmol/kg per min in PBS), SULFI/NO (0.16 μmol/kg per min in 25 mM NaOH, 0.9% NaCl), or the respective vehicle (PBS or 25 mM NaOH, 0.9% NaCl) were performed at a rate of 10 mL/kg per hour through the right internal jugular venous line. Continuous monitoring of mean arterial pressure and blood withdrawal was from an indwelling arterial (left common carotid) line. Blood was taken at defined time points (0, 5, 10, 30, 60, and 120 min) and processed as previously described for determination of NO metabolite concentrations by ion chromatography and gas-phase chemiluminescence (63). Cardiac function and heart rate were assessed by transthoracic echocardiography using a Vivid 7 (GE Healthcare) as described (64). A rectal probe (TES Electrical Electronic Corp.) inserted 3 cm in depth was used to measure core temperature.

Effects of Sulfide on NO Bioactivity and Detection of NO Release and Bioactivity of SSNO$^-$ and SULFI/NO in RFL-6 Cells. The effects of sulfide on Sper/NO-mediated activation of sGC were determined by measuring changes in intracellular cGMP levels in RFL-6 cells pretreated with a phosphodiesterase inhibitor (500 μM 3-isobutyl-1-metylxanthine), and then treated with 100 μM Sper/NO for 20 min in the absence or presence of increasing concentrations of sulfide (1, 10, and 100 μM Na_2S in 100 mM Tris, pH 7.4) as described (26). The NO/HNO bioactivities of SSNO$^-$ and SULFI/NO were compared by treating 3-isobutyl-1-metylxanthine–pretreated cells (as above) with either 20 μM SSNO$^-$ mix or 1, 10, and 100 μM SULFI/NO for 20 min. To test for HNO bioactivity, ∼7,000 U/mL SOD was added directly to the treatment medium 5 min before addition of SSNO$^-$ or SULFI/NO to enable extracellular conversion of HNO into NO. In select experiments, an NO scavenger (cPTIO; 500 μM) or a nitroxyl scavenger (1 mM Cys) was added 5 min before the other treatments. Intracellular cGMP levels and protein content were assessed in cell lysates using a DetectXHigh Sensitivity Direct cGMP Kit (Arbor Assay; Biotrend) and Roti$^-$Nanoquant (Carl Roth GmbH + Co. KG), respectively. Data were normalized for protein content and expressed as folds of untreated control to further account for the variability in sGC expression levels of RFL-6 cells of different batches and passages.

Detection of SSNO$^-$, SULFI/NO, and Polysulfides by UV-Visible Spectroscopy and HRMS. The spectroscopic and kinetic behaviors of the reaction between sulfide (1–10 mM) and NO (0.2 mM), DEA/NO (0.5–3 mM), or SNAP (0.2–1 mM) were followed by rapid scanning UV-visible spectroscopy as described (26). The identification of the reaction products was achieved by HRMS using an LTQ Orbitrap XL Hybrid Linear Ion Trap–Orbitrap Mass Spectrometer equipped with a nanospray ionization source controlled with XCalibur 2.1 (Thermo-Fisher). Samples for HRMS were mixed in 50 mM $(NH4)_3PO4$ buffer (pH 7.4), mixed 1:5 with acetonitrile through a T piece, and infused directly into the ion source. Spectra were acquired in negative ion mode with a spray voltage of 5 kV and nitrogen as sheath gas; capillary temperature was set at 300 °C, and capillary voltage was set at 20 V. Instrument parameters, especially those of the ion optics, were optimized for each individual compound of interest. Elemental analysis based on accurate mass and a priori information of likely elemental composition and isotope distribution simulation were performed using XCalibur 2.1.

Time-Resolved Measurement of NO Trapping and NO Release by Chemiluminescence. Trapping by Na_2S (33.4 and 334 μM) of NO released from DETA/NO (33.4 μM) and NO released from SSNO-containing mixtures (1–100 μM) after 1 min of incubation of SNAP and sulfide, SULFI/NO (100 μM), and SNAP (10 μM) alone was monitored by gas-phase chemiluminescence (CLD 77:00 AM sp; Ecophysics) using a custom-designed, water-jacketed glass reaction chamber (15 mL total volume) continuously bubbled with nitrogen or air as described elsewhere (26).

Detection of HNO Release by P-Rhod Fluorescence. HNO release form SSNO$^-$ (0.001–1 mM) and SULFI/NO (0.001–1 mM) was determined by using the HNO-specific probe P-Rhod (stock 50 mM in DMSO) (38). Briefly, N_2 gassed SSNO$^-$ mix (1 mM SNAP, 10 mM Na_2S), SULFI/NO (1 mM), or Angeli's salt (1 mM; all in 100 mM Tris·HCl, pH 7.4) were serially diluted in Tris·HCl in a dark 96-well plate. Buffer alone was used as blank. P-Rhod (5 μM) was added to all wells using an automatic injector, and fluorescence changes were recorded at excitation of 480 nm and emission of 520 nm using a multimode plate reader (FLUOstar Omega; BMG Labtech). Data are reported as percentage increases compared with background signal (blank).

Nitrous Oxide Quantification by GC. Stock solutions of DEA/NO (10–200 μM) were mixed with Na_2S (100 μM) in phosphate buffer, injected into a 10-mL round-bottom flask sealed with a rubber septum, flushed with either N_2 or air, and incubated at 37 °C, and at the indicated time points, headspace aliquots (100 μL) were injected through a gas-tight syringe onto a 7890 A Agilent Gas Chromatograph equipped with a microelectron capture detector and a 30 × 0.32-m (25 μm) HP-MOLSIV Capillary Column. The retention time of nitrous oxide was 3.4 min, and yields were calculated based on a standard curve for nitrous oxide (Matheson Tri-Gas). Angeli's salt was used as the reference compound for HNO. In some experiments, 200 μM triarylphosphine was used to trap HNO.

Statistical Analysis. Data are reported as means ± SEMs. ANOVA followed by an appropriate posthoc multiple comparison test was used to test for statistical significance.

ACKNOWLEDGMENTS. We thank Peter B. O'Connor, J. Derek Woollins, Catherine Botting, and many other colleagues for insightful discussions and critical reading of our paper. The authors acknowledge support from the German Research Council (DFG CO 1305/2-1 to M.M.C.K., SFB1116 TP B06 to M.M.C.K. and M.K.); the European Cooperation in Science and Technology (COST) action BM1005 (European Network on Gasotransmitters) allowing M.G. to conduct experiments in P.N.'s laboratory; the Slovak Research & Development Agency (APVV-0074-11 to K.O.), the Marie Curie International Reintegration Grant (PIRG08-GA-2010-277006 to P.N.), the Hungarian National Science Foundation (OTKA; Grant K 109843 to P.N.), and the János Bolyai Research Scholarship of the Hungarian Academy of Sciences (to P.N.); the Susanne-Bunnenberg-Stiftung of the Düsseldorf Heart Center (to M.K.); the UK Medical Research Council (G1001536 to M.F.) and the Faculty of Medicine, University of Southampton (to M.F.).

1. Urey HC (1952) On the early chemical history of the Earth and the origin of life. *Proc Natl Acad Sci USA* 38(4):351–363.

2. Feelisch M, Martin JF (1995) The early role of nitric oxide in evolution. *Trends Ecol Evol* 10(12):496–499.

3. Olson KR (2012) Mitochondrial adaptations to utilize hydrogen sulfide for energy and signaling. *J Comp Physiol B* 182(7):881–897.
4. Parker ET, et al. (2011) Primordial synthesis of amines and amino acids in a 1958 Miller H_2S-rich spark discharge experiment. *Proc Natl Acad Sci USA* 108(14):5526–5531.
5. Patel BH, Percivalle C, Ritson DJ, Duffy CD, Sutherland JD (2015) Common origins of RNA, protein and lipid precursors in a cyanosulfidic protometabolism. *Nat Chem* 7(4):301–307.
6. Goubern M, Andriamihaja M, Nübel T, Blachier F, Bouillaud F (2007) Sulfide, the first inorganic substrate for human cells. *FASEB J* 21(8):1699–1706.
7. Danovaro R, et al. (2010) The first metazoa living in permanently anoxic conditions. *BMC Biol* 8:30.
8. Searcy DG, Lee SH (1998) Sulfur reduction by human erythrocytes. *J Exp Zool* 282(3): 310–322.
9. Seel F, Wagner M (1988) Reaction of sulfides with nitrogen monoxide in aqueous solution. *Z Anorg Allg Chem* 558(3):189–192.
10. Seel F, Wagner M (1985) The reaction of polysulfides with nitrogen monoxide in non-acqueous solvents nitrosodisulfides. *Z Naturforsch C* 40(6):762–764.
11. Kurtenacker A, Löschner H (1938) Über die Einwirkung von Stickoxyd auf Thiosulfat und Sulfid. *Z Anorg Allg Chem* 238(4):335–349.
12. Bagster LS (1928) The reaction between nitrous acid and hydrogen sulphide. *J Chem Soc,* 2631–2643.
13. Cortese-Krott MM, Fernandez BO, Kelm M, Butler AR, Feelisch M (2015) On the chemical biology of the nitrite/sulfide interaction. *Nitric Oxide* 46(0):14–24.
14. Bruce King S (2013) Potential biological chemistry of hydrogen sulfide (H_2S) with the nitrogen oxides. *Free Radic Biol Med* 55:1–7.
15. Li Q, Lancaster JR (2013) Chemical foundations of hydrogen sulfide biology. *Nitric Oxide* 35:21–34.
16. Kimura H (2014) The physiological role of hydrogen sulfide and beyond. *Nitric Oxide* 41:4–10.
17. Shatalin K, Shatalina E, Mironov A, Nudler E (2011) H_2S: A universal defense against antibiotics in bacteria. *Science* 334(6058):986–990.
18. Ali MY, et al. (2006) Regulation of vascular nitric oxide in vitro and in vivo; a new role for endogenous hydrogen sulphide? *Br J Pharmacol* 149(6):625–634.
19. Whiteman M, et al. (2006) Evidence for the formation of a novel nitrosothiol from the gaseous mediators nitric oxide and hydrogen sulphide. *Biochem Biophys Res Commun* 343(1):303–310.
20. Yong QC, et al. (2011) Regulation of heart function by endogenous gaseous mediators-crosstalk between nitric oxide and hydrogen sulfide. *Antioxid Redox Signal* 14(11):2081–2091.
21. Filipovic MR, et al. (2012) Chemical characterization of the smallest S-nitrosothiol, HSNO; cellular cross-talk of H_2S and S-nitrosothiols. *J Am Chem Soc* 134(29):12016–12027.
22. Williams DLH (2004) Nitrosation *Reactions and the Chemistry of Nitric Oxide* (Elsevier, Amsterdam).
23. Goehring M, Messner J (1952) Zur Kenntnis der schwefligen Säure. III. Das Sulfinimid und seine Isomeren. *Z Anorg Allg Chem* 268(1-2):47–56.
24. Müller RP, Nonella M, Huber JR (1984) Spectroscopic investigation of HSNO in a low temperature matrix. UV, VIS, and IR-induced isomerisations. *Chem Phys* 87:351–361.
25. Nonella M, Huber JR, Ha TK (1987) Photolytic preparation and isomerization of thionyl imide, thiocyanic acid, thionitrous acid, and nitrogen hydroxide sulfide in an argon matrix: An experimental and theoretical study. *J Phys Chem* 91(20):5203–5209.
26. Cortese-Krott MM, et al. (2014) Nitrosopersulfide ($SSNO^{(-)}$) accounts for sustained NO bioactivity of S-nitrosothiols following reaction with sulfide. *Redox Biol* 2:234–244.
27. Munro AP, Williams DLH (2000) Reactivity of sulfur nucleophiles towards S-nitrosothiols. *J Chem Soc Perkin 2* 1(9):1794–1797.
28. Berenyiova A, et al. (2015) The reaction products of sulfide and S-nitrosoglutathione are potent vasorelaxants. *Nitric Oxide* 46:123–130.
29. Kimura Y, et al. (2013) Polysulfides are possible H2S-derived signaling molecules in rat brain. *FASEB J* 27(6):2451–2457.
30. Fukuto JM, et al. (2012) Small molecule signaling agents: The integrated chemistry and biochemistry of nitrogen oxides, oxides of carbon, dioxygen, hydrogen sulfide, and their derived species. *Chem Res Toxicol* 25(4):769–793.
31. Ida T, et al. (2014) Reactive cysteine persulfides and S-polythiolation regulate oxidative stress and redox signaling. *Proc Natl Acad Sci USA* 111(21):7606–7611.
32. Nagasaka Y, et al. (2008) Brief periods of nitric oxide inhalation protect against myocardial ischemia-reperfusion injury. *Anesthesiology* 109(4):675–682.
33. Vitvitsky V, Kabil O, Banerjee R (2012) High turnover rates for hydrogen sulfide allow for rapid regulation of its tissue concentrations. *Antioxid Redox Signal* 17(1):22–31.
34. Blackstone E, Morrison M, Roth MB (2005) H_2S induces a suspended animation-like state in mice. *Science* 308(5721):518.
35. Seel F, et al. (1985) PNP-Perthionitrit und PNP-Monothionitrit. *Z Naturforsch B* 40(12): 1607–1617.
36. Hrabie JA, Keefer LK (2002) Chemistry of the nitric oxide-releasing diazeniumdiolate ("nitrosohydroxylamine") functional group and its oxygen-substituted derivatives. *Chem Rev* 102(4):1135–1154.
37. Reisz JA, Zink CN, King SB (2011) Rapid and selective nitroxyl (HNO) trapping by phosphines: Kinetics and new aqueous ligations for HNO detection and quantitation. *J Am Chem Soc* 133(30):11675–11685.
38. Kawai K, et al. (2013) A reductant-resistant and metal-free fluorescent probe for nitroxyl applicable to living cells. *J Am Chem Soc* 135(34):12690–12696.
39. De Witt BJ, Marrone JR, Kaye AD, Keefer LK, Kadowitz PJ (2001) Comparison of responses to novel nitric oxide donors in the feline pulmonary vascular bed. *Eur J Pharmacol* 430(2-3):311–315.
40. Murphy ME, Sies H (1991) Reversible conversion of nitroxyl anion to nitric oxide by superoxide dismutase. *Proc Natl Acad Sci USA* 88(23):10860–10864.
41. Dunnicliff H, Mohammad S, Kishen J (1931) The interaction between nitric oxide and hydrogen sulphide in the presence of water. *J Phys Chem* 35(6):1721–1734.
42. Degener E, Seel F (1956) Zur Kenntnis der Salze der Nitrosohydroxylaminsulfonsäure. I. Chemischer Konstitutionsbeweis der Nitrosohydroxylaminsulfonate. *Z Anorg Allg Chem* 285(3-6):129–133.
43. Goehring M, Otto R (1955) Zur Kenntnis der Salze der stickoxyd-schwefligen Säure. *Z Anorg Allg Chem* 280(1-3):143–146.
44. Clusius K, Schumacher H (1957) Reaktionen mit ^{15}N. XXVI. Konstitution und Zerfall von Kaliumnitroso-hydroxylaminsulfonat. *Helv Chim Acta* 40(5):1137–1144.
45. Keefer LK, Nims RW, Davies KM, Wink DA (1996) "NONOates" (1-substituted diazen-1-ium-1,2-diolates) as nitric oxide donors: Convenient nitric oxide dosage forms. *Methods Enzymol* 268:281–293.
46. Steudel R (1996) Mechanism for the formation of elemental sulfur from aqueous sulfide in chemical and microbiological desulfurization processes. *Ind Eng Chem Res* 35(4):1417–1423.
47. Zamora R, Grzesiok A, Weber H, Feelisch M (1995) Oxidative release of nitric oxide accounts for guanylyl cyclase stimulating, vasodilator and anti-platelet activity of Piloty's acid: A comparison with Angeli's salt. *Biochem J* 312(Pt 2):333–339.
48. Ono K, et al. (2014) Redox chemistry and chemical biology of H2S, hydropersulfides, and derived species: Implications of their possible biological activity and utility. *Free Radic Biol Med* 77:82–94.
49. Toohey JI, Cooper AJ (2014) Thiosulfoxide (sulfane) sulfur: New chemistry and new regulatory roles in biology. *Molecules* 19(8):12789–12813.
50. Nagy P (2015) Mechanistic chemical perspective of hydrogen sulfide signaling. *Methods Enzymol* 554:3–29.
51. Cox E, Jeffrey G, Stadler H (1948) Structure of dinitrososulphite ion. *Nature* 162:770.
52. Reglinski J, Armstrong DR, Sealey K, Spicer MD (1999) N-nitrosohydroxylamine-N-sulfonate: A redetermination of its X-ray crystal structure and an analysis of its formation from NO and SO32-using ab initio molecular orbital calculations. *Inorg Chem* 38(4):733–737.
53. Szabó C (2007) Hydrogen sulphide and its therapeutic potential. *Nat Rev Drug Discov* 6(11):917–935.
54. King AL, et al. (2014) Hydrogen sulfide cytoprotective signaling is endothelial nitric oxide synthase-nitric oxide dependent. *Proc Natl Acad Sci USA* 111(8):3182–3187.
55. Bucci M, et al. (2010) Hydrogen sulfide is an endogenous inhibitor of phosphodiesterase activity. *Arterioscler Thromb Vasc Biol* 30(10):1998–2004.
56. Wang R (2011) Signaling pathways for the vascular effects of hydrogen sulfide. *Curr Opin Nephrol Hypertens* 20(2):107–112.
57. Burgoyne JR, et al. (2007) Cysteine redox sensor in PKGIa enables oxidant-induced activation. *Science* 317(5843):1393–1397.
58. Bucci M, et al. (2012) cGMP-dependent protein kinase contributes to hydrogen sulfide-stimulated vasorelaxation. *PLoS One* 7(12):e53319.
59. Olson KR (2013) Hydrogen sulfide as an oxygen sensor. *Clin Chem Lab Med* 51(3): 623–632.
60. Nyholm RS, Rannitt L, Drago RS (1957) N-nitrosohydroxylamine-N-sulfonates. *Inorg Synth* 5:117–122.
61. Stamler J, Feelisch M (1996) Preparation and detection of S-nitrosothiols. *Methods in Nitric Oxide Research*, eds Feelisch M, Stamler J (Wiley, Chichester, United Kingdom), pp 521–539.
62. Feelisch M (1991) The biochemical pathways of nitric oxide formation from nitrovasodilators. *J Cardiovasc Pharmacol* 17(Suppl 3):S25–S33.
63. Feelisch M, et al. (2002) Concomitant S-, N-, and heme-nitros(yl)ation in biological tissues and fluids: Implications for the fate of NO in vivo. *FASEB J* 16(13):1775–1785.
64. Dyson A, et al. (2011) An integrated approach to assessing nitroso-redox balance in systemic inflammation. *Free Radic Biol Med* 51(6):1137–1145.

SUPPORTING INFORMATION (SI) APPENDIX

to

The Key Bioactive Reaction Products of the NO/H_2S Interaction are S/N-Hybrid Species, Polysulfides and Nitroxyl

Miriam M. Cortese-Krott[a], Gunter G.C. Kuhnle[b,1], Alex Dyson[c,1], Bernadette O. Fernandez[d,1], Marian Grman[e], Jenna F. DuMond[f], Mark P Barrow[g], George McLeod[h], Hidehiko Nakagawa[i], Karol Ondrias[e], Péter Nagy[j], S. Bruce King[f], Joseph Saavedra[k], Larry Keefer[l], Mervyn Singer[c], Malte Kelm[a], Anthony R. Butler[m], Martin Feelisch[d,2]

[a]Cardiovascular Research Laboratory, Department of Cardiology, Pneumology and Angiology, Medical Faculty, Heinrich Heine University of Düsseldorf, Universitätstrasse 1, 40225 Düsseldorf, Germany; [b]Department of Nutrition, University of Reading, Whiteknights, Reading RG6 6AP, UK; [c]Bloomsbury Institute of Intensive Care Medicine, University College London, Gower Street, London, WC1E 6BT, UK; [d]Clinical & Experimental Sciences, Faculty of Medicine, University of Southampton, Southampton General Hospital, Tremona Road, Southampton, SO16 6YD, UK; [e]Center for Molecular Medicine, Slovak Academy of Sciences, Vlarska 7; 83101 Bratislava, Slovak Republic; [f]Department of Chemistry, Wake Forest University, Winston-Salem, NC 27109, USA; [g]Department of Chemistry, Warwick University, Coventry CV4 7AL, UK; [h]Bruker UK Ltd., Banner Lane, Coventry CV4 9GH, UK; [i]Department of Organic and Medicinal Chemistry, Graduate School of Pharmaceutical Sciences, Nagoya City University 3-1, Tanabedori, Mizuho-ku, Nagoya-shi, Aichi 467-8603, Japan; [j]Department of Molecular Immunology and Toxicology, National Institute of Oncology, Ráth György utca 7-9, 1122, Budapest, Hungary; [k]Leidos Biomedical Research, Inc., NCI-Frederick, Frederick, Maryland 21702; [l]NCI-Frederick, Frederick, MD 21702; and [m]Medical School, University of St-Andrews, St-Andrews, Fife, KY16 9AJ, Scotland.

[1] These authors contributed equally.

[2] To whom correspondence should be addressed: m.feelisch@soton.ac.uk

SI : Chemical Reactions

Reaction of sulfide with RSNO

As discussed previously (1), the reaction of excess sulfide with nitrosothiols (RSNO) mainly occurs via direct transnitrosation reaction and formation of thionitrite (SNO^-); its protonated form, thionitrous acid (HSNO) can react with a second HS^- leading to the formation of the more stable intermediate $SSNO^-$.

$$RSNO + HS(S)^- \longrightarrow RSH + SSNO^- \quad [1]$$

We suggest the following model for the formation of $SSNO^-$ that is consistent with all our data (for simplicity, we here use the protonated forms of all reactants because we do not have pH dependent kinetic data to elucidate the contribution of differently charged species):

$$RSNO + H_2S \longrightarrow RSH + HSNO \quad [2]$$

$$HSNO + H_2S \longrightarrow HSSH + HNO \quad [3]$$

$$HSSH + RSNO \longrightarrow HSSNO + RSH \quad [4]$$

$$HSSH + HSNO \longrightarrow HSSNO + H_2S \quad [5]$$

Reaction of sulfide with NO•

Although this reaction was studied a long time ago, the mechanisms involved are not fully understood, particularly as far as the reaction between NO and HS^- is concerned.

Early thermodynamic studies proposed that NO and H_2S should react to produce water, sulfur and nitrogen according to the following stoichiometric equation (4):

$$2NO\bullet + 2H_2S \longrightarrow 2H_2O + 2S + N_2 \quad [6]$$

However, calculations of this sort can rarely tell whether the reaction occurs or not; this is determined by the height of the energy barrier of the reaction profile, which could be impossibly high for the reaction of a radical with an anion. Experimental studies - carried out mainly under anaerobic conditions in (unbuffered) alkaline aqueous solutions or in polar organic solvents- suggested involvement of complex reaction mechanisms as nature and yield of the products obtained were strongly dependent on reaction conditions (pH, temperature, pO_2, solvent), in particular the concentration ratio of the reagents (5-8).

Since NO itself is not a very efficient nitrosating agent the question arises as to how it can react with HS^-. We propose 3 mechanisms involving: 1. prior oxidation of NO, 2. oxidation of HS^-, 3. direct reaction with formation of a radical intermediate.

1. NO is oxidized to N_2O_3, a nitrosating species (aerobic conditions)

The simplest assumption is that under aerobic conditions sulfide is nitrosated by reaction products of the NO autoxidation reaction in which NO is first oxidized to N_2O_3 which leads to formation of SNO^-; the latter reacts with excess sulfide as described above.

$$2\ NO\bullet + 1/2\ O_2 \longrightarrow N_2O_3 \qquad [7]$$

$$HS^- + N_2O_3 \longrightarrow HSNO + NO_2^- \qquad [8]$$

However, our results with DEA/NO and aqueous NO solution (Fig. 1A,B, main text), and previous literature (5, 7) clearly demonstrate that the reaction also occurs (to about the same extent) under strict exclusion of oxygen, rendering this an unlikely route of formation.

2. Sulfide undergoes a 1-electron oxidation to form sulfur radicals reacting with NO•

The 1-electron oxidation of sulfide leads to formation of thiyl radicals (HS•), which rapidly react to form HSS•-, as well as SO• and SO_2• radicals (9, 10). These radicals may intercept co-generated NO• to form HSNO (see Reaction 26 underneath).

$$HS^- \longrightarrow HS\bullet + 1\ e^- \qquad [9]$$

The pKa value of HS• is not known but suspected to be smaller than 7 (9). Therefore, at physiological pH the radical anion $S\bullet^-$ will be the major reactive form (9).

$$HS\bullet \longrightarrow S\bullet^- + H^+ \qquad [10]$$

The $S\bullet^-$ radical can either dimerise (Reaction 11) or react by addition to HS^- (Reactions 12-13) (9) or O_2 (Reaction 14) (10).

$$2\ S\bullet^- \longrightarrow S_2^{2-} \qquad [11]$$

$$S\bullet^- + HS^- \longrightarrow HSS\bullet^{2-} + H^+ \longrightarrow \longrightarrow HS_2^- \qquad [12]$$

$$S\bullet^- + HS_2^- \longrightarrow HSS\bullet^{2-} + HS^- \qquad [13]$$

$$S\bullet^- + O_2 \longrightarrow [SOO\bullet^-] \longrightarrow SO_2\bullet^- \qquad [14]$$

HS• and $HSS\bullet^{2-}$ radicals may be formed

a. by direct reaction with molecular oxygen (not very efficient);

$$HS^- + O_2 \longrightarrow S\bullet^- + H^+ + O_2\bullet^- \qquad [15]$$

b. by transition metal (e.g. copper or iron) catalysis;

$$Cu(II) + HS^- \longrightarrow Cu(I) + HS\bullet \qquad [16]$$

Copper ions, for example, may be present even in very pure aqueous buffers and have been shown to participate in chemical reactions even while complexed with metal chelators (11).

c. by homolytic cleavage of long-chain polysulfides (HS_n^-)

$$S_4^{2-} \longrightarrow 2\ S_2\bullet^- \qquad [17]$$

$$S_5^{2-} \longrightarrow S_2\bullet^- + S_3\bullet^- \qquad [18]$$

$$2\ S_5^{2-} \longrightarrow S_2\bullet^- + S_8 \downarrow \qquad [19]$$

This process may be transition metal catalyzed, and polysulfide will reduce transition metals in 1-electron processes (12). The presence of long-chain HS_n^- cannot be fully excluded from sodium sulfide stocks. A difficulty with such a mechanism is that sulfur tends to polymerize, and the driving force for the decomposition of polysulfides to anion radicals is not clear.

d. by homolytic cleavage of HSNO (or its isomers), or $SSNO^-$, once formed by other routes.

The mobile hydrogen of HSNO allows isomerisation of HSNO (1, 13-15) by a facile cyclic 1,3 shift.

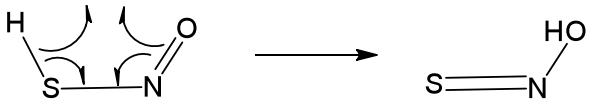

[20]

$$HNSO \rightleftharpoons HOSN \rightleftharpoons HSNO \rightleftharpoons HONS \qquad [21]$$

HSNO and its isomeric forms, as well as $SSNO^-$ can homolyse to generate NO and thiyl readicals

$$HSNO \longrightarrow HS\bullet + \bullet NO \qquad [22]$$

$$SSNO^- \longrightarrow SS\bullet^- + \bullet NO \qquad [23]$$

3. Direct reaction of NO with sulfide may form SNOH• radicals

In attempts to explain the direct nitrosation of GSH by NO under anoxic conditions, formation of an intermediate radical, GSNOH• has been proposed recently (16, 17). This radical would donate the electron to an electron acceptor, forming the nitrosothiol.

$$NO\bullet + GSH \longrightarrow [G\text{-}S\text{-}N\bullet\text{-}OH] \longrightarrow GSNO + 1\ e^- + H^+ \qquad [24]$$

In analogy an intermediate radical may be formed and undergo condensation reactions with other radicals forming S/N hybrid species.

$$NO\bullet + HS^- \longrightarrow [SNOH\bullet^-] \qquad [25]$$

This possibility remains speculative.

Formation and decomposition of HSNO and HSSNO

Generated $S^{\bullet -}$ and $S_2^{\bullet -}$ (according to reactions 9-19; 22,23) can react directly with NO to form HSNO and HSSNO.

$$HS^{\bullet} + NO^{\bullet} \longrightarrow HSNO \quad [26]$$

$$HS_2^{\bullet} + NO^{\bullet} \rightleftharpoons HSSNO \quad [27]$$

HSNO and $SSNO^-$ can undergo homolytic cleavage ($HSS^{\bullet -}$ and $NO^{\bullet}$) according to reactions 22 and 23; HSSNO can be formed also via transnitrosation of HSNO (Reaction 5).

As observed by Seel (6, 18), under non-aqueous anaerobic conditions there is an equilibrium between HSSNO and the blue trisulfide radical ($S_3^{\bullet -}$), depending on the presence of NO in the gas phase. According to Seel (18) this is due to an equilibrium between HSSNO and disulfide (inverse reaction 27). The latter leads to formation of the more stable trisulfide and tetrasulfide anion radicals (see below reactions 28,29,and 30), which can be observed by UV-Vis and/or EPR, respectively (18).

Formation and decomposition of polysulfides

$S^{\bullet -}$ and $S_2^{\bullet -}$ generated from sulfide (according to reactions 9-19) or from decomposition of HSNO or $SSNO^-$ (according to reactions 22, 23), can react with one another leading to formation of polysulfides.

$$S^{\bullet -} + S_2^{\bullet -} \longrightarrow S_3^{2-} \quad [28]$$

$$S^{\bullet -} + S_3^{2-} + H^+ \longrightarrow S_3^{\bullet -} + HS^- \quad [29]$$

$$S^{\bullet -} + S_4^{2-} + H^+ \longrightarrow S_5^{\bullet -} + HS^- \quad [30]$$

$$2\ S_2^{\bullet -} \longrightarrow S_4^{2-} \longrightarrow S_n^{2-} \longrightarrow S_{(n-1)}^{2-} + H_2S \quad [31]$$

Polysulfides are formed during $SSNO^-$ decomposition, but do not affect its kinetics of decomposition since decay was similar in the presence and absence of CN^- (**SI Fig. S5**). As expected, sulfur is extruded on addition of acid, and can be quantified by chloroform extraction (**SI Fig. S5**).

Formed polysulfide may undergo further reactions including: a) polymerization reaction to longer chain polysulfides (reaction 31) and inorganic sulfur (reaction 19); b) decomposition to sulfide in the presence of strong nucleophiles (such as thiolate and cyanide), a property we used in the present study to distinguish them from $SSNO^-$; c) homolytic cleavage (see reactions 17-19).

Formation and decomposition of SULFI/NO

A potential precursor in the formation of SULFI/NO from NO and sulfide is sulfite (SO_3^{2-}), as suggested by others earlier, not only for the reaction of sulfide with NO under anoxic conditions (5, 7), but also for explaining the formation of SULFI/NO by the reaction of NO with thiosulfate ($S_2O_3^{2-}$) and dithionite anion ($S_2O_4^{2-}$)(7).

$$HSO_3^- + 2\ NO\bullet \longrightarrow N(O)N(OH)SO_3^- \qquad [32]$$

In aqueous solution, sulfite may be formed either by reaction of sulfide with molecular oxygen (O_2)(19) or via formation of radical intermediates such as $SO_2\bullet^-$ (described in reaction 14). The $SO_2\bullet^-$ radical anions are identical to those obtained by dissociation of dithionite $S_2O_4^{2-}$ anion (9).

$$2SO_2\bullet^- \rightleftharpoons S_2O_4^{2-} \qquad [33]$$

The latter is known to react rapidly with O_2 and sulfide, leading to formation of SO_3^{2-} and $S_2O_3^{2-}$. Moreover, the $S_2O_4^{2-}$ anion is known to reduce polythionate to SO_3^{2-}, $S_2O_3^{2-}$ and S_8 (9, 20).

Alternatively, SO_3^{2-} is formed via hydrolysis of intermediate HONS, formed by isomerization of HSNO to thiosulfate as proposed by Goehring et al. (13):

$$HONS + 2\ H_2O \longrightarrow HONH_2 + S(OH)_2 \qquad [34]$$

$$2\ S(OH)_2 \longrightarrow S_2O_3^{2-} + H_2O + 2H^+ \qquad [35]$$

$$S_2O_3^{2-} + H^+ \longrightarrow HSO_3^- + S_8 \qquad [36]$$

Since no SO_3^{2-} was detected by HR-ESI-MS in freshly prepared sulfide stock solutions, and sulfide autoxidation is a rather slow process, production of $S_2O_3^{2-}$ via radical reactions and/or via HONS/HSNO would appear to be the most plausible route.

Decomposition of SULFI/NO leads to formation of SO_3^{2-}, sulfate (SO_4^{2-}) and nitrous oxide (N_2O). While it has been proposed that this process occurs directly (21), the formation of both HNO and NO from hyponitrite ($ON:NOH^-$) has been proposed by others (22-24).

$$O{=}NN(OH)\text{-}SO_3^- \longrightarrow N_2O + H_2SO_4 \qquad [37]$$

$$O{=}NN(OH)\text{-}SO_3^- + H_2O \longrightarrow ON:NOH^- + H_2SO_4. \qquad [38]$$

Indeed, evidence for trace levels of $ON:NOH^-$ in incubation mixtures of both SULFI/NO and DEA/NO (but not SNAP) with sulfide were observed by us using HR-ESI-MS (**SI Fig. S8**); in addition, sodium hyponitrite was found to release NO at pH 7.4 as detected by gas phase

chemiluminescence, and its release was markedly enhanced in the presence of the 1-electron oxidant ferricyanide, consistent with the generation of HNO (25).

$ON:NOH^-$ is known to decompose to N_2O and water via intermediate formation of HNO:NOH.

$$NO:NOH^- + H^+ \rightleftharpoons HNO:NOH \longrightarrow N_2O + H_2O \quad [39]$$

In addition, nitroxyl can be reduced by sulfide to hydroxylamine (NH_2OH) and then be nitrosated. The latter was found to occur by Bagster *et al*. in the reaction of NO with sulfide (8).

Parallel reactions

Alternatively, direct reaction of NO with polysulfides with subsequent formation of nitroxyl may be involved. In analogy to sulfhydryl radicals (26), polysulfides and persulfides have recently been proposed to be better radical reducing/capturing reagents compared to sulfide itself (because of resonance stabilization of the generated radical species by the adjacent sulfur atoms)(12) and hence they might be able to directly reduce NO:

$$HSSH + NO\bullet \longrightarrow HSS\bullet + HNO \quad [40]$$

$$HSS\bullet + HS^- \longrightarrow HSSSH\bullet^- \quad [41]$$

$$HSSSH\bullet^- + O_2 \longrightarrow HSSSH + O_2\bullet^- \quad [42]$$

$$O_2\bullet^- + NO\bullet \longrightarrow ONOO^- \quad [43]$$

Reactions 42 and 43 are known to be close to the diffusion controlled limit, and peroxynitrite is a powerful oxidant (27, 28).

SI : Materials and Methods

Materials. The potassium salt of N-nitrosohydroxylamine-N-sulfonate (SULFI/NO) was synthesized as described by Drago et al.(29) and found to release 1.03 mol of N_2O per mol of compound as measured by gas chromatography with electron capture detection (Shimadzu GC-2014). S-nitroso-N-acetyl-D,L-penicillamine (SNAP) was either prepared as described by Field et al (30) or *in situ* by nitrosation of N-acetyl-D,L-penicillamine with acidified nitrite (see below). Ultrapure water was generated using a Milli-Q system (Millipore), 3-isobutyl-1-methylxanthine (IBMX) and Angeli's salt were from Cayman Chemicals (Biomol, Hamburg, Germany), DETA/NO and DEA/NO from Alexis (Enzo Life Sciences, Exeter, UK). Unless otherwise specified, all other chemicals were of the highest purity available and purchased from Sigma-Aldrich (Schnelldorf, Germany or Gillingham, UK), cell culture plastics from Greiner (Frickenhausen, Germany), and other cell culture material from PAA (Pashing, Austria). Fetal bovine serum (FBS) was from Cambrex (Lonza, Cologne, Germany).

Cell culture. Rat fibroblastoid-like (RFL-6, ATCC CCL192™) cells were purchased from LGC Standards GmbH (Wesel, Germany) and cultured from passage 8-18 in T9 flasks using RPMI 1640, supplemented with 20% fetal bovine serum and antibiotics in a CO_2 incubator under standard cell culture conditions.

Animals. All experiments were performed following local ethics committee approval by either the Institutional Animal Care and Use Committee (IACUC) at Boston University School of Medicine (Boston, MA), University College London (London, UK), or the State Veterinary and Food Administration of the Slovak Republic. Animals were handled in accordance with the Guide for the Care and Use of Laboratory Animals published by the US National Institutes of Health (NIH publication no. 85-23, revised 1996) and Home Office (UK) guidelines under the 1986 Scientific Procedures Act. Male Wistar rats (270-325 g, Charles River) were kept on a normal 12/12 light cycle and allowed to acclimatize to local vivarium conditions for at least 7 days prior to experimental use.

Preparation of stock solutions $SSNO^-$, and polysulfide containing mixtures. Stock solutions of SNAP (100 mM, DMSO) and IBMX (50 mM, DMSO) were kept aliquoted at -20°C until use. Stock solutions of DEA/NO, DETA/NO, Sper/NO, SULFI/NO and Angeli's salt were freshly prepared in 0.01 M NaOH, diluted in PBS and used immediately. Stock

solutions of S-nitrosocysteine (CysNO), ^{15}N-SNAP, SNAP, and S-nitrosoglutathione (GSNO) in aqueous solution were freshly prepared either from crystalline material or via reaction of the reduced thiols with acidified nitrite (31) and used immediately. Saturated aqueous solutions of NO were prepared as described (32), kept sealed with minimal headspace under argon and used without further dilution; aliquots of this stock were directly transferred into cuvettes using argon-flushed Hamilton syringes. For *in vitro* and cell culture experiments Na_2S stock solutions (200 mM, anhydrous, Sigma-Aldrich) were prepared fresh before each experiment by dissolving anhydrous Na_2S in a strong buffer (1 M TRIS or phosphate buffer, pH 7.4) and diluted further in 100 mM TRIS or 50-100 mM phosphate buffer pH 7.4 immediately before use. For *in vivo* experiments NaHS stock solutions were prepared in 300 mM phosphate buffer pH 7.4, diluted in phosphate buffered saline (PBS) pH 7.4 and used immediately (10 mg/ml = 176.7 mM NaHS; anhydrous; Alfa Aesar; Heysham, UK). In near-neutral aqueous solution both Na_2S and NaHS will rapidly dissolve to S_2^{2-} and HS^-, respectively, and undergo protonation according to the following equilibrium (mean pKa_1 = 7; pKa_2 >12) (33).

$$S_2^{2-} \rightleftharpoons HS^- \rightleftharpoons H_2S\ (aq) \rightleftharpoons H_2S\ (g) \uparrow \qquad [44]$$

Therefore, at pH 7.4 both salts will give a solution mainly containing HS^- with only negligible amounts of S_2^{2-}, but a stronger buffer is needed to adjust the pH of Na_2S to physiological pH.

It is important to point out that the relative amounts of the three species at equilibrium depend on temperature, pH, ionic strength, amount of H_2S gas leaving the solution, as well as "side" reactions including sulfide oxidation to form sulfite, sulfate, and thiosulfate, and polymerization reactions generating polysulfides (33). Although all precautions were undertaken to avoid the presence of such contaminants, their presence in the stock solutions cannot be excluded. The presence of those species may even initiate some of the chemistry leading to observed products. Nitrosopersulfide ($SSNO^-$) enriched mixtures ('$SSNO^-$ mix') were obtained by adding appropriate volumes of the stock solutions directly to the incubation buffer to achieve final concentrations of 0.5-3 mM for SNAP or DEA/NO and 0.2–10 mM for sulfide and incubated for 1-10 min, as appropriate. Where indicated, excess sulfide was removed by purging solutions with Ar or N_2 for 10 min; the formation of $SSNO^-$ and the removal of sulfide were verified spectrophotometrically. For *in vitro* and *in vivo* bioactivity experiments, stock solutions of $SSNO^-$ were prepared by reacting 1 mM SNAP with 10 mM Na_2S in 1 ml PBS or TRIS 100 mM pH 7.4 and incubating for 10 min. The (theoretical) maximal yield of $SSNO^-$ under these conditions is 1 mM, corresponding to the concentration of added nitrosothiol (please refer to Fig. S9 for experimental determination of reaction yield). In a typical experiment, 10 µl of SNAP (100 mM/DMSO) and 100 µl Na_2S (100 mM/Tris 100 mM pH 7.4) stock solutions were added to an amber centrifugation tube containing 890 µl

Tris 100 mM pH 7.4. After 10 min of incubation at RT, excess sulfide was removed by 10 min bubbling with N_2. For cell culture experiments 20 µl of this mix was then added to cell culture medium of a total volume of 1 ml (corresponding to a 1:50 dilution) to yield a final concentration of 20 µM $SSNO^-$. For in vivo experiments the $SSNO^-$ solution was prepared in phosphate buffer pH 7.4, and further diluted in PBS to obtain the doses indicated for bolus i.v injection (dose range 0.03 -3 µmol/kg) or used directly for continuous i.v. infusion (0.16 µmol/kg/min). Mixtures of polysulfides were prepared by oxidation of sulfide with HOCl as described (34, 35). Briefly, 500 µl of 20 mM HOCl was added dropwise to 500 µl of 120 mM Na_2S upon continuous vortexing. Then, 600 µl of this solution were diluted by addition of 300 µl H_2O and 100 µl of 9% NaCl. To allow direct comparison, a sulfide solution was prepared under identical conditions by adding 200 µl of 120 mM Na_2S solution to 700 µl H_2O and 100 µl 9% NaCl.

Effects of sulfide, $SSNO^-$, SULFI/NO and polysulfides on cardiovascular hemodynamics. All procedures were conducted in male Wistar rats anesthetized with 2% isoflurane, as described (36). Briefly, the effects of bolus intravenous injection (i.v.) of increasing doses of NaHS (doses range 0.1 -1 mg/kg = 1.8 - 17.7 mg/kg in PBS), or $SSNO^-$ mix (dose range 0.03 -3 µmol/kg in PBS), or vehicle control (PBS only) , or SULFI/NO (stock 10 mM in 10 mM NaOH/ NaCl 0.9%, injected at dose range 0.03 -3 µmol/kg), or vehicle control (dose range 0.03 -3 µmol NaOH/kg in 0.9%NaCl) on cardiovascular hemodynamics and circulating NO stores were assessed at 10 min intervals. Continuous infusion of either NaHS (1 mg/ml = 17.7 mM in PBS pH 7.4) or $SSNO^-$ (1 mM in PBS pH 7.4) or PBS only, or SULFI/NO (1 mM in 0.25 mM NaOH/NaCl 0.9%) or vehicle control (0.25 mM NaOH/NaCl 0.9%) were administered at a rate of 10 ml/kg/h via a right internal jugular venous line. Final doses were 2.94 µmol/kg/min for NaHS, 0.16 µmol/kg/min for $SSNO^-$, and 0.16 µmol/kg/min SULFI/NO (in 25 mM NaOH/0.9% NaCl with 4.16 µmol NaOH/kg/min for the vehicle control). Continuous monitoring of mean arterial pressure (MAP) and blood withdrawal were performed from an indwelling arterial (left common carotid) line. Blood was taken at defined time points (0, 5, 10, 30, 60, 120 minutes) and processed as previously described for determination of NO metabolites by chemiluminescence (37). Cardiac function and heart rate were assessed by transthoracic echocardiography using a Vivid 7 device (GE Healthcare, Bedford, UK) as described (36). A rectal probe (TES Electrical Electronic Corp., Taiwan) inserted 3 cm in depth was used to measure core temperature. The hemodynamic effects of polysulfides were assessed by injecting 150 µl polysulfides/sulfide mixture (stock 6 mM HS_x^-/ 24 mM HS^- in NaCl 0.9%) or sulfide alone as a control (24 mM HS^- in NaCl 0.9%) corresponding to doses of ≈ 2.7 µmol/kg HS_x^- and 10.8 µmol/kg, respectively (35). Other

doses were obtained by 1:2 and 1:6 dilution and were 0.45 µmol/kg HS_x^- / 1.8 µmol/kg HS^- and 1.35 µmol/kg HS_x^- / 5.4 µmol/kg HS^-.

Determination of circulating NO stores. Blood was anti-coagulated with EDTA (2.5 mM), and N-ethylmaleimide (NEM, 10 mM) was added to prevent artificial thiol nitrosation and minimize anion exchange processes across blood cell membranes. Plasma and erythrocytic fractions were obtained by centrifugation at 800xg at 4°C for 10 min. Once separated, samples were frozen with liquid N_2 and kept at -80°C for later NO metabolite analyses, as described (37). Plasma was harvested as described above, thawed, and analyzed. After thawing, erythrocytes were subjected to hypotonic lysis in 4 volumes of a solution of NEM (10 mM) and EDTA (2.5 mM) in water prior to analyses. In both blood compartments, NO oxidation products (nitrite and nitrate) were quantified using HPLC ion chromatography (ENO-20, Eicom). Plasma and erythrocytic nitrosation products (RXNO) and erythrocytic nitrosylation products (NO-heme) were measured by gas phase chemiluminescence (CLD 77am/sp, Eco Physics AG, Dürnten, Switzerland).

Effects of sulfide on NO bioactivity, and detection of NO release and bioactivity of $SSNO^-$ and SULFI/NO in RFL-6 cells. The effects of sulfide on Sper/NO mediated activation of sGC were determined by measuring changes in intracellular cGMP levels in RFL-6 cells in response to 100 µM Sper/NO in the absence or presence of increasing concentrations of sulfide (1 µM, 10 µM and 100 µM Na_2S in Tris 100 mM pH 7.4) as described (1), with minor modifications. Briefly, 1.5 x 10^5 RFL-6 cells were seeded on 6-well plates and grown to confluence for 48 hours in complete RPMI 1640 growth medium containing 20% FCS (complete medium), washed with PBS, and pre-treated for 15 min with 500 µM IBMX in 1 ml complete medium without serum (treatment medium) to inhibit PDE activity. The medium was removed, and fresh treatment medium was added (1 ml/well). Sulfide treatments were added directly to the culture medium, immediately (< 1 min) followed by addition of Sper/NO. Cells were incubated for 20 min, washed with cold PBS and lysed in 0.1M HCl for 20 min at room temperature (RT). The incubation time and the concentration of the NO donor were carefully optimized in preliminary experiments by testing 10 and 100 µM Sper/NO, and incubating cells for time intervals between 1 and 30 min. The NO/HNO bioactivity of $SSNO^-$ and SULFI/NO were compared by treating IBMX-pretreated cells (as above) with 20 µM $SSNO^-$ mix, with 1 µM, 10 µM and 100 µM SULFI/NO, or with 1 µM, 10 µM and 100 µM of the HNO donor Angeli's salt for 20 min. In some experiments, ~7000 U/ml SOD (stock 10 mg/ml in PBS pH 7.4, specific activity 4557 U/mg) was added directly to the treatment medium 5 min before addition of $SSNO^-$ mix, SULFI/NO or Angeli's salt to enable

extracellular conversion of HNO into NO. In selected experiments, an sGC inhibitor (ODQ, 50 µM), an NO scavenger (cPTIO, 500 µM) or a nitroxyl scavenger (1 mM Cys) were added 5 min prior to the other treatments. Intracellular cGMP levels were assessed in cell lysates by using DetectX®High Sensitivity Direct Cyclic GMP kit by Arbor Assay (Biotrend, Cologne, Germany) as per manufacturer's instructions. Protein concentrations in the supernatant were determined by a modified Bradford's protein assay (Roti-Nanoquant, Carl Roth GmbH + Co. KG, Karlsruhe, Germany) after pH equilibration with 200 mM TRIS pH 8. Data were normalized for protein content and expressed as folds of untreated control to further account for the variability in basal cGMP levels of RFL-6 cells of different batches and passages.

Time-resolved NO detection, NO trapping and NO release by chemiluminescence. Time-resolved detection of NO release from DEA/NO, Sper/NO, GSNO and SNAP and their reaction mixtures, was carried out by gas phase chemiluminescence detection (CLD 77am sp) using a custom-designed, water jacketed glass reaction chamber (15 ml total volume) kept at 25±0.1°C using a circulating water bath and continuously bubbled with N_2, essentially as described (1).

NO trapping by sulfide, sulfite and thiosulfate was monitored as described above, with NO generated using a slow-releasing NO-donor (DETA/NO). Briefly, DETA/NO was injected from a concentrated alkaline stock solution into the reaction chamber containing buffer to achieve a final concentration of 33.4 µM; after NO release reached a steady-state, this was followed by injection of 33.4 and 334 µM of Na_2S, or 664 µM of Na_2SO_3, Na_2SO_4, and $Na_2S_2O_3$.

NO formation from $SSNO^-$ enriched mixtures, in the presence or absence of the metal chelator DTPA (100 µM), in 1 M Tris/HCl or 100 mM phosphate buffer pH 7.4 was monitored by chemiluminescence detection as described above. Briefly, 1 ml volumes of the respective SNAP/sulfide mixtures were pre-mixed in Eppendorff vials, vortexed, and after 1 min of incubation a 150 µl aliquot of the reaction mixture was transferred into the reaction chamber containing 15 ml buffer (dilution 1 : 100) by means of a gas-tight syringe. NO concentration in the sample gas was recorded continuously and peak areas were integrated using an EPC-500/PowerChrom data processing system (eDAQ).

Determination of reaction kinetics by UV-visible spectroscopy. The spectroscopic and kinetic behavior of the reaction between sulfide and DEA/NO, Sper/NO, GSNO and SNAP was followed by rapid scanning UV-visible spectroscopy in 3 ml quartz cuvettes, kept at either 25.0 or 37.0±0.02°C with continuous stirring (t2 peltier-type cuvette holder with TC1

temperature controller, Quantum Northwest, Liberty Lake, WA) using a Cary 60 UV/Vis spectrophotometer and analyzed using WinUV software (Agilent Technologies, Wokingham, UK) as described (1). No differences in spectral changes were observed whether reactions were carried out in the presence or absence of DTPA (100 μM), suggesting that transition metal contamination of our buffers was negligible.

High-resolution mass spectrometry for detection of $SSNO^-$, polysulfides and SULFI/NO. High-resolution mass spectrometry (HRMS) was conducted using an LTQ Orbitrap XL hybrid linear ion trap-orbitrap mass spectrometer equipped with a nanospray ionization source (Thermo-Fisher, Hemel Hempstead, UK). Sample mixtures were prepared as described above except that all final incubations were carried out in 50 mM ammonium phosphate buffer pH 7.4; reaction mixtures were prepared on-site and infused directly into the ion source using a gas-tight glass syringe and peek tubing. Acetonitrile (HPLC grade, Fisher Scientific Ltd, Loughborough, UK) was used as make-up solvent and mixed with the reaction solutions at a ratio of 1:5 via a T-piece to improve ionization efficiency. The instrument was controlled with XCalibur 2.1 (Thermo-Fisher). Spectra were acquired in negative ion mode with a spray voltage of 5 kV and nitrogen as sheath gas; capillary temperature was set at 300°C, and capillary voltage at 20 V. Instrument parameters, especially those of the ion optics, were optimized for each individual compound of interest. Elemental analysis, based on accurate mass and *a priori* information of likely elemental composition, and isotope distribution simulation were performed using XCalibur 2.1.

Electrospray ionization high-resolution mass spectrometry for HSNO detection. All experiments were carried out using a maXis Impact instrument (Bruker Daltonik GmbH, Bremen, Germany) operating in positive ionization mode (ESI^+; capillary voltage 4700 V, dry gas flow and temperature 4.0 L/min, 180°C; scan 30-500 m/z). The instrument was calibrated in the mass range of 45-156 using a mixture of low-mass calibrants and found to perform at a mass accuracy of 1-2 ppm using Li-formate clusters. In some experiments ESI^+ was carried out at lower temperatures (4° or -20°C) using a Bruker Cryospray unit, with and without acetonitrile or methanol (1:1-1:4) to enhance ionization efficiency using an infusion rate of 240 μl/h.

GSNO and SNAP stock solutions were prepared approximately 1h ahead of the experiments by mixing equal volumes of equimolar solutions of the corresponding reduced thiols (L-glutathione and N-acetyl-D,L-penicillamine) in 1N HCl with aqueous sodium nitrite (or ^{15}N-nitrite) to produce a 10 mM GSNO (pink) and 2 mM SNAP (green) stock solution which was kept on ice in the dark. These stocks were diluted 1:5 in ice-cold 1N $(NH_3)_3PO_4$ pH 7.4

immediately before each incubation run. Sulfide stock solutions were prepared anaerobically in 1 M $(NH_4)_3PO_4$ buffer pH 7.40 from Na_2S and kept under argon. Incubations were carried out at pH 7.4 / RT in 10 mM ammonium phosphate buffer under the following conditions: GSNO 1 mM, Na_2S 1 or 8 mM; SNAP 0.2 mM, Na_2S 0.2 mM, with final buffer concentrations varying between 50 and 500 mM. Nitrosothiol solutions and reaction mixtures were infused at a rate of 4 µL/min directly into the electrospray source and spectra were recorded for up to 10 min.

Determination of sulfide release from $SSNO^-$ by the methylene blue method. An $SSNO^-$ mix was prepared by incubating 500 µM SNAP and 5 mM H_2S in 175 mM Tris/HCl buffer containing 87.5 µM DTPA (pH 7.4). After 5 min of incubation at RT (necessary to complete $SSNO^-$ formation), 5 mM DTT (or H_2O in the control) was added to the samples. To ensure the assay only measures sulfide that is released by $SSNO^-$, polysulfides (which also form in the reaction of SNAP with sulfide) were reduced by DTT to H_2S, which was subsequently eliminated from reaction mixtures by bubbling with Ar. When polysulfide reduction by DTT was completed (10 min) the system was bubbled with Ar for 30 min (>98% of polysulfides and H_2S is removed by this method before substantial $SSNO^-$ decomposition). This was followed by the addition of another 5 mM DTT aliquot, and the pH was raised to 9.3 by addition of 100 mM NH_4OH. The reaction mixture was kept in the dark to avoid photolytic decomposition reactions. The amount of sulfide that was released by $SSNO^-$ decomposition from this reaction mixture was measured by the methylene blue method (into 500 µL of 10x diluted sample, 250 µL of 54.7 mM zinc acetate, 133 µL of 31.6 mM DPD (N,N-dimethyl-p-phenylenediamine, sulfate salt) in 7.2 M HCl and 133 µL of 18 mM $FeCl_3 \cdot 6H_2O$ in 1.2 M HCl were added). After 15 min incubation at RT, sulfide content was quantified spectrophotometrically at 670 nm with the aid of a calibration curve that was constructed using authentic sulfide standards. The presence of DTT had no effect on the assay.

Determination of polysulfides by the cold cyanolysis method. Sample preparation was as described under the Methylene blue method section above except that DTT addition was excluded from this protocol. After Ar bubbling and raising the pH to 9.3, 55 mM KCN was added to the reaction mixture (which was again stored in the dark). Polysulfide content was quantified at the indicated time points by adding 15 µL of 37% formaldehyde and 150 µL of Goldstein reagent (62 mM $FeCl_3 \cdot 6H_2O$ in 18.4% HNO_3) into a 675 µL sample aliquot (that was incubated with KCN). Quantification was based on the measured absorbance values at 460 nm following 15 min incubation at RT with the reagent solutions. A baseline correction was applied by subtracting the spectrum of the starting solution, which was measured after

eliminating polysulfides and sulfide from the reaction mixture (by adding 500 μM DTT followed by Ar bubbling at pH 7.4 before the pH jump to 9.3) before substantial $SSNO^-$ decomposition occurred. Calibration curves were developed using standard KSCN solutions. Polysulfides that were generated in the reaction of SNAP with sulfide were quantified by incubating the reaction mixture for 10 min only with cyanide before the addition of formaldehyde and the Goldstein reagent. In independent experiments we verified that (under similar conditions) 10 min was enough to have >90% of the polysulfides reacting with cyanide. The amount of sulfane sulfur that was released during $SSNO^-$ decomposition was quantified by subtracting the polysulfide content that is not originating from $SSNO^-$ from the total amount of the measured sulfane sulfur after complete decomposition of $SSNO^-$.

Determination of sulfane sulfur by extraction into chloroform. The amounts of polysulfides other than $SSNO^-$ that were generated in the reaction of SNAP with sulfide and the amount of sulfane sulfur that forms upon the decomposition of $SSNO^-$ were also quantified spectrophotometrically after extraction of sulfane sulfur into chloroform. A SNAP/sulfide (1:10 molar ratio) reaction mixture was prepared by mixing 500 μM SNAP with 5 mM H_2S in DTPA-contaning Tris/HCl buffer pH 7.4 as described above. However, this mixture was not bubbled with Ar and the pH was not adjusted to 9.3. Two volume equivalents of chloroform were added to the reaction mixtures immediately upon completion of $SSNO^-$ formation (5 min after mixing SNAP with sulfide) or at 540 min (i.e. after complete decomposition of $SSNO^-$). Extraction was achieved by 30 min vortexing of the heterogeneous mixture. Sulfane sulfur content of the organic phase after the extraction was quantified spectrophotometrically at 280 nm based on a calibration curve (repeated 3x) that was developed by dissolution of known amounts of authentic *cyclo*-octasulfur; this gave us an extinction coefficient for sulfur of 925.9 M^{-1} cm^{-1} at 280 nm.

Nitroxyl detection by metHb trapping. Trapping of HNO by methemoglobin (metHb) with subsequent formation of HbNO following reductive nitrosylation was assessed as increase in absorbance at 542 nm and 583 nm of a solution of 10 mg/ml in Tris Buffer 1M pH 7.4 (100 μl) treated with 1-100 μl of 50 mM Angeli's salt in 0.01 M NaOH or an NO/sulfide reaction mixture, respectively. Control incubations were carried out with metHb and sulfide alone.

Nitroxyl detection by P-Rhod fluorescence. Nitroxyl formation was assessed also using the nitroxyl-specific fluorescence probe P-Rhod (38). Stock solutions of P-Rhod (50 mM in DMSO) were aliquoted and kept at -20°C. N_2 gassed $SSNO^-$ mix (1 mM SNAP/ 10 mM Na_2S

in Tris 100 mM pH 7.4), SULFI/NO (1 mM in Tris 100 mM), or Angeli's salt (1 mM in Tris 100 mM) were serially diluted in Tris/HCl 100 mM in a dark 96 well plate. Buffer alone was used as blank. P-Rhod (5 µM) was added to all wells using an automatic injector and fluorescence changes were recorded at ex 480 nm, em 520 nm using a multi-mode plate reader (FLUOstar Omega, BMG Labtech, Offenburg, Germany). Data are reported as percent increases compared to background signal.

Nitrous oxide quantification by gas chromatography. Stock solutions of NO donors/RSNOs were mixed with Na_2S in phosphate buffer and injected into a 10 mL round bottom flask sealed with a rubber septum. Angeli's salt (NaN_2O_3) was used as reference compound for HNO generation. To some air-treated samples 200 µM TXPTS in phosphate buffer (10 mM, pH 7.4) was added to trap HNO. Incubation vials were flushed with either N_2 or air, incubated at 37°C, and at the indicated time points headspace aliquots (100 µl) were injected via a gas-tight syringe onto a 7890A Agilent gas chromatograph equipped with a micro-electron capture detector (µECD) and a 30 m × 0.32 m (25 µm) HP-MOLSIV capillary column as described (39). The oven was operated at 200 °C for the duration of the run (4.5 min). The inlet was held at 250°C and run in split mode (split ratio 1:1) with a total flow (N_2 as carrier gas) of 4 ml/min and a pressure of 37.9 psi. The detector was held at 325°C with a makeup flow (N_2) of 5 ml/min. The retention time of nitrous oxide was 3.4 min, and yields were calculated based on a standard curve for nitrous oxide (Matheson Tri-Gas).

Determination of nitrite and nitrate by ion chromatography. An air-equilibrated stock solution of SNAP (100 mM) was injected into a septum-sealed glass container containing 50 mM phosphate buffer (pH 7.4). The formation of nitrite and nitrate over time was monitored at 5.7 min intervals post mixing (30 s) using high pressure liquid ion chromatography (37). For all mixtures, the final concentration of SNAP was adjusted to 100 µM. SNAP/Sulfide incubations (final sulfide concentrations 100 µM and 1000 µM) were prepared by addition of appropriate volumes of sulfide from freshly prepared anaerobic stocks (10 mM) to the buffered SNAP solution to obtain a final molar concentration ratio of either 1:1 or 1:10 SNAP:HS^- and monitored as above. For all mixtures the total volume was kept constant at 5 ml. A 10 µl volume of an air-equilibrated stock solution of 1 mM DEA/NO was injected into a septum-sealed container containing 50 mM phosphate buffer (pH 7.4). After 30s of mixing the decomposition of DEA/NO was monitored over time using the same intervals and methods as described for SNAP above. For all mixtures, the final DEA/NO concentration was 2 µM. Various concentrations of sulfide (final concentrations 1 µM, 2 µM, 4 µM, and 20 µM) were individually mixed from freshly prepared stock solutions (100 mM, 10 mM, or 1

mM) to the DEA/NO solution to obtain molar ratios of 1:0.5, 1:1, 1:2, and 1:10 DEA/NO:HS^-. The total volume was kept constant at 5 ml.

Statistical analysis. If not otherwise described, data are reported as means+/- SEM. Statistical significance was tested by using GraphPad Prism 6.0 for Mac OS (GraphPad Software Inc.) or with SPSS 22 (IBM). Multiple comparisons were tested with ANOVA followed by an appropriate *post hoc* test as indicated in the figure legends. Outliers were identified graphically by analyzing a box&whiskers plots according to Tuckey.

SI : Figure and Legends

Figure S1

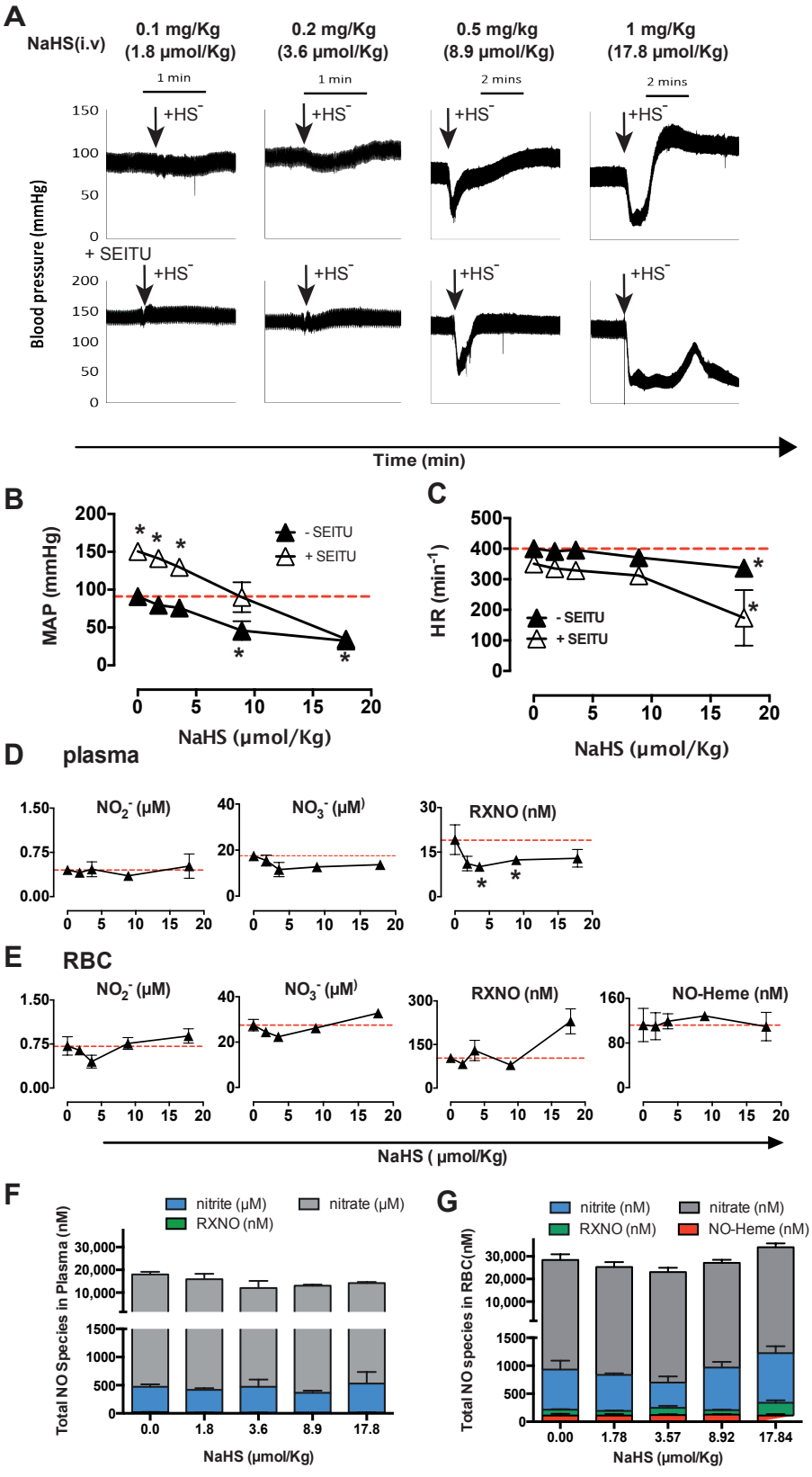

Figure S1. Association between hemodynamic changes to i.v. bolus application of sulfide (dose range 1.8 - 17.8 µmol/kg) and changes in systemic NO status in rats. (**A**) Representative blood pressure tracings in the absence (upper panels) and presence (lower panels) of the NOS inhibitor S-ethylisothiourea (SEITU; 1.5 mg/kg/min i.v. infusion) (**B**) mean arterial pressure (MAP) and (**C**) heart rate (HR) with or without NOS blockade by SEITU. (**D,E**) Levels of nitrite (NO_2^-), nitrate (NO_3^-) and total nitroso (RXNO) species in plasma and, (along with NO-heme) in red blood cells (RBC); Levels of nitrite, nitrate and nitroso (RXNO) species in blood (**F,G**). Total NO species in plasma (**F**) and in RBC (**G**). n = 3; * $p<0.05$ vs. baseline # $p<0.05$ paired T-Test vs. baseline.

Figure S2

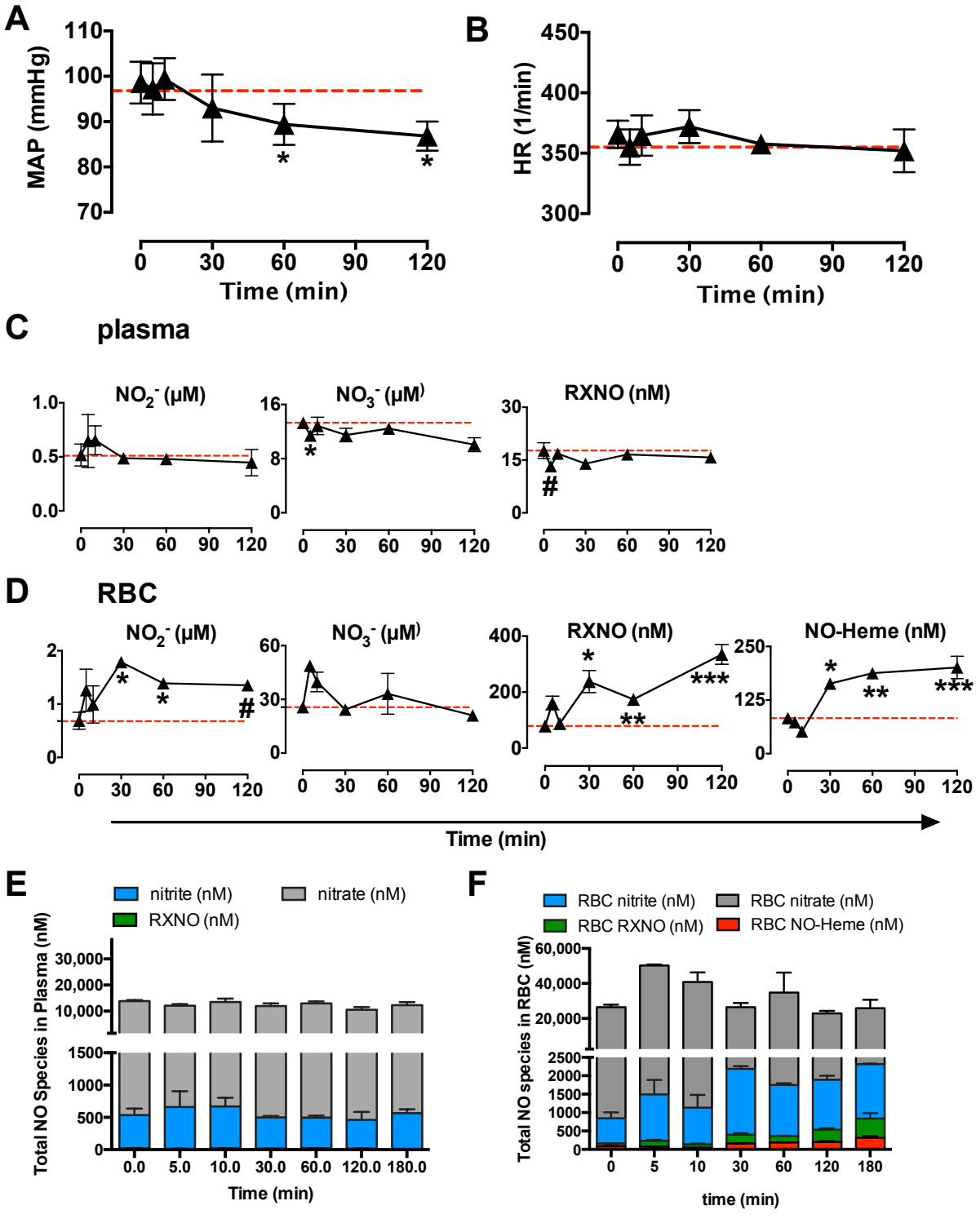
A
MAP (mmHg)
110
100
90
80
70
0 30 60 90 120
Time (min)
B
HR (1/min)
450
400
350
300
0 30 60 90 120
Time (min)
C
plasma
NO2- (µM)
1.0
0.5
0.0
NO3- (µM)
16
8
0
RXNO (nM)
30
15
0
D
RBC
NO2- (µM)
2
1
0
NO3- (µM)
60
30
0
RXNO (nM)
400
200
0
NO-Heme (nM)
250
125
0
0 30 60 90 120
Time (min)
E
nitrite (nM)
nitrate (nM)
RXNO (nM)
Total NO Species in Plasma (nM)
30,000
20,000
10,000
1500
1000
500
0
0.0 5.0 10.0 30.0 60.0 120.0 180.0
Time (min)
F
RBC nitrite (nM)
RBC nitrate (nM)
RBC RXNO (nM)
RBC NO-Heme (nM)
Total NO species in RBC (nM)
60,000
40,000
20,000
2500
2000
1500
1000
500
0
0 5 10 30 60 120 180
time (min)

Figure S2. Continuous i.v. infusion of sulfide (NaHS, dose 2.8 µmol/kg/min) in anesthetized rats leads to an initial decrease followed by an increase in NO bioavailability. (**A**) mean arterial pressure (MAP) (**B**) heart rate (HR). (**C,D**) Levels of nitrite (NO_2^-), nitrate (NO_3^-) and total nitroso (RXNO) species in plasma (**C**) and, along with NO-heme, in red blood cells (RBC) (**D**); (**E,F**) Total NO species in plasma (**E**) and in RBC (**F**). 1-way ANOVA $p<0.01$; Dunnet * $p<0.05$; ** $p<0.01$; ***$p<0.001$ vs. baseline # $p<0.05$ T-Test between groups.

Figure S3

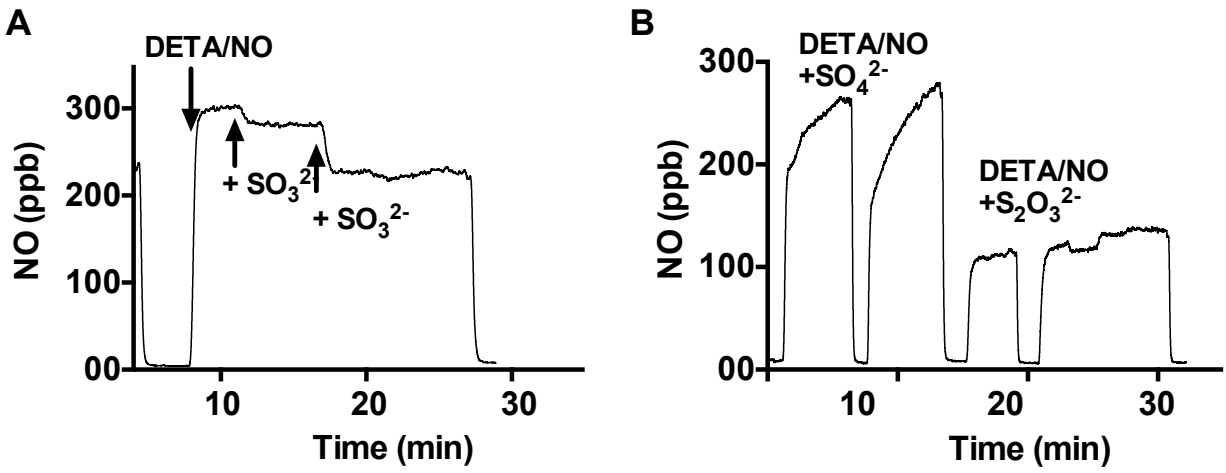

Figure S3. Sulfite but not thiosulfate and sulfate scavenge NO. Time-resolved chemiluminescence recordings of NO release from 33.4 μM DETA/NO in phosphate-buffered saline (pH 7.4) after addition of 664 μM sulfite (**A**) or 664 μM sulfate or 664 μM thiosulfate (**B**); tracings are representative of 3 independent experiments.

Figure S4

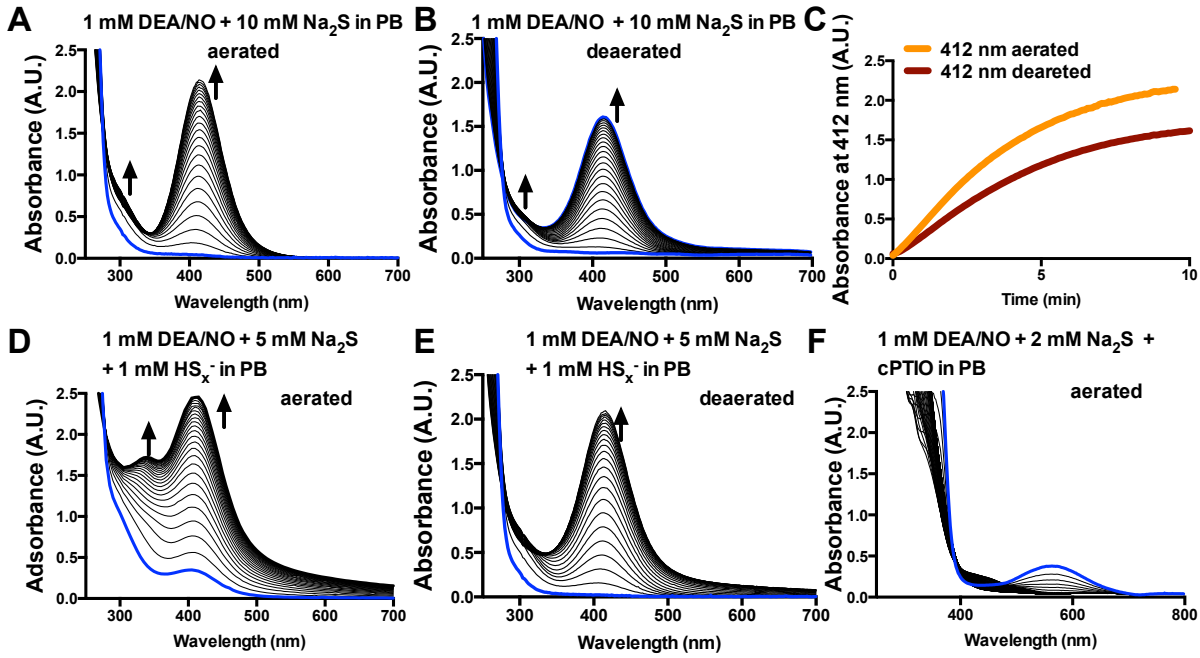

Figure S4. Accumulation of $SSNO^-$ (λ_{max} 412 nm) in the reaction between DEA/NO and sulfide in the presence (aerated) and absence (deaerated) of oxygen. (**A**,**B**) The reaction between 1 mM DEA/NO with 10 mM Na_2S under aerated (**A**) and deaerated (**B**) conditions was monitored by UV-visible spectrophotometry. (**C**) Kinetics of accumulation of $SSNO^-$ (λ_{max} 412 nm). (**D**,**E**) The reaction between 1 mM DEA/NO with 5 mM Na_2S in the presence of 1 mM polysulfide (S_x^{2-}) from K_xS_x was monitored under aerated und deaerated conditions. (**F**) The reaction between 1 mM DEA/NO with 2 mM Na_2S in the presence of the NO scavenger cPTIO does not produce $SSNO^-$ (λ_{max} 412 nm). Blue lines depict spectra at start of the reaction.

Figure S5

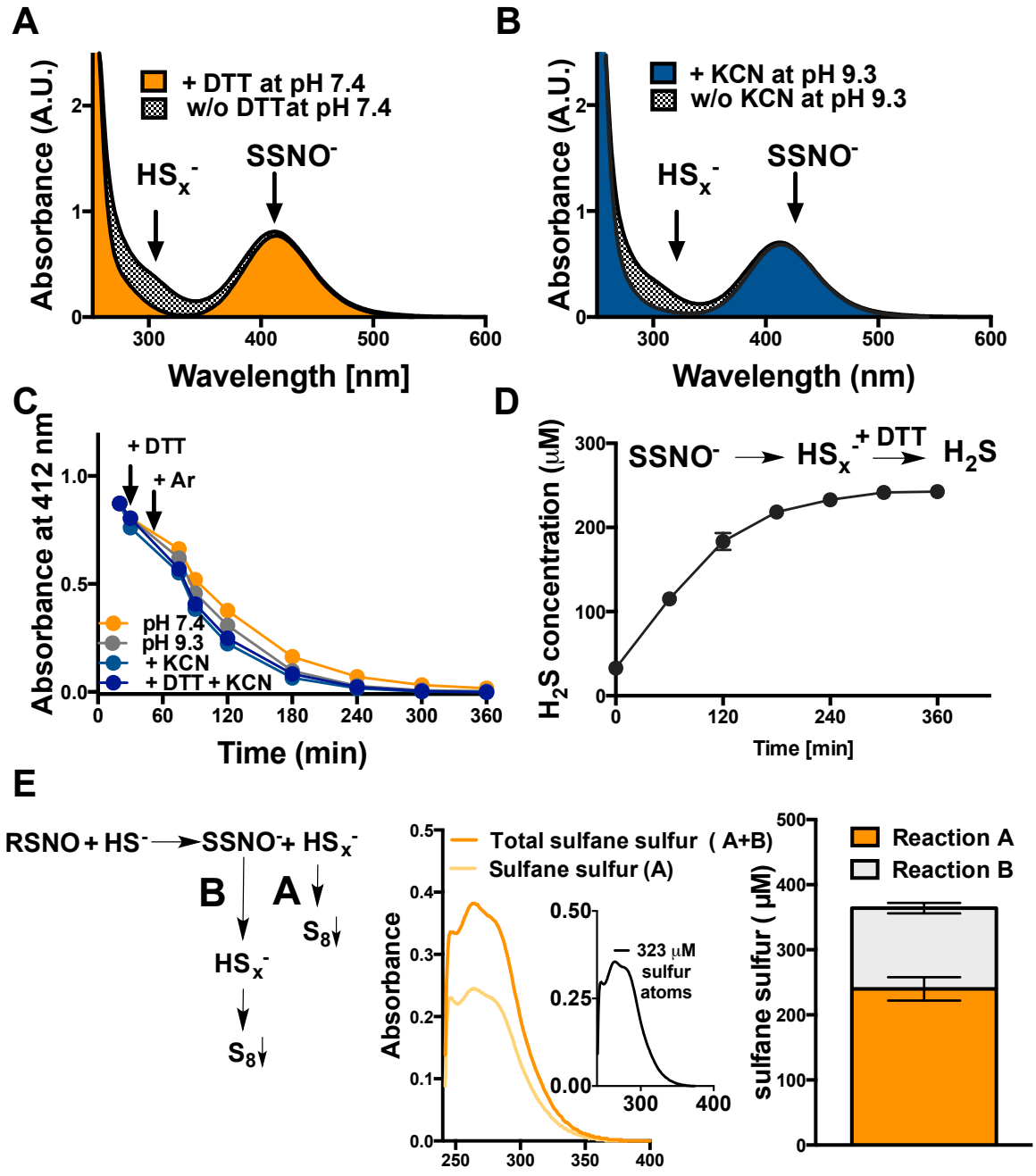
A
+ DTT at pH 7.4
w/o DTTat pH 7.4
HSx-
SSNO-
Absorbance (A.U.)
Wavelength [nm]
B
+ KCN at pH 9.3
w/o KCN at pH 9.3
HSx-
SSNO-
Absorbance (A.U.)
Wavelength (nm)
C
+ DTT
+ Ar
pH 7.4
pH 9.3
+ KCN
+ DTT + KCN
Absorbance at 412 nm
Time (min)
D
SSNO- → HSx- + DTT → H2S
H2S concentration (μM)
Time [min]
E
RSNO + HS- → SSNO- + HSx-
B
A
S8
HSx-
S8
Total sulfane sulfur (A+B)
Sulfane sulfur (A)
323 μM sulfur atoms
Absorbance
Reaction A
Reaction B
sulfane sulfur (μM)

Figure S5. $SSNO^-$ is resistant to DTT decomposition and $SSNO^-$ contains two sulfur atoms one of which is a sulfane sulfur. (**A,B**) Addition of DTT or KCN to the SNAP (500 μM)/sulfide (5 mM) reaction mixture fully decomposes polysulfide products to H_2S (approx 250 μM sulfide), but leaves $SSNO^-$ intact. (**A**) UV-vis spectra taken in the absence (grey) or in the presence of 5 mM dithiothreitol (DTT; orange) at pH 7.4 in TRIS buffer; (**B**) UV-vis spectra in the presence (blue) or in the absence (gray) of potassium cyanide (55 mM KCN pH 9.3); (**C**) the decomposition of $SSNO^-$ is not affected by basic pH or by high concentrations of dithiothreitol (500 μM DTT) and potassium cyanide (55 mM KCN pH 9.3) (n = 3). +Ar –denotes argon gassing for removal of excess sulfide. (**D**) Release of sulfide from polysulfides formed during $SSNO^-$ decomposition, as assessed in the presence of 5 mM DTT using the Methylene Blue method (n = 3). (**E**) Determination of sulfane sulfur by extraction with $CHCl_3$. Left panel: Schematic representation of the formation of sulfane sulfur equivalents by catenation reaction of polysulfide formed during formation of $SSNO^-$ (**Reaction A**), and during decomposition of $SSNO^-$ (**Reaction B**). Center panel: Representative spectra of sulfur atoms (i.e. sulfane sulfur equivalents) generated according to reactions A and B. Inset: representative standard spectrum. Right panel: Concentration of sulfane sulfur equivalents generated in reaction A and B (n = 3), showing that $SSNO^-$ decomposition accounts for ~30% of the detected sulfane sulfur, while polysulfide decomposition account for ~50% of the detected sulfane sulfur. The fact that two times as much sulfide (shown in **D**) as compared to sulfane sulfur (shown in **E**) was released upon $SSNO^-$ decomposition corroborates that $SSNO^-$ contains two sulfur atoms one of which is a sulfane sulfur.

Figure S6

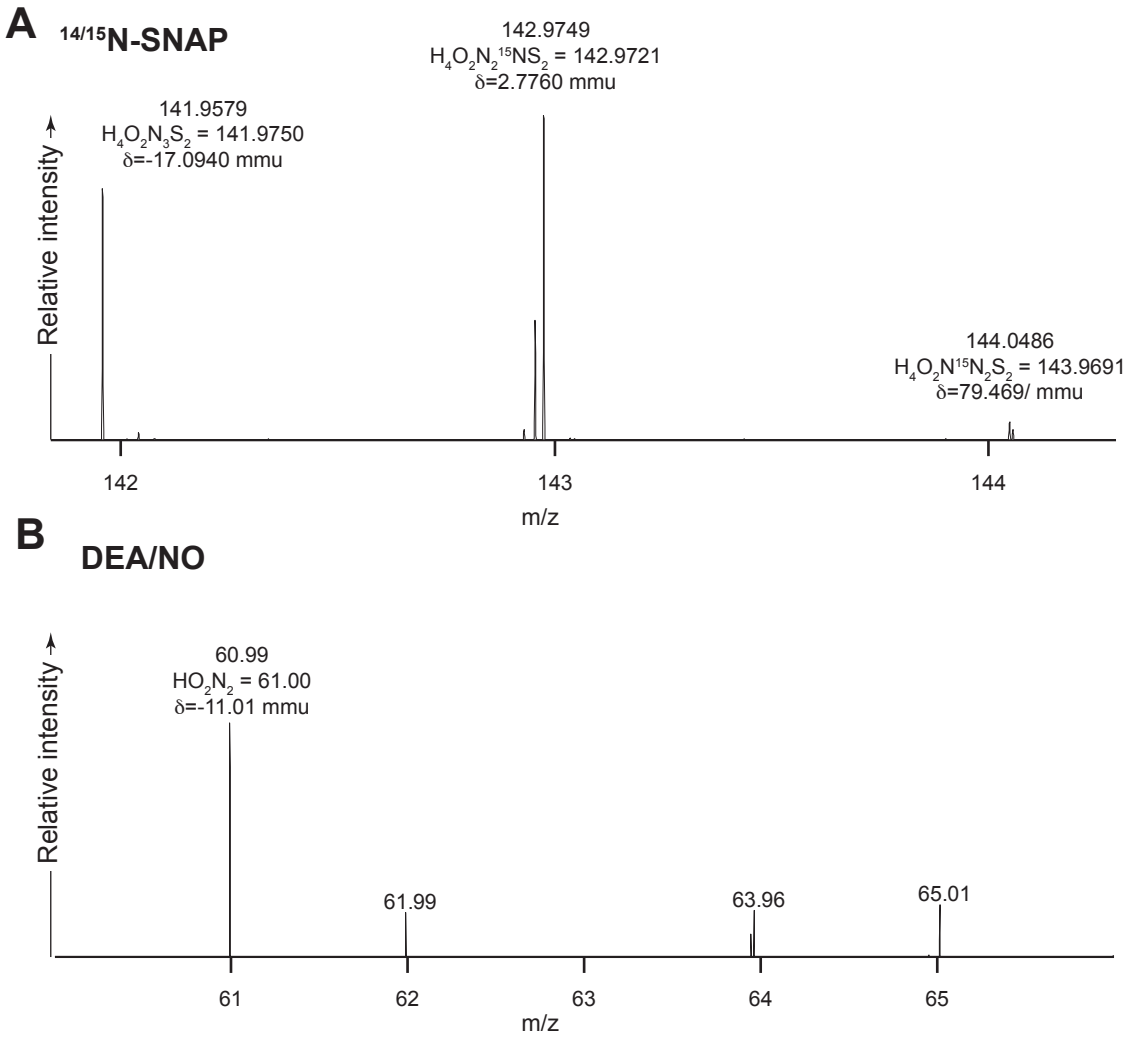

Figure S6. Dinitrosopersulfide and hyponitrite are also formed in the reaction between NO/RSNO and sulfide. (A) High resolution mass spectrum of $[SS(NO)NOH]^-$ (panel **A**) obtained by the reaction of a 50/50 mixture of 1 mM ^{14}N and ^{15}N- labelled SNAP with 2 mM Na_2S. **(B)** High resolution mass spectrum of hyponitrite ($ON:NOH^-$) from 1 mM DEA/NO/ 2 mM sulfide incubates in ammonium phosphate buffer (10 mM, pH 7.40, RT). The reaction solution was analyzed by high-resolution MS using an LTQ OrbiTrap with electrospray ionization source operated in negative ion mode. Samples were introduced into the source by direct infusion, and acetonitrile was used as make-up solvent to facilitate ionization. Representative of 3 independent experiments.

Figure S7

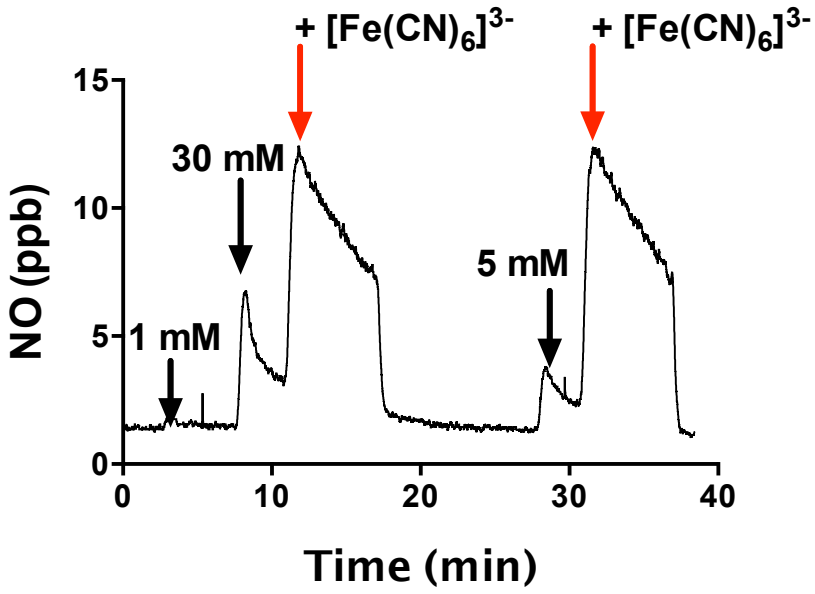

Figure S7. Time-resolved chemiluminescence of the generation of NO and HNO from hyponitrite. Hyponitrite (1 mM , 5 mM or 30 mM, black arrows) decomposes to release NO in phosphate buffer (pH 7.4, at 37°C) that reaches a steady-state level after approximately 3 minutes. Addition of potassium ferricyanide ($[Fe(CH)_6]$ (red arrows 1.67 mM) 3 min after hyponitrite addition potentiates NO release via conversion of HNO into NO. Representative of 3 independent experiments.

Figure S8 Panel A

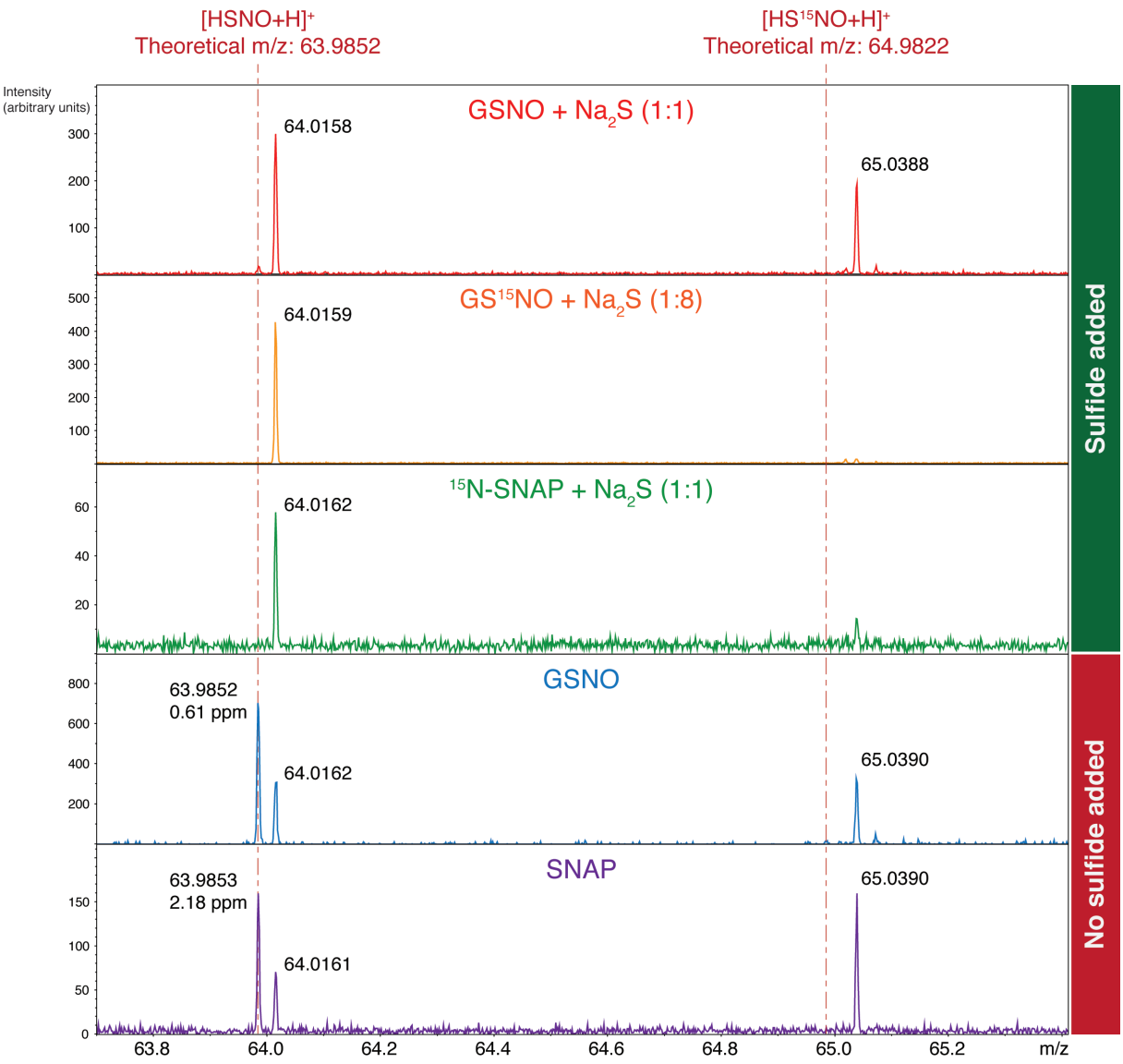

Figure S8 Panel B

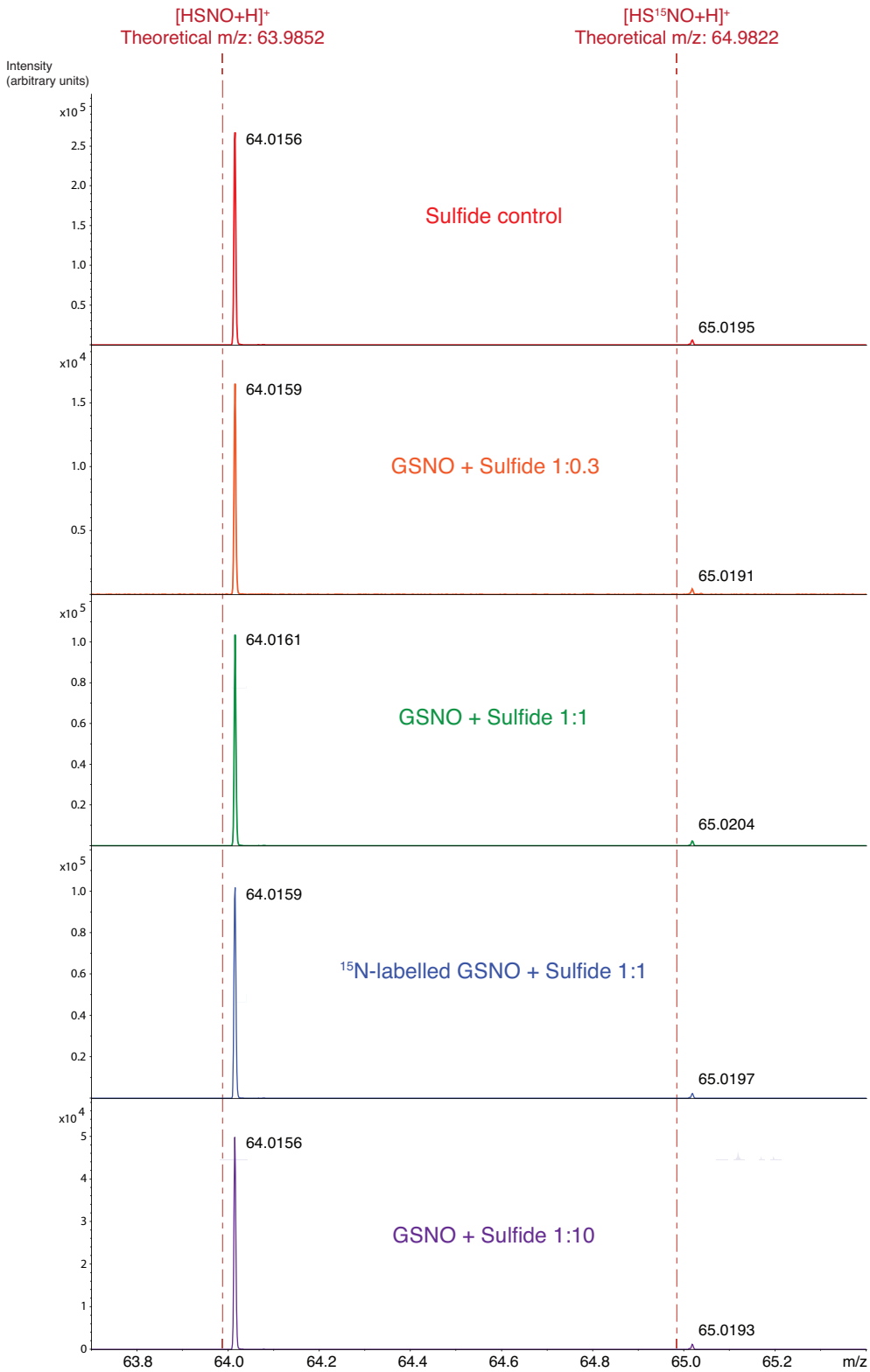

Figure S8 Panel C

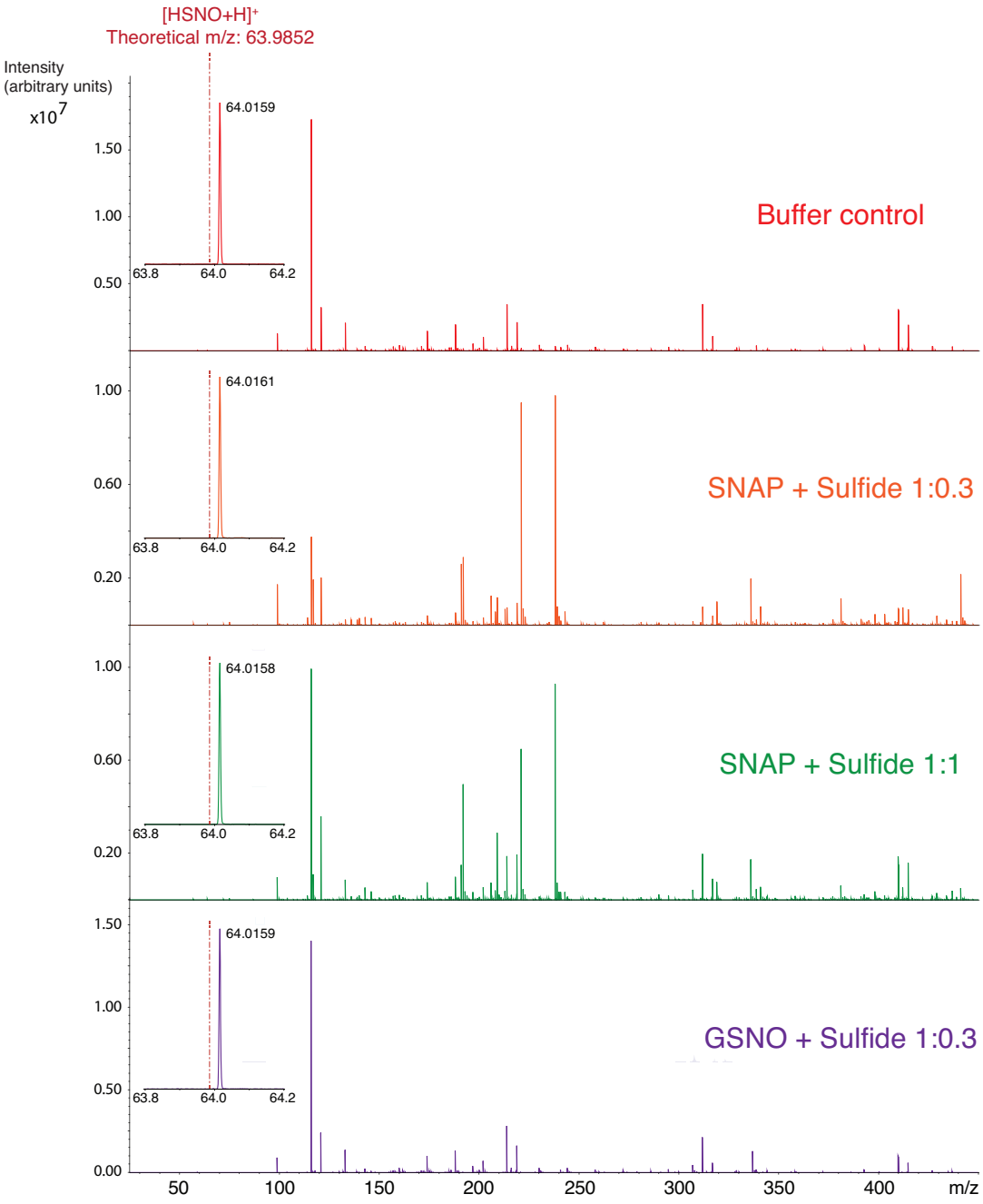

Figure S8. Panel A. Incubations of GSNO (1 mM) with equimolar sulfide produce a very small peak at m/z 63.9852 suggestive of the presence of HSNO; two more pronounced peaks were present at m/z of 64.0158 and 65.0388 (upper panel). The potential "HSNO peak" and the peak at m/z 65 were not observed in the presence of higher sulfide concentrations, suggesting the products are thiol sensitive. Importantly, the "HSNO peak" did not shift 1 m/z to the right on ^{15}N-labelling of the NO group of GSNO (neither at equimolar concentration nor with excess sulfide; 2nd panel). No "HSNO peak" was observed with SNAP/sulfide incubations under any reaction condition (shown for SNAP 1mM/sulfide 1 mM in panel 3 where SNAP stock solution). Disturbingly, the apparent "HSNO peak" was much more prominent on infusion of GSNO or SNAP in the absence of sulfide (lower two panels). Very similar results were obtained when electrospray ionization of buffered aqueous reaction mixtures was carried out at -20°C. Unexpectedly, neither lower sulfide concentrations (GSNO 1mM/sulfide 0.3 mM instead of 1:1 or 1:10 ratio) nor lower temperatures increased signal intensity of the peak at m/z 63.9852.

A separate series of experiments was carried out using cryospray ionization in conjunction with either acetonitrile or methanol coinfusion in attempts to enhance ionization efficiency while minimizing thermolytic cleavage of unstable reaction intermediates. This was accomplished by mixing aqueous ammonium phosphate-buffered reaction incubates (kept at either RT or 4°C) with the solvents at a ratio of 1:1 or 1:3 (v/v) via a T-piece right in front of the sprayer inlet. **Panel B** depicts results from the series with acetonitrile. GSNO or ^{15}N-labelled GSNO (both 1 mM) was mixed with substoichiometric (0.3 mM), equimolar (1 mM) or excess sulfide (10 mM; incubation solution dark yellow within <30s) and infused immediately into the ionization source. Under neither condition any new m/z features appeared besides the intense peak for the sodium adduct of acetonitrile at 64.015-64.016, which is a common background ion in ESI+ experiments. **Panel C** depicts the results from our subsequent attempts with either SNAP (0.2 mM) or GSNO (1 mM)/sulfide incubations and methanol coinfusion showing full scans and the m/z 64 region of interest (insets). Spectra are dominated by phosphate and sodium or ammonium adducts of the reaction products. Despite an extended wash-out period between experiments the 64 peak originating from the acetonitrile used in preceding experiments, albeit now at lower intensity, remained the dominating feature in the m/z range of 63-66 with no other peaks being detected during any time of the incubation (1-6 min).

Collectively, these results demonstrate that the apparent "HSNO peak" (m/z 63.9852) reacts with excess sulfide, is not particularly temperature-sensitive and quenched on attempts to improve ionization efficiency, is generated (presumably within the ion source) from

nitrosothiols already in the absence of any added sulfide, but does not originate from the NO group of the parent nitrosothiol as it does not shift with ^{15}N-NO labelling.

Figure S9

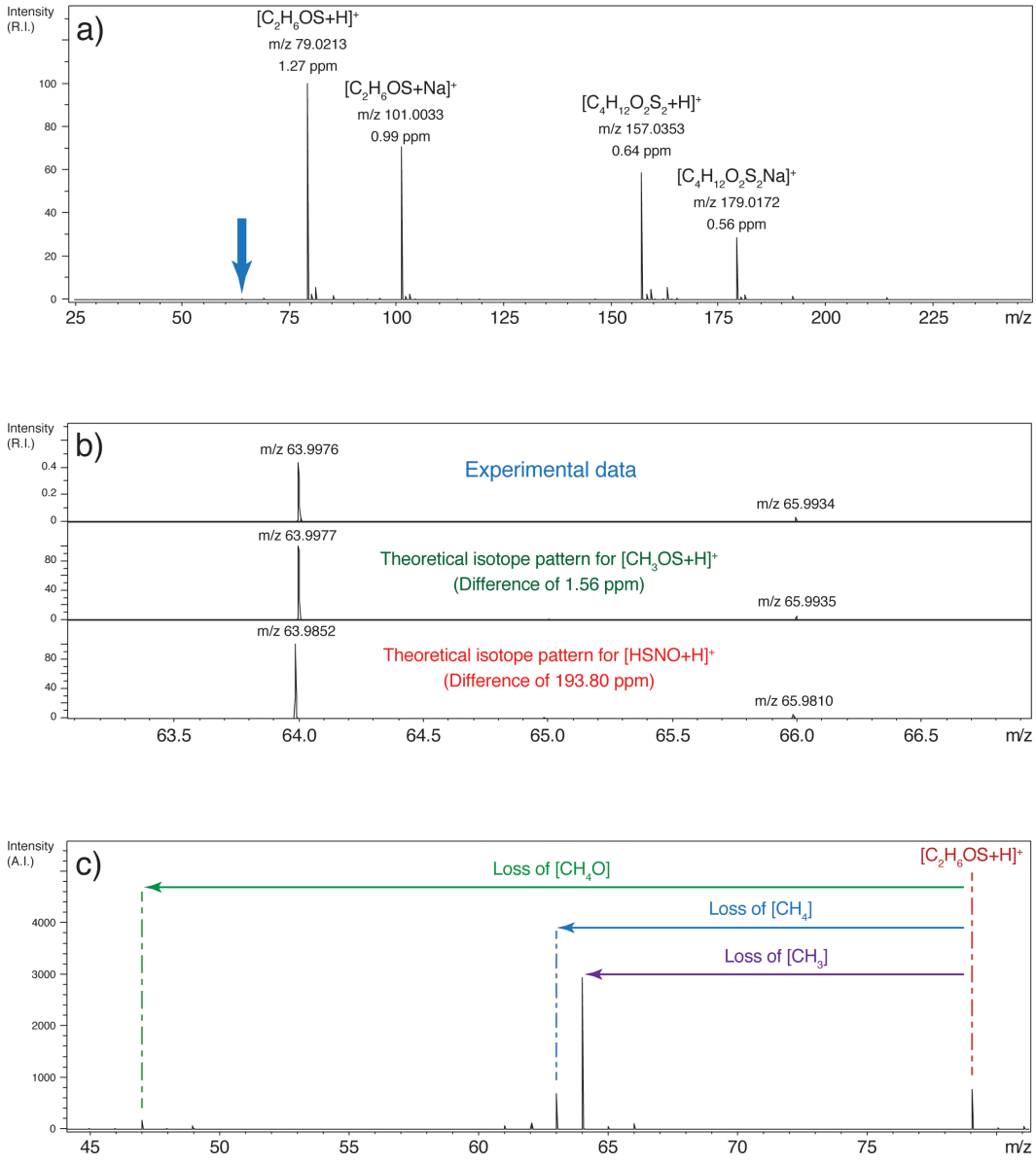

Fig. S9. The solvent dimethylsulfoxide also produces a peak at m/z 64.

In earlier experiments we used DMSO to prepare SNAP stock solutions because of its lower water solubility compared to GSNO. Accordingly, in positive ionization mode the spectrum of incubation mixtures of SNAP and sulfide (**A)** was dominated by DMSO adducts (arrow indicates the blown-up view of the m/z region around 64). **B)** In those experiments, a peak near m/z 64 was observed in SNAP/Sulfide (1:1 and 1:10) incubation mixtures, but not in those of DMSO-free GSNO/Sulfide mixtures. A comparison of the theoretical isotope pattern for the DMSO fragment (middle panel) and protonated HSNO (lower panel) with the experimental data (upper panel; SNAP 1 mM, Na_2S 1 mM; pH 7.4, RT; 2-6 min) reveals that the 64 peak observed in the SNAP/Sulfide mixture was due to DMSO and not HSNO. **C)** Controls with only DMSO confirmed that the peaks in the region of m/z 63-65 are in fact odd-electron species originating by loss of $CH_{3/4}$ and CH_4O from DMSO.

These finding are of relevance to other researchers in this area (in particular when relying on multi-user core instruments) as they document that a frequently used solvent known to be notorious for sticking to tubings and other surfaces may cause artifactual peaks in the lower m/z region around 64, which may originate from remnant material of previous runs. This finding adds to the known problems with acetonitrile when working with ESI+ at trace level in the m/z region around 64.

Figure S10

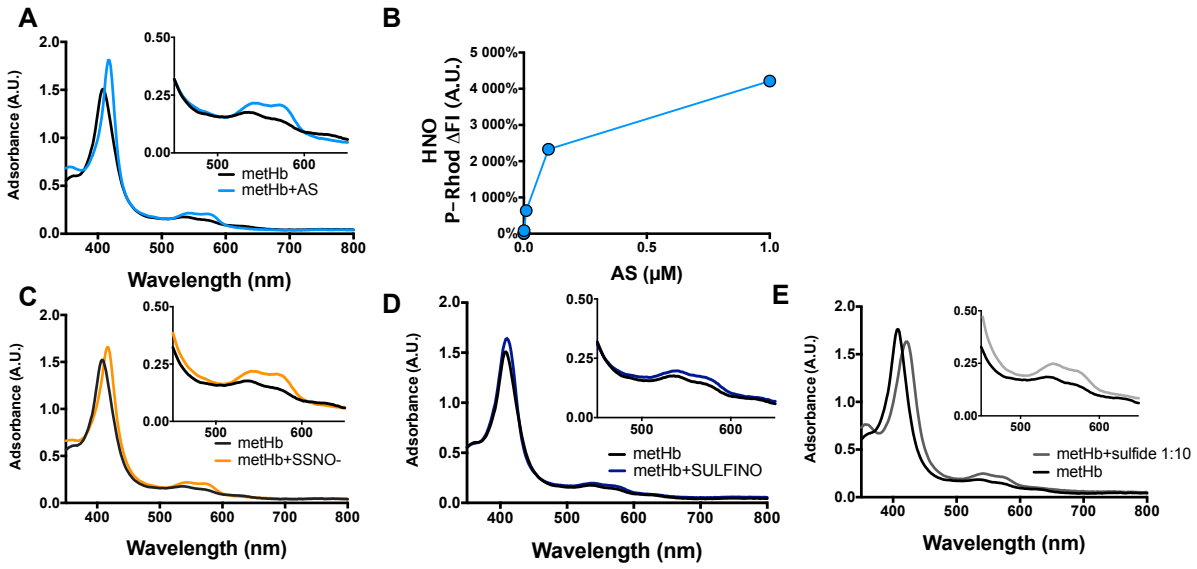

Figure S10. Detection of nitroxyl release from $SSNO^-$ and SULFI/NO as compared to Angeli's salt by reductive nitrosylation of metHb and P-Rhod. (**A,B**) Nitroxyl trapping by methemoglobin (metHb) results in an increase in absorbance at 542 nm and 583 nm, as shown by reaction of 1 mM Angeli's salt (AS) with metHb in panel **A**. In panel **B** production of nitroxyl by AS was assessed by reaction with P-Rhod. (**C**) The 'SSNO$^-$ mix' (prepared by reacting 1 mM SNAP with 5 mM sulfide, followed by removal of excess sulfide gassing the solution with N_2 increased absorbance at 542 nm and 583 nm. (**D**) 1 mM SULFI/NO increased absorbance at 542 nm and 583 nm to a lesser degree than AS. (**E**) Sulfide alone increases absorbance at 542 nm and 583 nm.

The use of metHb trapping to test nitroxyl production during the reaction of sulfide with nitrogenous species is not reliable, because sulfide reacts with metHb forming a Fe^{3+}-sulfide complex (40, 41) with similar absorbance characteristics.

Figure S11

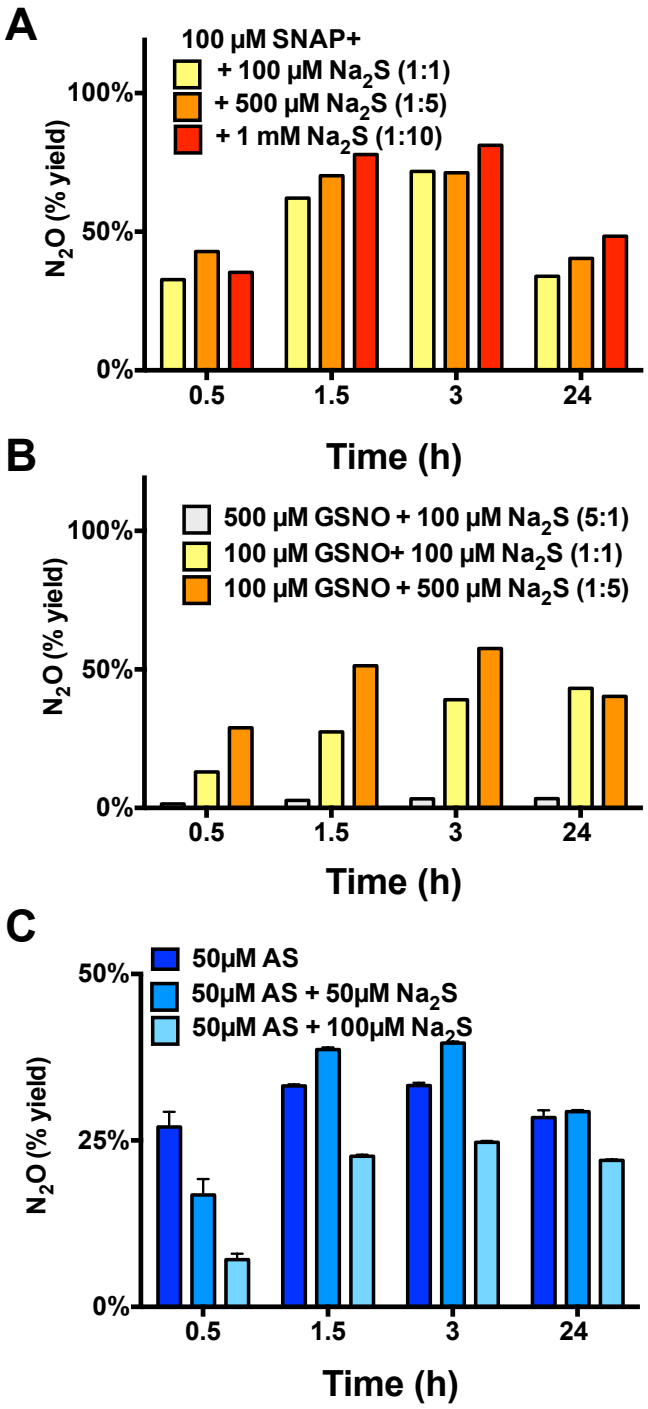

Figure S11. Release of N_2O from SNAP + HS^-, GSNO + HS^- and Angeli's salt + HS^- as assessed by gas chromatography. (A,B) Increase in N_2O production during formation and decomposition of $SSNO^-$ and SULFI/NO in the reaction between SNAP and Na_2S (**A**) or GSNO with Na_2S (**B**) at the indicated concentrations. (**C**) N_2O released by 50 µM Angeli's salt (AS) is decreased by addition of Na_2S in a concentration-dependent manner.

Figure S12

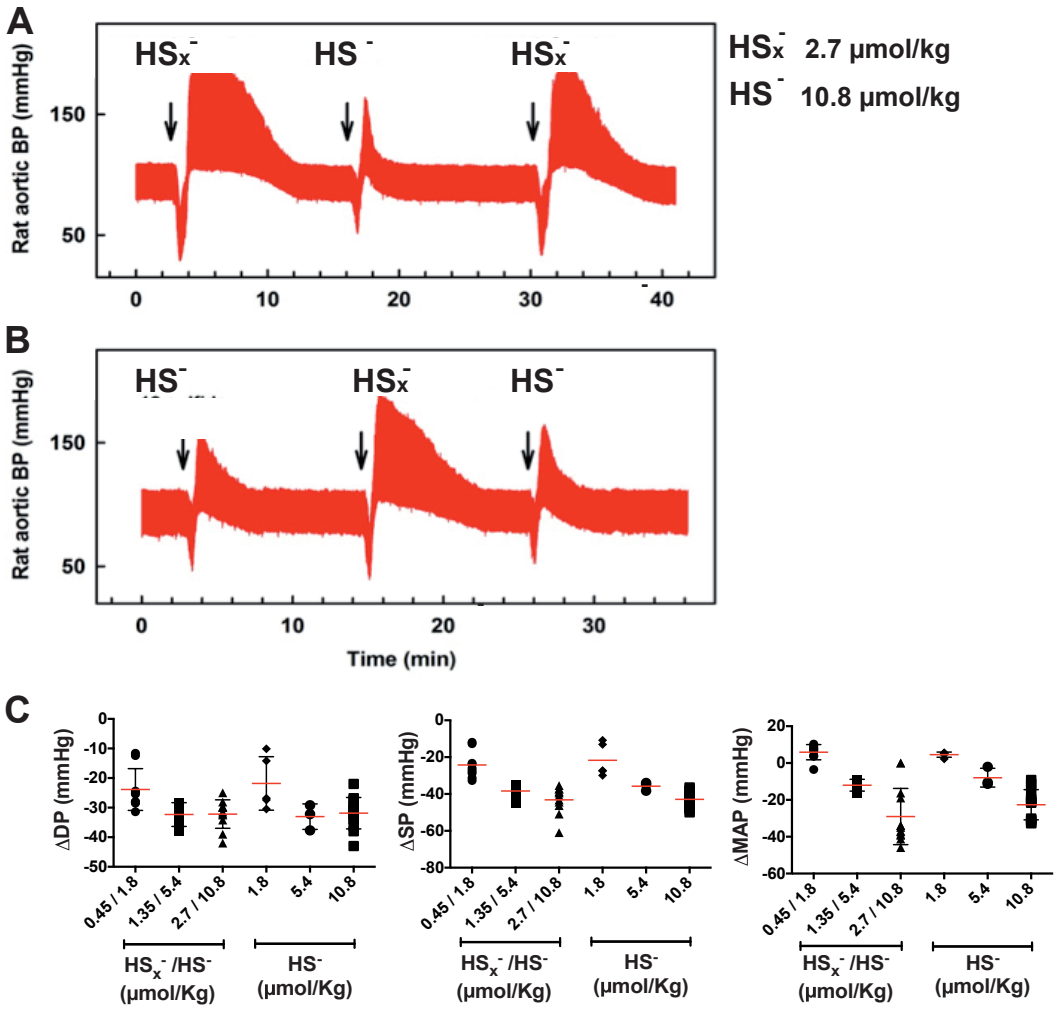

Figure S12: Polysulfides (HS_x^-) decrease blood pressure in rats. Intravenous (i.v.) administration of polysulfde (2.7 µmol/kg HS_x^-) / sulfide (10.8 µmol/kg HS^-) mixtures obtained by in situ oxidation of sulfide (see Materials and Methods and (34)) decrease systolic blood pressure (SP), diastolic blood pressure (DP) and mean arterial pressure (MAP) in anaesthetized rats. (**A,B**) Representative traces of effects of i.v. bolus applications of HS_x^- /HS^- mixture (2.7 µmol/kg HS_x^-/ 10.8 µmol/kg HS^-) or of sulfide alone (10.8 µmol/kg HS^-) on BP. (**C**) Concentration-dependent effects of the HS_x^-/HS^- mixture (0.45 - 2.7 µmol/kg HS_x^-/ 1.8 -10.8 µmol/kg HS^-), as compared to equivalent total amounts of sulfide (1.8 - 10.8 µmol/kg HS^-) on systolic (SP), diastolic (DP) and mean arterial blood pressure (MAP) compared to baseline (measurements performed in 8 rats). The magnitude of blood pressure

reduction by polysulfides appears to be similar to that of sulfide alone, yet its duration of action is prolonged as are duration and magnitude of the reactive pressor effects elicited.

Figure S13

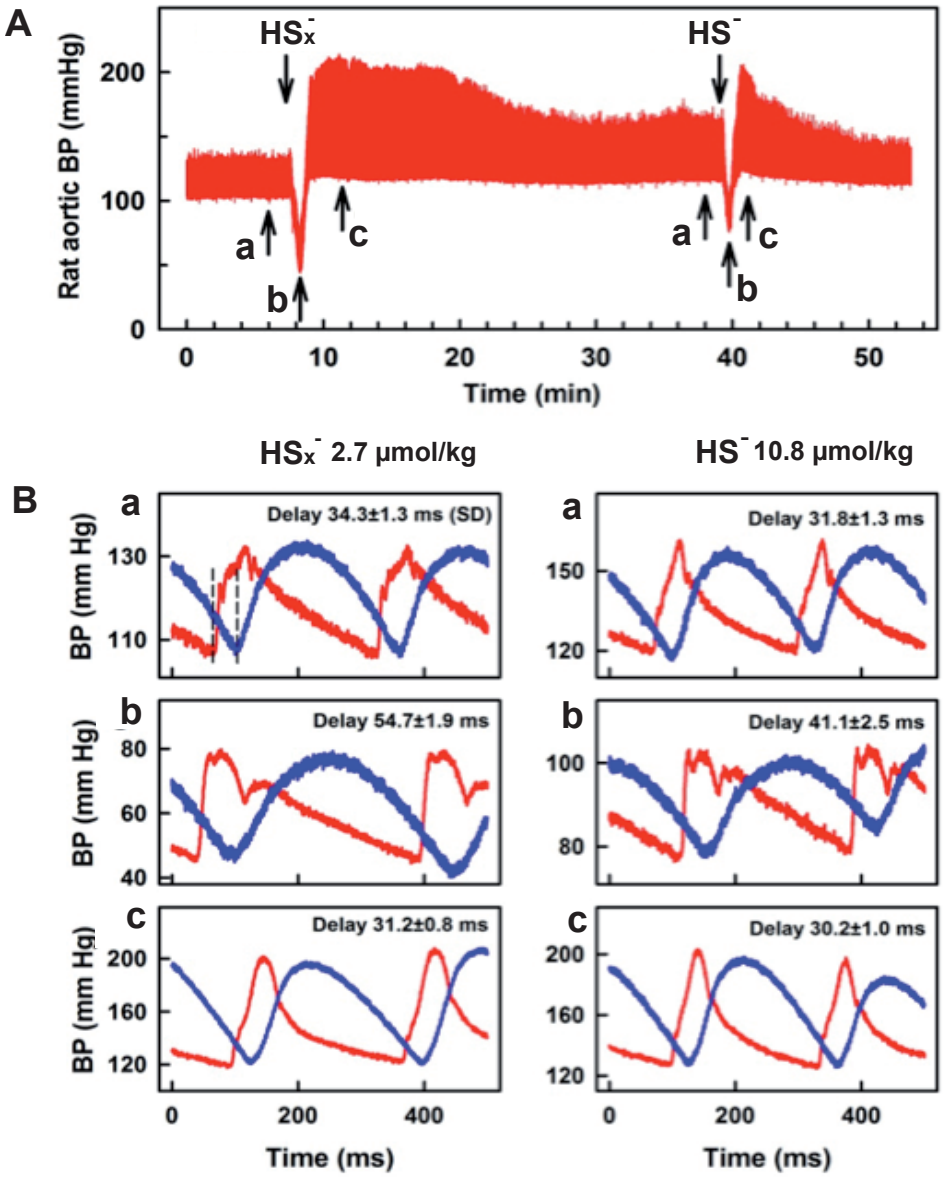

Figure S13: Polysulfides (HS_x^-) and sulfide modulate arterial stiffness. (**a)** Both polysulfides (2.7 µmoles/kg HS_x^-/10.8 µmol/kg HS^-) and sulfide alone (10.8 µmoles/kg) decrease blood pressure in anaesthetized rats. The arrows indicate the point of recording of the waveforms (**B**). Polysulfide and sulfide increase the time delay between the wave assessed in the carotic artery (heart, red line) and the tail artery (periphery, blue line) to a similar extent. (**a**) Baseline recording of the waves before administration of polysulfides or sulfide; (**b**) recording of the wave immediately after administration of polysuflde/sulfide; (**c**)

recording of the waves after reaching baseline again. The delay values are mean±SD (n=10). Data were calculated as described elsewhere (42).

Figure S14

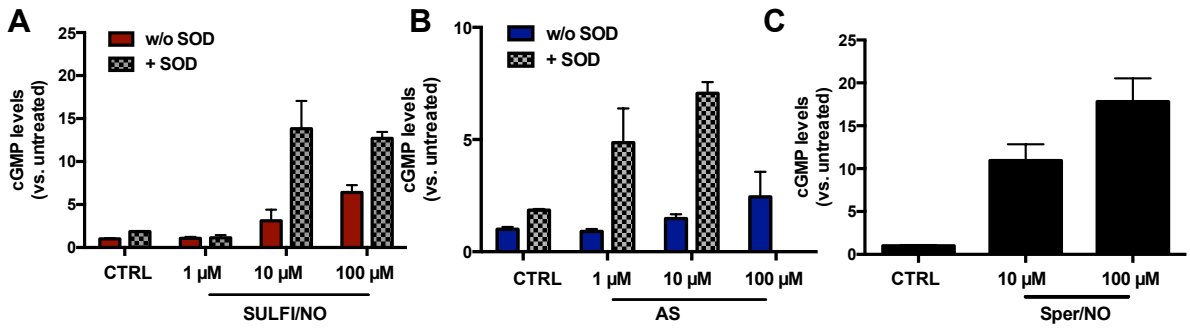

Figure S14. NO-dependent soluble guanylate cyclase (sGC) activation by SULFI/NO as compared to the NO donor Sper/NO and the nitroxyl donor Angeli's salt (AS). Concentration-dependent activation of sGC in RFL-6 cells (pre-treated with IBMX) by (**A**) 1 µM, 10 µM and 100 µM SULFI/NO, (**B**) 1 µM 10 µM and 100 µM Angeli's salt, and (**C**) 10 µM and 100 µM Sper/NO (**C**). Activation of sGC by 1 µM SULFI/NO and 1-10 µM AS occurs in the presence of high concentrations of SOD converting HNO into NO.

Figure S15

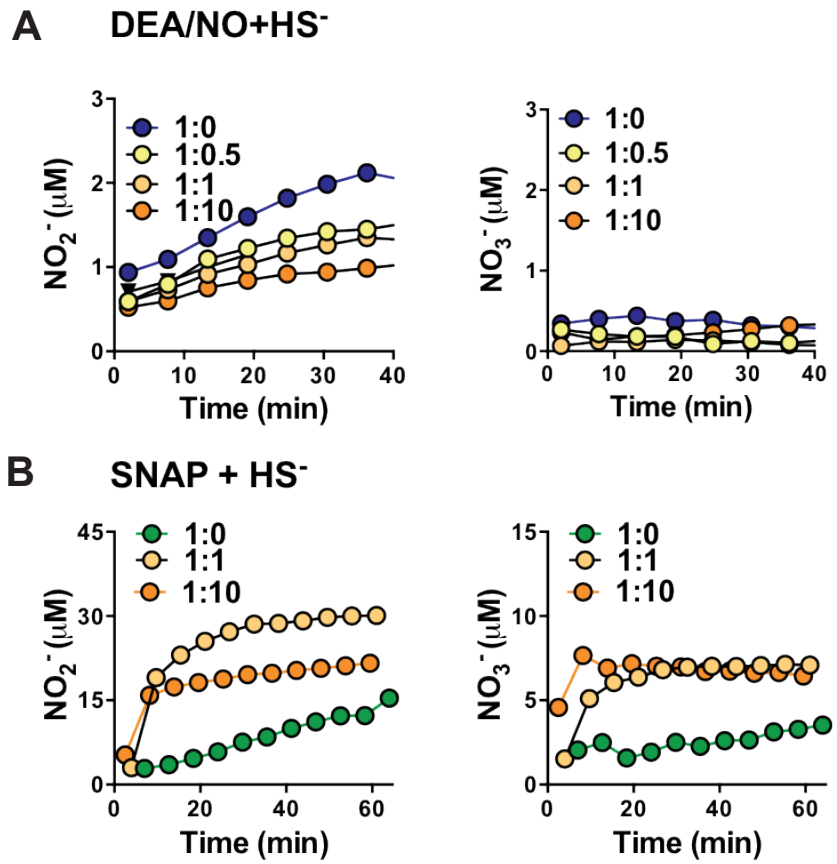

Figure S15. **Profile of nitrite (NO_2^-) and nitrate (NO_3^-) formation in incubation mixtures of DEA/NO or SNAP with HS^-. (A)** Nitrite and nitrate generation from aerated mixtures of 2 μM DEA/NO with 0 μM, 1 μM, 2 μM and 20 μM Na_2S incubated over 60 min at RT in phosphate buffer 50 mM pH 7.4. (B) Nitrite and nitrate generation from aerated mixtures of 100 μM SNAP with 0 μM, 2 μM and 20 μM sulfide (HS^-) in 50 mM phosphate buffer pH 7.4.

SI Tables

Tab. S1: Changes in hemodynamic parameters after i.v. bolus administration of NaHS (dose range 1.8 - 17.8 µmol/kg).

	Dose (mg/Kg) [µmol/kg]										
	0 [0]		0.1 [1.8]		0.2 [3.6]		0.5 [8.9]		1.0 [17.8]		
	mean	SD	mean	SD	mean	SD	mean	SD	mean	SD	n
Peak blood flow velocity (m/s)	1.19	0.09	0.91	0.14	0.98	0.14	0.94	0.08	0.82	0.20	3
Resp rate (1/min)	73	12	69	19	62	18	54	4	53	3	3
Stroke volume (ml) (Doppler)	0.36	0.04	0.30	0.05	0.32	0.05	0.32	0.02	0.31	0.06	3
Cardiac output (ml/min)[a]	143	5	115	17	121	12	114	9	100**	10	3
Ejection fraction (%)	88	1	84	3	87	1	87	3	85	4	3
Fractional shortening (%)	60	3	57	5	57	2	58	5	56	6	3

[a]ANOVA p = 0.029 F = 3.934 ; Bonferroni post hoc ** p = 0.03 vs. untreated.

Tab. S2: Changes in hemodynamic parameters during continuous i.v. infusion of NaHS (2.8 µmoles/kg/min).

	Time (min)												
	0		5		10		30		60		120		
	mean	SD	mean	SD	mean	SD	mean	SD	mean	SD	mean	SD	n
Peak blood flow velocity (m/s)	1.14	0.18	1.18	0.17	1.19	0.17	1.16	0.20	1.17	0.11	1.19	0.09	3
Resp rate (per min)	78	15	77	20	80	19	84	23	78	17	81	16	3
Stroke volume (ml) (Doppler)	0.35	0.03	0.38	0.04	0.37	0.03	0.38	0.05	0.38	0.03	0.40	0.03	3
Cardiac output (ml/min)	128	19	133	12	136	8	140	20	136	6	140	2	3
% Ejection fraction[a]	82.0	4.4	77.3	5.0	85.1	0.1	89.9[#]	2.9	79.1	6.1	79.7	1.7	3
% Fractional shortening[b]	52.5	6.7	48.1	5.4	56.7	0.2	64.5[##]	5.5	48.9	6.3	48.5	3.2	3

[a]ANOVA p = 0.20 F = 4.181; Post Hoc Sidak [#]p<0.05 vs. 5 min; p<0.05 vs. 60 min

[b]ANOVA p= 0.012 F = 4.820; Post Hoc Sidak [##]p<0.05 vs. 5 min; p<0.05 vs. 60 min

Tab. S3: Changes in hemodynamic parameters after bolus i.v. administration of $SSNO^-$ (dose range 0.03 - 3 µmol/kg)

	Doses (nmol) [µmol/Kg]												
	0 [0]		10 [0.03]		30 [0.09]		100 [0.3]		300 [0.9]		1000 [3]		
	mean	*SD*	*mean*	*SD*	*mean*	*SD*	*mean*	*SD*	*mean*	*SD*	*mean*	*SD*	*n*
Heart rate (per min)	368	19	396	9	396	5	410	58	401	59	415	57	3
Peak blood flow velocity (m/s)	1.0	0.1	1.0	0.1	1.1	0.2	1.0	0.2	1.1	0.1	1.0	0.1	3
Resp rate (per min)	71	5	75	2	69	7	72	5	69	9	57	9	3
Stroke volume (ml) (Doppler)	0.30	0.01	0.31	0.04	0.33	0.05	0.29	0.04	0.31	0.06	0.31	0.05	3
Cardiac output (ml/min)	112	9	121	11	133	19	117	14	122	6	125	3	3
% Ejection fraction	83	4.3	87	5.4	83	1.8	84	8.2	86	6.2	86	2.8	3
% Fractional shortening	51	4.7	59	7.6	53	2.1	57	10.3	56	11.1	61	7.6	3

Tab. S4: Changes in cardiovascular hemodynamic parameters during continuous infusion of $SSNO^-$ (0.16 µmol/kg/min).

	Time (mins)												
	0		5		10		30		60		120		
	mean	*SD*	*mean*	*SD*	*mean*	*SD*	*mean*	*SD*	*mean*	*SD*	*mean*	*SD*	*n*
Heart rate (per min)	389	34	375	60	338	25	371	48	368	39	375	32	3
Peak blood flow velocity (m/s)	0.9	0.0	1.0	0.0	0.9	0.1	1.0	0.1	1.1	0.1	1.2	0.2	3
Resp rate (per min)	66	1	72	6	77	8	74	7	77	6	75	2	3
Stroke volume (ml) (Doppler)	0.29	0.02	0.29	0.03	0.30	0.03	0.32	0.03	0.35	0.04	0.36	0.03	3
Cardiac output (ml/min)	111	2	109	8	100	18	119	17	129	17	136	23	3
% Ejection fraction	82.4	2.0	77.2	4.0	78.5	4.3	83.1	2.7	83.7	4.1	81.4	4.6	3
% Fractional shortening	53.0	3.8	46.9	4.7	48.3	5.3	53.6	1.6	54.7	4.5	52.5	4.9	3

Tab. S5: **Changes in cardiovascular hemodynamic parameters during bolus i.v. injection of SULFI/NO (dose range 0.03 - 3 µmol/kg)**

	Doses (nmol) [µmol/Kg]												
	0 [0]		10 [0.03]		30 [0.09]		100 [0.3]		300 [0.9]		1000 [3]		
	mean	*SD*	*mean*	*SD*	*mean*	*SD*	*mean*	*SD*	*mean*	*SD*	*mean*	*SD*	*n*
Heart rate (per min)	405.67	23.46	430.00	22.52	431.67	16.50	412.67	33.17	408.33	31.79	417.00	31.32	3
Peak flow velocity (m/s)[a]	1.06	0.12	1.11	0.15	1.17	0.12	1.19	0.06	1.39	0.16	1.49[#]	0.16	3
Resp rate (per min)	78.33	1.53	82.67	6.43	79.67	10.02	74.67	6.66	78.00	3.61	74.33	8.08	3
Stroke volume (ml) (Doppler)[b]	0.33	0.04	0.34	0.06	0.28[##]	0.03	0.35	0.02	0.40	0.06	0.40[§]	0.01	3
Cardiac output (ml/min)	132.60	21.80	144.76	24.73	120.74	15.48	144.39	4.82	163.94	15.30	167.89	15.44	3
% Ejection fraction	n.d.	n.d.	n.d.	n.d.	n.d.	n.d.	n.d.	n.d.	n.d.	n.d.	n.d.	n.d.	3
% Fractional shortening	54.64	3.03	52.09	4.90	54.72	9.40	54.63	1.26	54.35	6.09	57.40	10.11	3

10 mM SULFI/NO stock solution was prepared in 10 mM NaOH/0.9% NaCl. None of the parameter analyzed was significantly different from the vehicle control (NaOH dose range 0.03 - 3 µmol/kg)

[a]ANOVA p=0.014 F=4.652; [#]Post hoc Sidak p = 0.031 vs. baseline. [§]T-Test vs. baseline p = 0.02137

[b]ANOVA p = 0.022 F = 4.066; [##]Post hoc Sidak p<0.05 vs. 300 µmol p<0.05 vs. 1000 µmol; [§§]T-Test vs. baseline p = 0.0406

n.d. not determined

Tab. S6: Changes in cardiovascular hemodynamic parameters during continuous infusion of SULFI/NO (0.16 µmol/kg/min) or vehicle control (4.16 µmol NaOH/kg/min).

	Time (mins)												
	0		5		10		30		60		120		
SULFI/NO	***mean***	***SD***	***mean***	***SD***	***mean***	***SD***	***mean***	***SD***	***mean***	***SD***	***mean***	***SD***	***n***
Blood pressure (mmHg)[a]	88.3[n.s.]	8.6	93.8[n.s.]	7.8	80.4[n.s.]	6.5	76.0[n.s.]	11.1	78.2[n.s.]	8.0	75.4[n.s.]	10.5	3
VTI (cm)[b]	5.20	0.53	5.67	0.21	6.60	0.26	7.33**	0.58	7.43***	0.32	8.23***	0.59	3
Heart rate (per min)	369.0	20.5	392.0	29.5	394.3	32.3	348.3	12.1	349.7	23.2	355.3	38.7	3
Peak blood flow velocity (m/s)[c]	1.1	0.1	1.1	0.1	1.3	0.0	1.4*	0.1	1.4**	0.0	1.5***	0.1	3
Resp rate (per min)	77.0	12.1	70.3	8.1	71.0	13.0	73.0	14.7	76.7	17.2	75.7	11.0	3
Stroke volume (ml) (Doppler)[d]	0.32	0.03	0.35	0.01	0.41	0.02	0.45**	0.04	0.46**	0.02	0.51***	0.04	3
Cardiac output (ml/min)[e]	117.7	6.7	136.6	7.7	160.4	16.3	157.6	18.0	160.3	17.1	179.5*	14.0	3
Vehicle (NaOH)	***mean***	***SD***	***mean***	***SD***	***mean***	***SD***	***mean***	***SD***	***mean***	***SD***	***mean***	***SD***	***n***
Blood pressure (mmHg)	87.1	3.7	101.8	27.3	94.9	16.8	80.1	5.2	95.8	12.6	92.8	5.1	3
VTI (cm)	5.53	0.60	5.30	0.20	5.70	0.26	5.90	0.52	5.67	0.06	5.5	0.46	3
Heart rate (per min)	386.3	28.7	378.0	44.2	393.7	24.9	381.7	10.1	354.7	11.9	402.7	70.8	3
Peak blood flow velocity (m/s)	1.1	0.1	1.1	0.1	1.2	0.1	1.2	0.1	1.2	0.0	1.2	0.1	3
Resp rate (per min)	78.3	11.9	76.7	11.9	74.7	16.2	71.3	5.0	70.7	7.5	75.0	8.5	3
Stroke volume (ml) (Doppler)	0.34	0.04	0.33	0.01	0.35	0.02	0.36	0.03	0.35	0.00	0.34	0.03	3
Cardiac output (ml/min)	131.7	19.0	123.0	9.8	137.9	3.3	138.8	14.3	123.7	3.6	137.6	34.0	3

In order to keep SULFI/NO stable during infusion, a 1 mM SULFI/NO stock solution was prepared in 25 mM NaOH/0.9% NaCl. The effects of SULFI/NO infusion were compared to the effects of the vehicle control.

[a] 2-way-ANOVA vs. vehicle p = 0.0906 n.s. vs. vehicle; [b] 2-way ANOVA p<0.0001 **p<0.01 ***p<0.001 vs. vehicle; [c] 2-way ANOVA p = 0.0002 Bonferroni *p<0.05 **p<0.01 ***p<0.001 vs. vehicle; [d] 2-way ANOVA p = 0.0001 Bonferroni **p<0.01 ***p<0.001 vs. vehicle; 2-way ANOVA p = 0.0138 Bonferroni *p<0.05 vs. vehicle

Tab. S7: Identification by ESI-HR mass spectrometry of SULFI/NO and $SSNO^-$ as S/N hybrid species formed in the reaction of sulfide with DEA/NO or SNAP. The corresponding mass spectra are shown in Figure 3.

Assignment	Panel	Experimental [m/z]	Theoretical [m/z]	d [ppm]
$SSNO^-$	a - mass spectrum	93.9427	93.9427	<0.1
$S_3^{\cdot-}$	a - mass spectrum	95.9168	95.9168	<0.1
$SSNO^-$	a - fragmentation	93.9431	93.9427	0.4
$S_2^{\cdot-}$	a - fragmentation	63.9452	63.9447	0.5
$S^{15}SNO^-$	a - ^{15}N labeling	94.9398	94.9397	0.1
$S^{14}SNO^-$	a - ^{15}N labeling	93.9428	93.9427	0.1
$SULFI/NO^-$	b - mass spectrum	140.9617	140.9612	0.5
$HN_3S_3^-$	b - mass spectrum	138.9154	138.9338	-18.4
$SULFI/NO^-$	b - fragmentation	140.9615	140.9612	0.3
HSO_4^-	b - fragmentation	96.9606	96.9601	0.5
$HO_5{}^{15}N_2S^-$	b- ^{15}N labeling	142.9550	142.9552	0.2
$HO_5{}^{14}N{}^{15}NS^-$	b- ^{15}N labeling	141.9579	141.9582	0.3
$HO_5{}^{14}N_2S^-$-	b- ^{15}N labeling	140.9609	140.9612	0.3

SI : References

1. Cortese-Krott MM*, et al.* (2014) Nitrosopersulfide ($SSNO^-$) accounts for sustained NO bioactivity of S-nitrosothiols following reaction with sulfide. *Redox Biol* 2:234-244.
2. Munro AP & Williams DLH (2000) Reactivity of sulfur nucleophiles towards S-nitrosothiols. *J Chem Soc, Perkin Trans 2* (9):1794-1797.
3. Ondrias K*, et al.* (2008) H_2S and HS^- donor NaHS releases nitric oxide from nitrosothiols, metal nitrosyl complex, brain homogenate and murine L1210 leukaemia cells. *Pflugers Arch* 457(2):271-279.
4. Pierce JA (1928) A study of the reaction between nitric oxide and hydrogen sulphide. *J Phys Chem* 33(1):22-36.
5. Seel F & Wagner M (1988) Reaction of sulfides with nitrogen monoxide in aqueous solution. *Z Anorg Allg Chem* 558:189-192.
6. Seel F & Wagner M (1985) The reaction of polysulfides with nitrogen monoxide in non-acqueous solvents: nitrosodisulfides. *Z Naturforsch* 40(6):762.
7. Kurtenacker A & Löschner H (1938) Über die Einwirkung von Stickoxyd auf Thiosulfat und Sulfid. *Z Anorg Allg Chem* 238(4):335-349.
8. Bagster LS (1928) The reaction between nitrous acid and hydrogen sulphide. *J Chem Soc* 2631 - 2643.
9. Steudel R (1996) Mechanism for the formation of elemental sulfur from aqueous sulfide in chemical and microbiological desulfurization processes. *Ind Eng Chem Res.* 35(4):1417-1423.
10. Zhu J, Petit K, Colson A, DeBolt S, & Sevilla M (1991) Reactions of sulfhydryl and sulfide radicals with oxygen, hydrogen sulfide, hydrosulfide, and sulfide: formation of SO_2^-, $HSSH•^-$, $HSS•^{2-}$ and HSS•. *J Phys Chem* 95(9):3676-3681.
11. Pawelec M, Stochel G, & van Eldik R (2004) Mechanistic information on the copper-catalysed autoxidation of mercaptosuccinic acid in aqueous solution. *Dalton Trans* (2):292-298.
12. Ono K*, et al.* (2014) Redox chemistry and chemical biology of HS•, hydropersulfides, and derived species: Implications of their possible biological activity and utility. *Free Radic Biol Med* 77C:82-94.
13. Goehring M & Messner J (1952) Zur Kenntnis der schwefligen Säure. III Das Sulfinimid und seine Isomeren. *Z Anorg Allg Chem* 268(1-2):47-56.
14. Müller RP, Nonella M, & Huber JR (1984) Spectroscopic investigation of HSNO in a low temperature matrix. UV, VIS, and IR-induced isomerisations. *Chem Phys* 87:351-361.
15. Nonella M, Huber JR, & Ha TK (1987) Photolytic preparation and isomerization of thionyl imide, thiocyanic acid, thionitrous acid, and nitrogen hydroxide sulfide in an argon matrix: an experimental and theoretical study. *J Phys Chem* 91(20):5203-5209.
16. Gow AJ, Buerk DG, & Ischiropoulos H (1997) A novel reaction mechanism for the formation of S-nitrosothiol in vivo. *J Biol Chem* 272(5):2841-2845.
17. Kolesnik B*, et al.* (2013) Efficient nitrosation of glutathione by nitric oxide. *Free Radic Biol Med* 63:51-64.
18. Seel F*, et al.* (1986) Untersuchung der Umsetzung von Schwefel mit Natriumnitrit in DMF, DMSO und HMPT. *Z. anorg. allg. Chem.* 538(7):177-190.

19. Morse JW, Millero FJ, Cornwell JC, & Rickard D (2002) The chemistry of the hydrogen sulfide and iron sulfide systems in natural waters. *Earth-Sci Rev* 24(1):1-42.

20. Münchow V & Steudel R (1994) The Decomposition of Aqueous Dithionite and its reactions with polythionates $S_nO_6^{2-}$ (n= 3–5) studied by ion-pair chromatography. *Z Anorg Allg Chem* 620(1):121-126.

21. Hrabie JA & Keefer LK (2002) Chemistry of the nitric oxide-releasing diazeniumdiolate ("nitrosohydroxylamine") functional group and its oxygen-substituted derivatives. *Chem Rev* 102(4):1135-1154.

22. Goehring M & Otto R (1955) Zur Kenntnis der Salze der stickoxyd-schwefligen Säure. *Z Anorg Allg Chem* 280(1-3):143-146.

23. Degener E & Seel F (1956) Zur Kenntnis der Salze der Nitrosohydroxylaminsulfonsäure. I. Chemischer Konstitutionsbeweis der Nitrosohydroxylaminsulfonate. *Z Anorg Allg Chem* 285(3-6):129-133.

24. Clusius K & Schumacher H (1957) Reaktionen mit ^{15}N. XXVI. Konstitution und Zerfall von Kaliumnitroso-hydroxylaminsulfonat. *Helv Chim Acta* 40(5):1137-1144.

25. Zamora R, Grzesiok A, Weber H, & Feelisch M (1995) Oxidative release of nitric oxide accounts for guanylyl cyclase stimulating, vasodilator and anti-platelet activity of Piloty's acid: a comparison with Angeli's salt. *Biochem J* 312 (Pt 2):333-339.

26. Das T, Huie R, Neta P, & Padmaja S (1999) Reduction potential of the sulfhydryl radical: pulse radiolysis and laser flash photolysis studies of the formation and reactions of •SH and $HSSH^{\bullet -}$ in aqueous solutions. *J Phys Chem A* 103(27):5221-5226.

27. Winterbourn CC (1993) Superoxide as an intracellular radical sink. *Free Radic Biol Med* 14(1):85-90.

28. Koppenol W (1993) A thermodynamic appraisal of the radical sink hypothesis. *Free Radic Biol Med* 14(1):91-94.

29. Nyholm RS, Rannitt L, & Drago RS (1957) N-Nitrosohydroxylamine-N-Sulfonates. *Inorg Synth 5*:117-122.

30. Field L, Dilts RV, Ravichandran R, Lenhert PG, & Carnahan GE (1978) An unusually stable thionitrite from N-acetyl-D, L-penicillamine; X-ray crystal and molecular structure of 2-(acetylamino)-2-carboxy-1, 1-dimethylethyl thionitrite. *J Chem Soc, Chem Commun* (6):249-250.

31. Stamler J & Feelisch M (1996) Preparation and detection of S-nitrosothiols. *Methods in Nitric Oxide Research*, eds Feelisch M & Stamler J (John Wiley & Sons, Chichester), pp 521-539.

32. Feelisch M (1991) The biochemical pathways of nitric oxide formation from nitrovasodilators. *J Cardiovasc Pharm* 17(Supplement 3):S25-S33.

33. Nagy P*, et al.* (2014) Chemical aspects of hydrogen sulfide measurements in physiological samples. *Biochim Biophys Acta* 1840(2):876-891.

34. Nagy P & Winterbourn CC (2010) Rapid reaction of hydrogen sulfide with the neutrophil oxidant hypochlorous acid to generate polysulfides. *Chem Res Toxicol* 23(10):1541-1543.

35. Berenyiova A*, et al.* (2015) The reaction products of sulfide and S-nitrosoglutathione are potent vasorelaxants. *Nitric Oxide* 46:123-130.

36. Dyson A*, et al.* (2011) An integrated approach to assessing nitroso-redox balance in systemic inflammation. *Free Radic Biol Med* 51(6):1137-1145.

37. Feelisch M*, et al.* (2002) Concomitant S-, N-, and heme-nitros(yl)ation in biological tissues and fluids: implications for the fate of NO in vivo. *FASEB J* 16(13):1775-1785.

38. Kawai K*, et al.* (2013) A reductant-resistant and metal-free fluorescent probe for nitroxyl applicable to living cells. *J Am Chem Soc* 135(34):12690-12696.

39. DuMond JF, Wright MW, & King SB (2013) Water soluble acyloxy nitroso compounds: HNO release and reactions with heme and thiol containing proteins. *J Inorg Biochem* 118:140-147.

40. Keilin D (1933) On the combination of methaemoglobin with H_2S. *Proc. R. Soc. London, Ser. A* 393-404.

41. Vitvitsky V, Yadav PK, Kurthen A, & Banerjee R (2015) Sulfide oxidation by a noncanonical pathway in red blood cells generates thiosulfate and polysulfides. *J Biol Chem* 290(13):8310-8320.

42. Tomasova L*, et al.* (2015) Effects of AP39, a novel triphenylphosphonium derivatised anethole dithiolethione hydrogen sulfide donor, on rat haemodynamic parameters and chloride and calcium Cav3 and RyR2 channels. *Nitric Oxide* 46(0):131-144.